ABSTRACT

Supervisor: Professor K.R. Dixon

The synthesis, reactivity, and spectroscopic properties of a series of triangular phosphido-bridged rhodium, iridium, palladium and platinum clusters are described. Throughout the project, X-ray diffraction and $^{31}P\{^{1}H\}$ NMR spectroscopy are the main techniques for characterizing compounds. In the first part of this report, the lability of μ-X and terminal phosphines in $[M_3(\mu\text{-}X)(\mu\text{-}PPh_2)_2(PPh_3)_3][BF_4]$(M= Pd, X= Cl; M=Pt,X= H) is utilized to prepare a number of compounds where the integrity of the triangular framework is maintained. The molecular structures of three representative examples: $[Pd_3(\mu\text{-}SCH_2Ph)(\mu\text{-}PPh_2)_2(PEt_3)_3][BF_4]$ $[Pt_3(\mu\text{-}Cl)(\mu\text{-}PPh_2)_2(PR_3)_3][BF_4]$ (R= Ph, Et) were determined and are described. Reaction of these palladium and platinum trinuclear clusters with chelating ligands, $R'_2PYPR"_2$ (Y= O, CH_2), results in unusual cluster fragmentation to give novel dinuclear monocations, $[M_2(\mu\text{-}PPh_2)(\mu\text{-}R'_2PYPR"_2)(PR_3)_2]^+$ (M= Pd, Pt) in which a metal-metal bond is supported by both dppm and phosphido bridges. These dimers are very inert failing to react with a number of reagents including C_4H_6, $HCCCO_2Me$, CH_2N_2, CO, CH_3I (when M= Pd), H_2, HBF_4 and CH_2I_2. The cluster, $[Pt_3(\mu\text{-}H)(\mu\text{-}PPh_2)_2(PPh_3)_3][BF_4]$, also reacts with Bu^tNC to afford the dinuclear species $[Pt_2(\mu\text{-}PPh_2)_2(Bu^tNC)(PPh_3)_3]^+$. The

crystal structures of fragmentation products $[Pd_2(\mu\text{-}PPh_2)(\mu\text{-}Pr^i{}_2PCH_2PPh_2)(PPh_3)_2][BF_4]$, $[Pt_2(\mu\text{-}PPh_2)(\mu\text{-}Me_2PCH_2PMe_2)(PPh_3)_2]_2[C_2O_4]$ and $[Pt_2(\mu\text{-}PPh_2)(Bu^tNC)(PPh_3)_3]_2[C_2O_4]$ are reported and discussed.

In the last part, the synthesis of a novel trinuclear iridium cluster, $[Ir_3(\mu\text{-}PPh_2)_3(CO)_5]$, is described , and the reactions of this cluster and its previously reported rhodium analogue, $[Rh_3(\mu\text{-}PPh_2)_3(PPh_3)_2(CO)_3]$, with dppm afford not fragmentation, but substitution products. The complex $[Ir_3(\mu\text{-}PPh_2)_3(CO)_5]$ also reacts with Bu^tNC to yield $[Ir_3(\mu\text{-}PPh_2)_3(CO)_5(Bu^tNC)_2]$. The crystal structures of the compounds, $[M_3(\mu\text{-}PPh_2)_3(\mu\text{-dppm})(CO)_3]$(M= Rh, Ir) and $[Ir_3(\mu\text{-}PPh_2)_3(CO)_5(Bu^tNC)_2]$, are also reported.

Examiners:

Dr. K.R. Dixon

Dr. P.J. Romaniuk

Dr. T.M. Fyles

Dr. G.W. Bushnell

Dr. A. Watton

Dr. T. Chivers

TABLE OF CONTENTS

LIST OF TABLES

LIST OF FIGURES

LIST OF ABBREVIATIONS

AcOH	acetic acid
Bu^n	normal-butyl
Bu^t	tertiary-butyl
COE	cyclooctene
Cy	cyclohexyl
dmpm	bis(dimethylphosphino)methane
dppm	bis(diphenylphosphino)methane
Et	ethyl
h	hour
IR	infrared
L	ligand
μ	bridging
M	metal
Me	methyl
MO	molecular orbital
NMR	nuclear magnetic resonance
Ph	phenyl
POP	tetraethylpyrophosphite
Pr^i	iso-propyl
R	alkyl or aryl
THF	tetrahydrofuran
UV	ultraviolet

ACKNOWLEDGMENTS

I would like to thank my supervisor, Professor K.R. Dixon, and my co-workers, Dr. D.E. Berry, Dr. N.J. Meanwell, and Dr. R. Vefghi, for all their invaluable help and advice throughout my years at UVic.

CHAPTER ONE

GENERAL INTRODUCTION

A metal cluster may be defined as a network of metal atoms held together by metal-metal bonds with at least two different metal-metal bonds to each metal atom.[1] By this definition, in any metal cluster each metal atom is part of a ring, making the smallest cluster complex possible a triangle. The study of transition metal cluster complexes has been the subject of a great deal of interest in recent years. This interest derives mainly from two ideas: firstly, the idea that adjacent metal centers offer the possibility for cooperative reactivity leading to more active, or more selective catalysts;[2-6] secondly, the idea that metal clusters and their reactions can be used as models to understand what happens on metal surfaces during heterogeneous catalysis.[2,4,7] Based on the first idea it was hoped that clusters would bridge the gap between traditional homogeneous and heterogeneous catalysis, combining high selectivity with high activity associated with the respective systems. A good example is the hydrogenation of CO by $[Ir_4CO_{12}]$ to yield methane.[8]

Perhaps the best example of the second idea is provided by the Fischer-Tropsch synthesis. This reaction is normally catalyzed by a number of solid metal oxides (e.g. Fe_2O_3), where the mechanism is not clearly understood. The accepted view, however, is that CO molecules dissociate on the

surface to form surface carbides. The carbides are then hydrogenated to form surface μ-methyne, μ-methylene, and methyl groups. These groups then combine to form different hydrocarbons.[9] The important features of this mechanism, CO bond weakening and cleavage, C-H -and C-C bond formation, mobility of surface species, and release of products from the surface have all been modeled with organometallic cluster complexes.[10]

The stepwise cleavage of coordinated carbon monoxide under acid conditions, as demonstrated by $[Fe_4(\mu^3\text{-}CO)(CO)_{12}]^{2-}$, provides a good example of C-O bond cleavage and C-H bond formation. The triply bridging CO is sequentially reduced upon protonation to afford the carbide cluster, $[Fe_4(\mu^4\text{-}C)(\mu\text{-}H)(CO)_{12}]^-$, which can further be protonated to get the the methylidyne cluster $[Fe_4(\mu\text{-}CH)(\mu\text{-}H)(CO)_{12}]^-$. These reactions show that coordination has weakened the CO bond sufficiently to be cleaved to form a carbide, and for the carbide to hydrogenate.[11] An example of a C-C bond forming reaction is the reaction of the triruthenium clusters, $[H_3Ru_3(\mu^3\text{-}CX)(CO)_9]$ (X= OMe, Me, Ph, SEt), with two molecules of alkyne. The subsequent hydrogenation and loss of one alkyne forms $[HRu_3(\mu^3\text{-}CX)(alkyne)(CO)_9]$ (X= OMe, Me, Ph).[12,13] These compounds undergo C-C bond formation between the μ-CX and the alkyne to give $[HRu_3(\mu^3\text{-}$

$C(X)C_2HR)(CO)_9]$ (R= Ph, Bu^n). Hydrogenation of the coupled compounds under mild conditions yields $[H_3Ru_3(\mu^3\text{-}CCHRCH_3)(CO)_9]$ in which the original alkylidyne has been extended by two carbon atoms. These examples show that it is possible for surface carbides to form, for carbides to hydrogenate, and finally for μ-alkyl fragments to combine to form hydrocarbons.

In cluster-mediated catalytic reactions, there is little evidence that the nuclearity of the cluster is maintained throughout the reaction. One way to stop the possibility of fragmentation is to utilize an inert, strongly binding, and flexible bridge to hold the metal framework together . In that respect, phosphido-bridges have been one of the most widely used units,[14] even though some recent reports indicate that $\mu\text{-}PPh_2$ is not always as inert as it was originally thought.[15-16] An example of the flexibility of the formally three electron donor $\mu\text{-}PPh_2$ is provided by $[Fe_2(CO)_6(PPh_2)_2]$, where the Fe-P-Fe angle is 72° with an Fe-Fe bond length of 2.62Å. Upon oxidation to $[Fe_2(CO)_6(PPh_2)]^{2+}$, the Fe-P-Fe angle increases to 105.5° with an Fe-Fe distance of 3.63Å.[17] In this case, the flexibility of the phosphido bridge allows for the formation and cleavage of the M-M bond without complex decomposition.

Another reason for the interest in phosphines in general, and phosphido bridges in particular, has been the greater availability of the very powerful tool of ^{31}P NMR spectroscopy. For example, μ-PR_2 bridges exhibit a wide range of chemical shifts extending from -181.6 ppm in $[Pt_2(\mu\text{-}PPh_2)_2(dppe)_2][Cl]_2$[18] to 1362 ppm in $[Cr_2(\mu\text{-}PBu^t_2)(CO)_{10}]$,[19] and their chemical shift can also be used as a diagnostic tool for the presence of M-M bonds as demonstrated by various groups.[20]

Metal clusters may be prepared by a variety of methods. Ligand substitution, addition, and condensation reactions have all been used. The usual method, however, involves pyrolysis of transition metal compounds under very severe conditions where there is no control over the complex formed.[21-28] In the past fifteen years hundreds of cluster structures have been synthesized and reported in the literature. Despite this large number, examples containing palladium and platinum are relatively rare. The work presented in this thesis involves synthetic and reactivity studies of a number of triangular palladium and platinum clusters which contain phosphido bridges. This was later extended to cover analogous rhodium and iridium complexes. It may be divided into three areas:

1) The study of the reactivity of clusters $[M_3(\mu\text{-}X)(\mu\text{-}$

$PPh_2)_2(PR_3)_3]][Y]$ (M= Pd, Pt, X= Cl, H, Y= BF_4, C_2O_4), where the integrity of the cluster is maintained through the reaction.

2) The study of the reactions of phosphido-bridged trinuclear rhodium, iridium, palladium, and platinum clusters with ligands such as $Ph_2PCH_2PPh_2$ and Bu^tNC, which in the case of palladium and platinum leads to fragmentation.

3) The study of the reactivity of the fragmentation products formed.

Throughout this project, $^{31}P\{^1H\}$ NMR spectroscopy and X-ray crystallography were the major tools for characterizing compounds. The phosphorus chemical shifts are reported in parts per million with respect to external $P(OMe)_3$.

CHAPTER TWO

$[M_3(\mu\text{-}X)(\mu\text{-}PPh_2)_2(PR_3)_3][Y]$ (M= Pd, Pt) CLUSTERS AND THEIR REACTIVITY

INTRODUCTION:

The number of triangular palladium clusters reported in the literature is very limited. Earliest examples are the palladium(0) complexes: $[Pd_3(\mu\text{-}CO)_3(L)_3]$ (L= tertiary phosphine)[29,30] and $[Pd_3(\mu\text{-}SO_2)_2(Bu^tNC)_5]$.[31] $[Pd_3(\mu\text{-}CO)_3(PPh_3)_3]$ was prepared by the reaction of $[(PPh_3)_2PdCl_2]$ with CO at room temperature in methanol using a primary or secondary amine. $[Pd_3(\mu\text{-}SO_2)_2(Bu^tNC)_5]$ was synthesized from $[Pd(Bu^tNC)_2]$ and an excess of SO_2. The structure was determined by X-ray diffraction and was shown to contain a nearly equilateral triangle of metal atoms with Pd-Pd distances averaging 2.74Å. $[Pd_3(\mu_3\text{-}CO)(dppm)_3]^{2+}$, the only example of a dicationic palladium cluster to date, was prepared by the reaction of $[Pd(OAc)_2]$ with dppm under CO in aqueous acetone containing excess of CF_3CO_2H.[32] The metal atoms lie in a plane and are joined by a triply bridging carbonyl group and bridging dppm ligands.

Recently it was reported that the reaction of $[Pd(CO)(Cl)]_n$ with $[LiBu^t_2P]$ in THF produces the trinuclear cluster $[Pd_3(\mu\text{-}PBu^t_2)_3(CO)_2(Cl)]$.[33] The crystal structure indicates that the Pd, P and Cl atoms and the CO ligands are all virtually in the same plane with an average Pd-Pd distance of 2.98Å. $[Pd(CO)(Cl)]_n$ also reacts with $C_5H_5MgCl.THF$ to yield the dimer $[Pd_2(C_5H_5)_2(\mu\text{-}CO)_2]$ which further reacts

with HBF_4 or CF_3SO_3H to give the trinuclear cluster $[Pd_3(C_5H_5)_3(\mu^3\text{-}CO)_2]^+$.[34] The structure consists of an approximately equilateral triangle of palladium atoms with each face capped with a triply bridging carbonyl ligand and the three corners capped by C_5H_5 ligands. The mean Pd-Pd bond distance is 2.63Å.

In the late 70's, this laboratory reported that the prolonged heating of $[PdCl(PPh_3)_3]][BF_4]$ in THF at 125°C in vacuo gives red crystals of the tripalladium cluster $[Pd_3(\mu\text{-}Cl)(\mu\text{-}PPh_2)_2(PPh_3)_3][BF_4]$, a precursor for some of the compounds that will be discussed in this chapter.[35] The cluster was fully analyzed and characterized by $^{31}P\{^1H\}$ NMR and X-ray crystallographic techniques.[36]

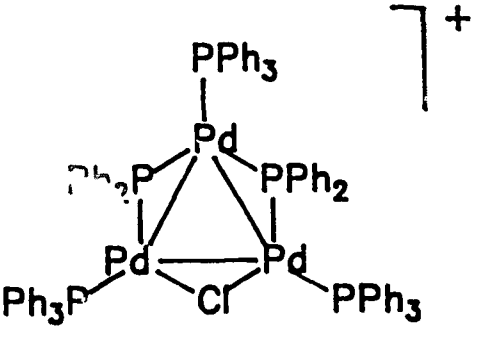

The palladium triangle is almost equilateral with the Cl-bridged Pd-Pd distance 2.89Å and the other two Pd-Pd distances equal at 2.93Å. The formal oxidation state of the palladium atoms is 4/3. Reactivity studies of $[Pd_3(\mu\text{-}Cl)(\mu\text{-}$

$PPh_2)_2(PPh_3)_3][BF_4]$ have shown that the bridging chloride and the terminal tertiary phosphine ligands are all labile. The bridging chloride can be replaced by bromide, iodide, SCF_3 or another PPh_2 group and the terminal phosphines may be substituted by more basic ones. The cluster can also be oxidatively degraded by H_2O_2 to yield a linear array of palladium atoms bridged by phosphides and halides. Further reaction with tertiary phosphines leads to the formation of mononuclear and dinuclear species.[37]

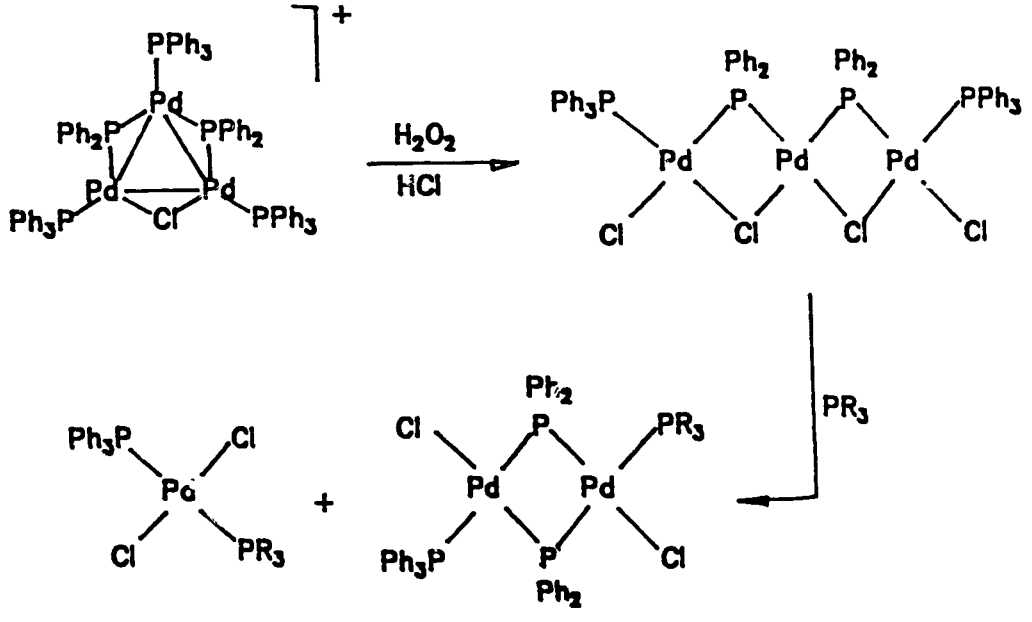

Similar to the palladium case, the number of triangular platinum clusters reported to date is relatively small. Platinum(0) examples include: $[Pt_3(\mu\text{-}CO)_3(PR_3)_3]$,[38-40] $[Pt_3(\mu\text{-}CO)_3(PR_3)_4]$,[41] $[Pt_3(\mu\text{-}SO_2)_3(PR_3)_3]$,[42,43] and

$[Pt_3(RNC)_6]$.[44,45] $[Pt_3(\mu_3\text{-}CO)(\mu\text{-}dppm)_3]^{2+}$,[46] $[Pt_3(\mu\text{-}CO)(\mu\text{-}dmpm)_4]^{2+}$,[47] and $[Pt_3(\mu\text{-}X)(\mu\text{-}SO_2)_2(PCy_3)_3]^+$ (X= Br, Cl, N_3)[48] are examples of cationic platinum clusters. The structure of all these clusters consists of a nearly equilateral triangle of metal atoms with Pt-Pt bond lengths in the range of 2.60Å-2.80Å.

$[Pt_3(Ph)(\mu\text{-}PPh_2)_3(PPh_3)_2]$,[49] $[Pt_3(\mu\text{-}Ph)(\mu\text{-}PPh_2)(\mu\text{-}SO_2)(PPh_3)_3]$,[50] and $[Pt_3(\mu\text{-}H)(\mu\text{-}PPh_2)_2(PPh_3)_3][BF_4]$[51] are the only reported examples of triangular platinum clusters with phosphido bridges. $[Pt_3(Ph)(\mu\text{-}PPh_2)_3(PPh_3)_2]$ was prepared by heating $Pt(PPh_3)_4$ in benzene under reflux for a period of several days. The structure is based on an open Pt_3 triangle with two Pt-Pt bonds (2.785Å) and three phosphido bridges.

In 1980, Evans et al. reported the synthesis of $[Pt_3(\mu\text{-}Ph)(\mu\text{-}PPh_2)(\mu\text{-}SO_2)(PPh_3)_3]$ a closed platinum cluster with phenyl, SO_2 and phosphido bridges. It was prepared from the reaction of SO_2 with $[Pt(1,2\text{-}C_4H_5R)(PPh_3)_2]$. An interesting point is that the different Pt-Pt bond lengths reflect the number of electrons contributed by each bridging ligand. Thus, the Pt-Pt bond lengths 2.69Å, 2.78Å and 2.81Å correspond to the bridging ligands Ph, SO_2 ,and PPh_2, which are respectively one-, two- and three-electron donors. The

Pt atoms in $[Pt_3(\mu\text{-}Ph)(\mu\text{-}PPh_2)(\mu\text{-}SO_2(PPh_3)_3]$ have an average oxidation state of 4/3.

In 1982, Bellon et al. showed by X-ray structural analysis and ^{31}P NMR studies that the previously reported cationic cluster, $[Pt_3(PPh_3)_4]^+$, is in fact $Pt_3(\mu\text{-}H)(\mu\text{-}PPh_2)_2(PPh_3)_3]^+$.

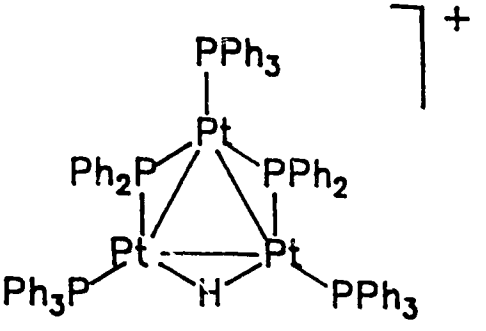

The compound was prepared by UV irradiation of an ethanolic solution of $[Pt(PPh_3)_2(C_2O_4)]$ under an H_2 atmosphere. The three platinum atoms lie in one plane. Two Pt-Pt bond distances to the unique platinum, are 2.796Å while the third Pt-Pt is 2.638Å. The presence of a bridging hydrogen atom was not established by X-ray analysis. However, high field ^{31}P NMR studies unambiguously showed one of the Pt-Pt edges to be H-bridged. In contrast to $[Pd_3(\mu\text{-}Cl)(\mu\text{-}PPh_2)_2(PPh_3)_3]^+$, no reactivity studies were reported for $[Pt_3(\mu\text{-}H)(PPh_2)_2(PPh_3)_3]^+$.

The only example of a mixed palladium /platinum triangular

cluster, $[PtPd_2(\mu\text{-}Cl)(\mu\text{-}PPh_2)_2(PPh_3)_3][BF_4]$, was prepared in this laboratory from the reaction of $[PdCl(PPh_3)_3][BF_4]$ with $[PtCl(PPh_3)_3][BF_4]$ at 125°C in vacuo.[52]

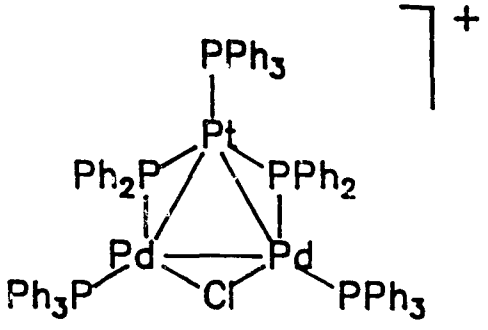

The structure was determined by ^{31}P, ^{195}Pt NMR, and X-ray crystallographic techniques. It has a similar structure to $[Pd_3(\mu\text{-}Cl)(\mu\text{-}PPh_2)_2(PPh_3)_3][BF_4]$, consisting of a triangle of metal atoms each bearing a terminal tertiary phosphine group with two edges bridged by phosphido groups and one bridged by a chloride. Some $[Pd_3(\mu\text{-}Cl)(\mu\text{-}PPh_2)_2(PPh_3)_3][BF_4]$ is always produced along with the heteronuclear species and successful separation has yet to be achieved.

The interesting features of $[M'M_2(\mu\text{-}X)(\mu\text{-}PPh_2)_2(PPh_3)_3]^+$ (M= M'= Pd, Pt; X= Cl, H) clusters may be summarized as follows:

1) the presence of three metal centers bonded together

2) the presence of strong yet flexible phosphido bridges

3) the presence of a potentially reactive μ-X bridge

4) the presence of potentially reactive terminal sites

These properties prompted us to further investigate the reactivity patterns of these clusters. This chapter deals with the reactivity of the μ-X moiety and the terminal sites. Reactions with diphosphines and other reagents which fragment the cluster are discussed in chapter three.

RESULTS AND DISCUSSION:

Reactions of $[Pd_3(\mu\text{-}Cl)(\mu\text{-}PPh_2)_2(PR_3)]^+$(R= Ph, Et):

There are a large number of transition metal complexes with sulphide ligands. The study of these complexes has been of interest as models for the activation of their oxo analogues or the development of desulphurization catalysts and for use in the preparation of organo sulphur compounds.[53-54] Sulphur has also been extensively used as a bridging unit to stabilize transition metal cluster complexes.[55-56]

The reaction of Na_2S with $[Pd_3(\mu\text{-}Cl)(\mu\text{-}PPh_2)_2(PR_3)_3][BF_4]$ (R= Ph, Et) in methanol yields the sulphido-bridged neutral species, $[Pd_3(\mu\text{-}S)(\mu\text{-}PPh_2)_2(PR_3)_3]$(R= Et, Ph).

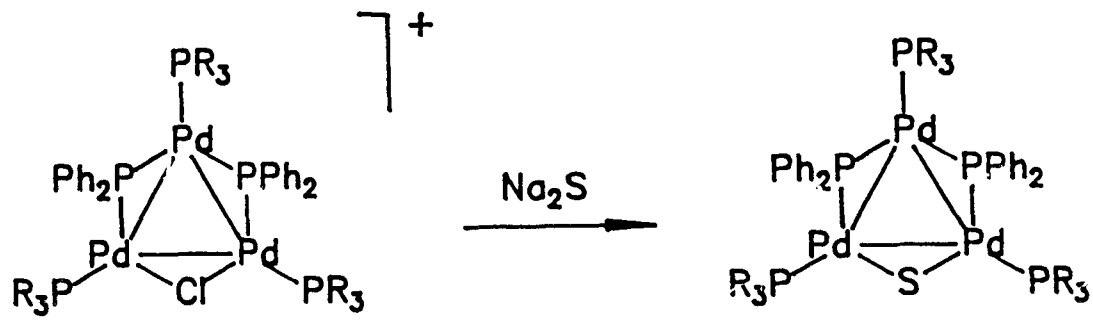

Both complexes were characterized by $^{31}P\{^1H\}$ NMR spectroscopy. The $^{31}P\{^1H\}$ NMR spectrum of $[Pd_3(\mu\text{-}S)(\mu\text{-}$

$PPh_2)_2(PEt_3)_3]$ is shown in figure 2-1. It consists of three sets of peaks. The peak at low field (0.4 ppm) belongs to the phosphido bridges. The doublet at -120.3 ppm and triplet at -140.4 ppm are due to the one unique and two equivalent terminal phosphine ligands respectively coupling to each other. The coupling constant between them is 103 Hz.

$[Pd_3(\mu\text{-}S)(\mu\text{-}PPh_2)_2(PPh_3)_3]$ proved to be unstable in solution. It decomposes in a matter of hours to give an insoluble black solid, assumed to be palladium metal, along with other products which were not characterized. The PEt_3 analogue, however, was stable. $[Pd_3(\mu\text{-}S)(\mu\text{-}PPh_2)_2(PEt_3)_3]$ may be prepared either by first synthesizing the PPh_3 analogue and then adding PEt_3, or by first preparing $[Pd_3(\mu\text{-}Cl)(\mu\text{-}PPh_2)_2(PEt_3)][BF_4]$ and then reacting it with Na_2S. Both methods work equally well with comparable yields. No reaction occurs when anhydrous Li_2S is used as the source of sulphide.

Previous reports on sulphido-bridged species have shown that the sulphide ligand is susceptible to electrophilic attack by protonating and alkylating reagents. Examples are $[Pt_2(\mu\text{-}S)_2(PPh_3)_4]$,[57] $[Pt_2(\mu\text{-}S)(CO)_2(PBu^t{}_2Ph)_2]$,[58] and $[Pt_2(\mu\text{-}S)(CO)(PPh_3)_3]$.[59] In all cases the sulphide could be

Figure 2-1

The $^{31}P\{^{1}H\}$ NMR Spectrum of
$[Pd_3(\mu\text{-}S)(\mu\text{-}PPh_2)_2(PEt_3)_3]$

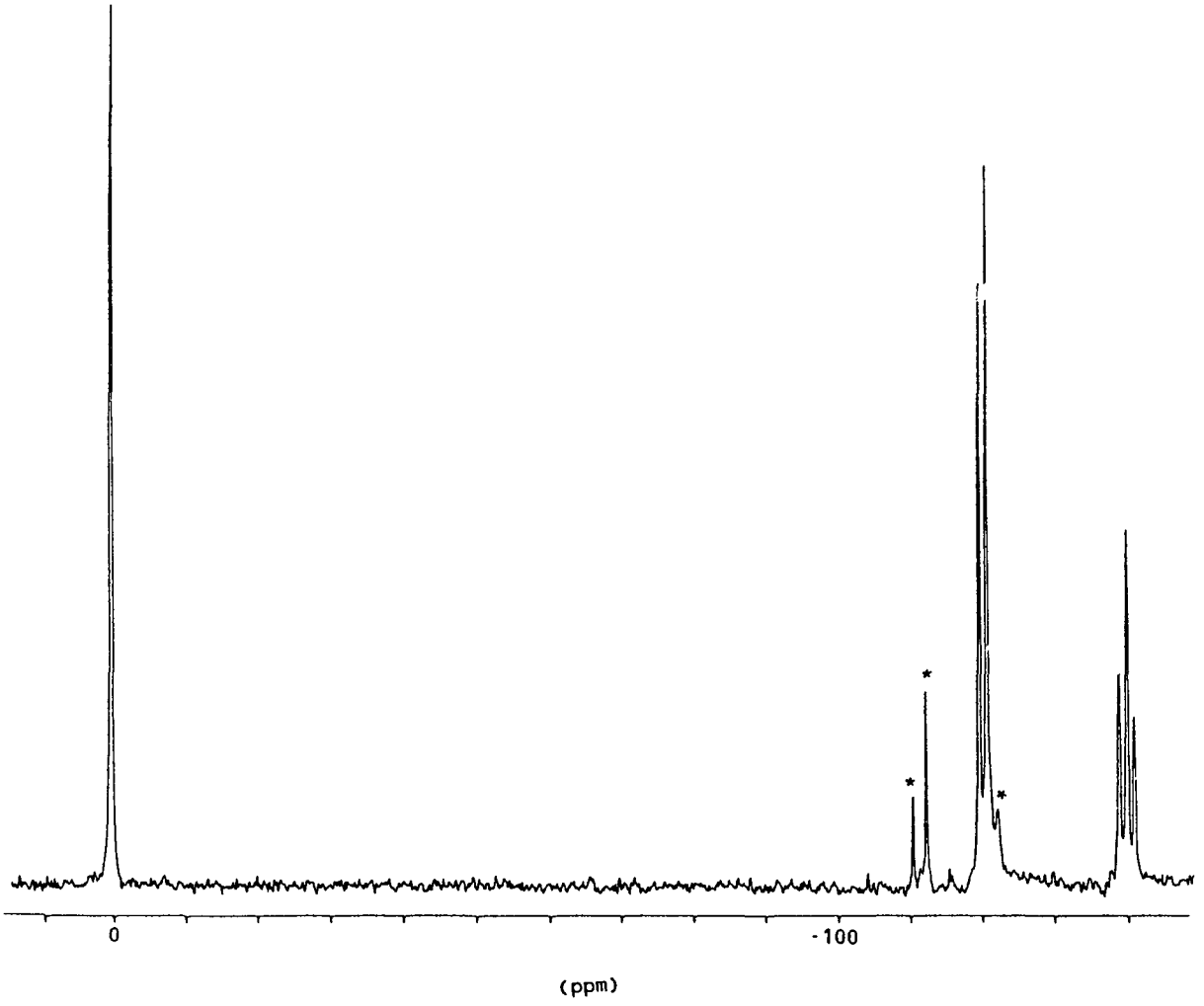

*= Impurity

alkylated by CH_3I. In the case of $[Pt_2(\mu\text{-}S)_2(PPh_3)_4]$ the nucleophilicity of μ-S is so high that it readily undergoes alkylation with both $CHCl_3$ and CH_2Cl_2. In the case of $[Pd_3(\mu\text{-}S)(\mu\text{-}PPh_2)_2(PR_3)_3]$ (R= Et, Ph) the bridging sulphide is also sufficiently nucleophilic to allow for easy protonation and alkylation.

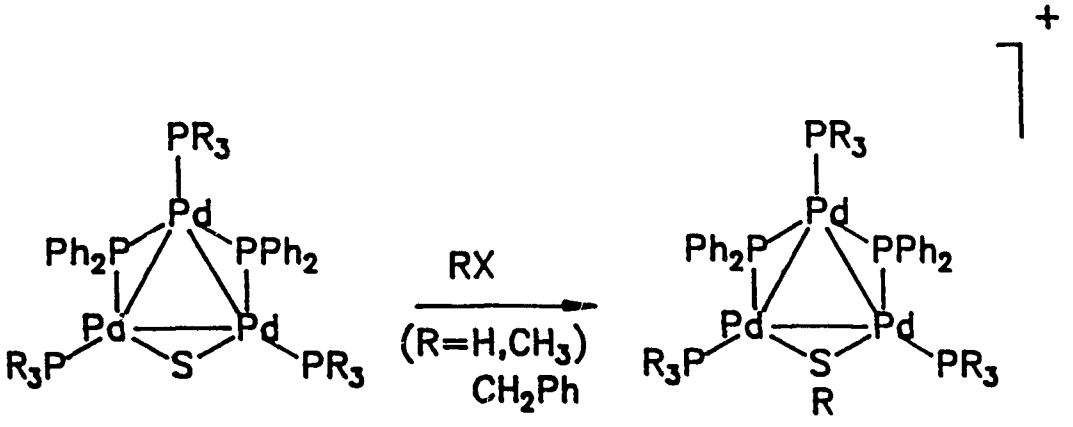

Protonation of $[Pd_3(\mu\text{-}S)(\mu\text{-}PPh_2)_2(PPh_3)_3]$ with $HBF_4.Et_2O$ in CH_2Cl_2 yields $[Pd_3(\mu\text{-}SH)(\mu\text{-}PPh_2)_2(PPh_3)_3][BF_4]$. The reaction proceeds cleanly and quantitatively. $(CH_3)_3OBF_4$ easily alkylates $[Pd_3(\mu\text{-}S)(\mu\text{-}PPh_2)_2(PPh_3)_3]$ to give $[Pd_3(\mu\text{-}SCH_3)(\mu\text{-}PPh_2)_2(PPh_3)_3][BF_4]$. Reaction with CH_3I, however, does not produce the desired product. Instead $[Pd_3(\mu\text{-}I)(\mu\text{-}PPh_2)_2(PPh_3)_3][I]$ is formed, which was identified by its identical $^{31}P\{^1H\}$ NMR spectrum with a previously synthesized pure sample of $[Pd_3(\mu\text{-}I)(\mu\text{-}PPh_2)_2(PPh_3)_3]^+$. The μ-SR complexes were all characterized by $^{31}P\{^1H\}$ NMR spectroscopy and elemental analysis (for values see chapter seven).

The reaction of $[Pd_3(\mu\text{-}S)(\mu\text{-}PPh_2)_2(PEt_3)_3]$ with excess benzyl bromide produces $[Pd_3(\mu\text{-}SCH_2Ph)(\mu\text{-}PPh_2)_2(PEt_3)_3]^+$. The $^{31}P\{^1H\}$ NMR spectrum of this compound (figure **2-2**) is similar to the previous case discussed. However, in this case, the coupling constant between the terminal phosphines is 95 Hz. A suitable crystal of this compound was obtained and its X-ray crystal structure was determined by Dr. J. Browning of our group. An ORTEP diagram of the compound is depicted in figure **2-3**. The relevant crystallographic parameters are listed in table **2-1**. Table **2-2** contains a list of selected bond lengths and angles. The palladium-palladium bond distances on the phosphido-bridged edges are 2.977Å and 2.953Å; and the benzylsulphido-bridged edge is 2.924Å. These bonds are slightly longer than the palladium-palladium bond lengths in the μ-Cl cluster. There are small distortions from planarity which are probably due to ligand crowding in the proximity of the palladium triangle. There is also an asymmetry in the bond lengths of the phosphorus of the phosphido bridges with the palladiums. For example P(4)-Pd(2) bond length is 2.268Å, whereas P(4)-Pd(3) bond length is 2.237Å. This small effect is probably due to the trans influences of the ligands most nearly trans to the affected bonds. The longer bonds are almost trans to another $\mu\text{-}PPh_2$ group (P-Pd-P angle averages 154°), and the

Figure 2-2

The $^{31}P\{^{1}H\}$ NMR Spectrum of
$[Pd_3(\mu\text{-}SCH_2Ph)(\mu\text{-}PPh_2)_2(PEt_3)_3][BF_4]$

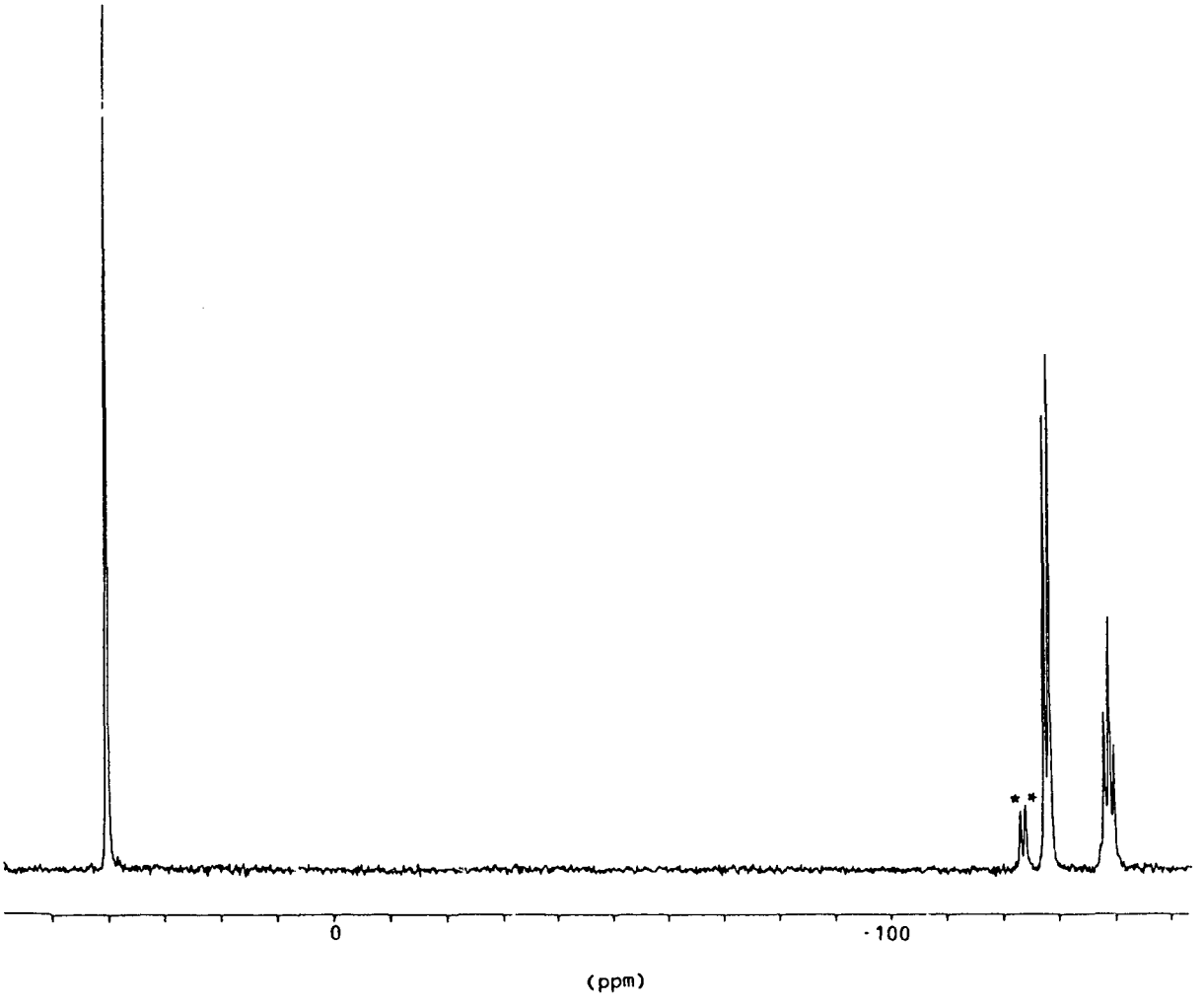

*= Impurity

Figure 2-3

The Molecular Structure of
$[Pd_3(\mu\text{-}SCH_2Ph)(\mu\text{-}PPh_2)_2(PEt_3)_3][BF_4]$

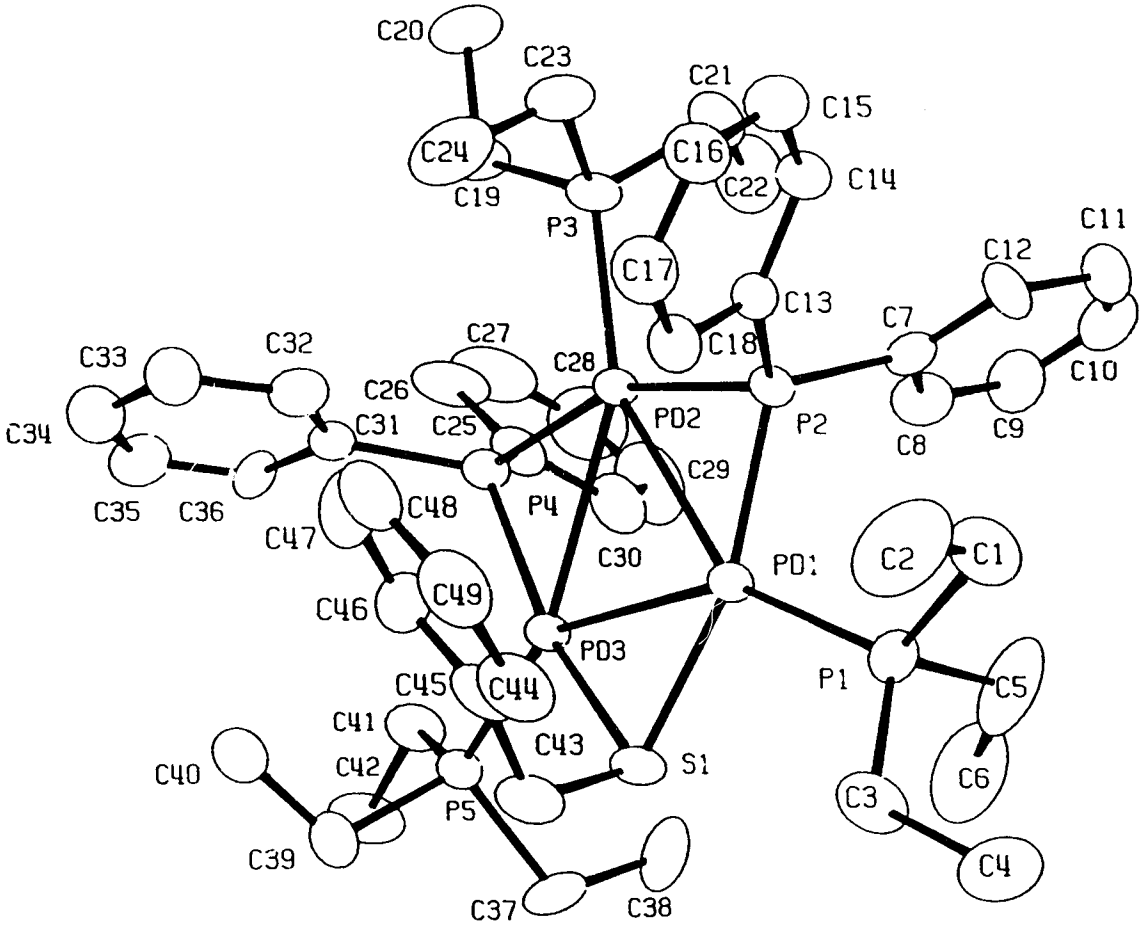

Table 2-1

Crystallographic Parameters for
$[Pd_3(\mu\text{-}SCH_2Ph)(\mu\text{-}PPh_2)_2(PEt_3)_3][BF_4]$

formula	$C_{49}H_{72}BF_4P_5Pd_3S$
fw	1254
space group	$P2_1/c$
a (Å)	16.689(5)
b (Å)	19.739(5)
c (Å)	17.078(3)
α (degrees)	90.00
β (degrees)	97.86(4)
ɣ (degrees)	90.00
volume ($Å^3$)	5573
Z	4
calculated density (g/cm^3)	1.4945
μ (cm^{-1})	11.67
radiation (Å)	Mo 0.71069
temperature (K)	295
scan method	$\omega/2\theta$
total reflections collected	5026
parameters refined	568
R	0.0542
R_w	0.0543

Table 2-2

Selected Bond Lengths(Å) and Angles(°) for $[Pd_3(\mu\text{-}SCH_2Ph)(\mu\text{-}PPh_2)_2(PEt_3)_3][BF_4]$

Atoms	Distance
Pd(2)-Pd(3)	2.953(1)
Pd(2)-Pd(1)	2.977(1)
Pd(3)-Pd(1)	2.924(1)
P(3)-Pd(2)	2.293(3)
P(5)-Pd(3)	2.282(3)
P(1)-Pd(1)	2.273(3)
P(4)-Pd(2)	2.268(3)
P(4)-Pd(3)	2.237(3)
P(2)-Pd(2)	2.265(3)
P(2)-Pd(1)	2.231(3)
S(1)-Pd(3)	2.355(1)
S(1)-Pd(1)	2.354(3)

Atoms	Angle
Pd(3)-Pd(2)-Pd(1)	59.1(1)
Pd(2)-Pd(3)-Pd(1)	60.9(1)
Pd(2)-Pd(1)-Pd(3)	60.0(1)
Pd(3)-S(1)-Pd(1)	76.8(1)
Pd(2)-P(4)-Pd(3)	81.9(1)
Pd(2)-P(2)-Pd(1)	82.9(1)
P(4)-Pd(2)-Pd(3)	48.6(1)
P(2)-Pd(2)-Pd(1)	48.1(1)
P(2)-Pd(1)-Pd(2)	49.0(1)
P(4)-Pd(3)-Pd(2)	49.5(1)
Pd(1)-Pd(3)-S(1)	51.6(1)
P(5)-Pd(1)-S(1)	104.1(1)
P(3)-Pd(2)-P(4)	100.7(1)
P(5)-Pd(3)-P(4)	102.9(1)
P(1)-Pd(1)-P(2)	101.3(1)
P(5)-Pd(3)-S(1)	95.8(1)
P(1)-Pd(1)-S(1)	98.0(1)

(Estimated standard deviations are given in parentheses.)

shorter bonds are essentially trans to the μ-SCH_2Ph group (P-Pd-S angle averages 161°).

$[Pd_3(\mu\text{-}Se)(\mu\text{-}PPh_2)_2(PEt_3)_3]$ was prepared by the reaction of $[Pd_3(\mu\text{-}Cl)(\mu\text{-}PPh_2)_2((PEt_3)_3]$ with excess Na_2Se. It proved to be very unstable and was only characterized by $^{31}P\{^1H\}$ NMR spectroscopy. Attempts to protonate and alkylate this μ-Se complex failed.

Reactions of $[Pt_3(\mu\text{-}H)(\mu\text{-}PPh_2)_2(PPh_3)_3]^+$:

Reaction of HCl with $[Pt_3(\mu\text{-}H)(\mu\text{-}PPh_2)_2(PPh_3)_3]^+$ in methanol proceeds quantitatively to yield the chloride-bridged species $[Pt_3(\mu\text{-}Cl)(\mu\text{-}PPh_2)_2(PPh_3)_3]^+$.

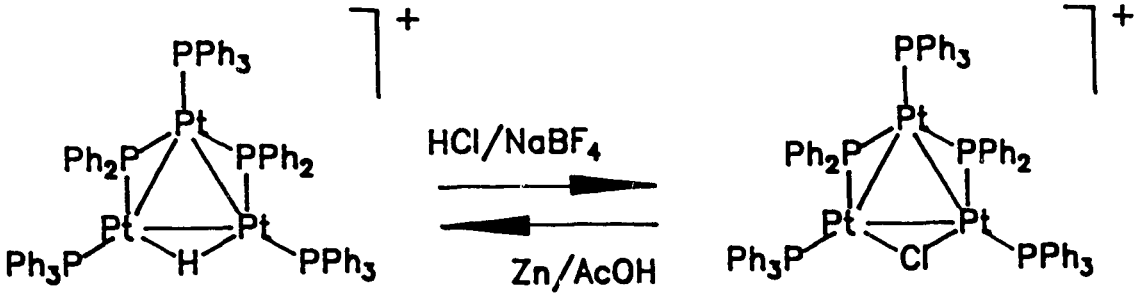

The $^{31}P\{^1H\}$ NMR spectrum of this compound is shown in figure **2-4**. The spectrum is basically first order and most of the parameters may be extracted directly from the spectrum. For

Figure 2-4

The $^{31}P\{^{1}H\}$ NMR Spectrum of
$[Pt_3(\mu\text{-}Cl)(\mu\text{-}PPh_2)_2(PPh_3)_3][BF_4]$

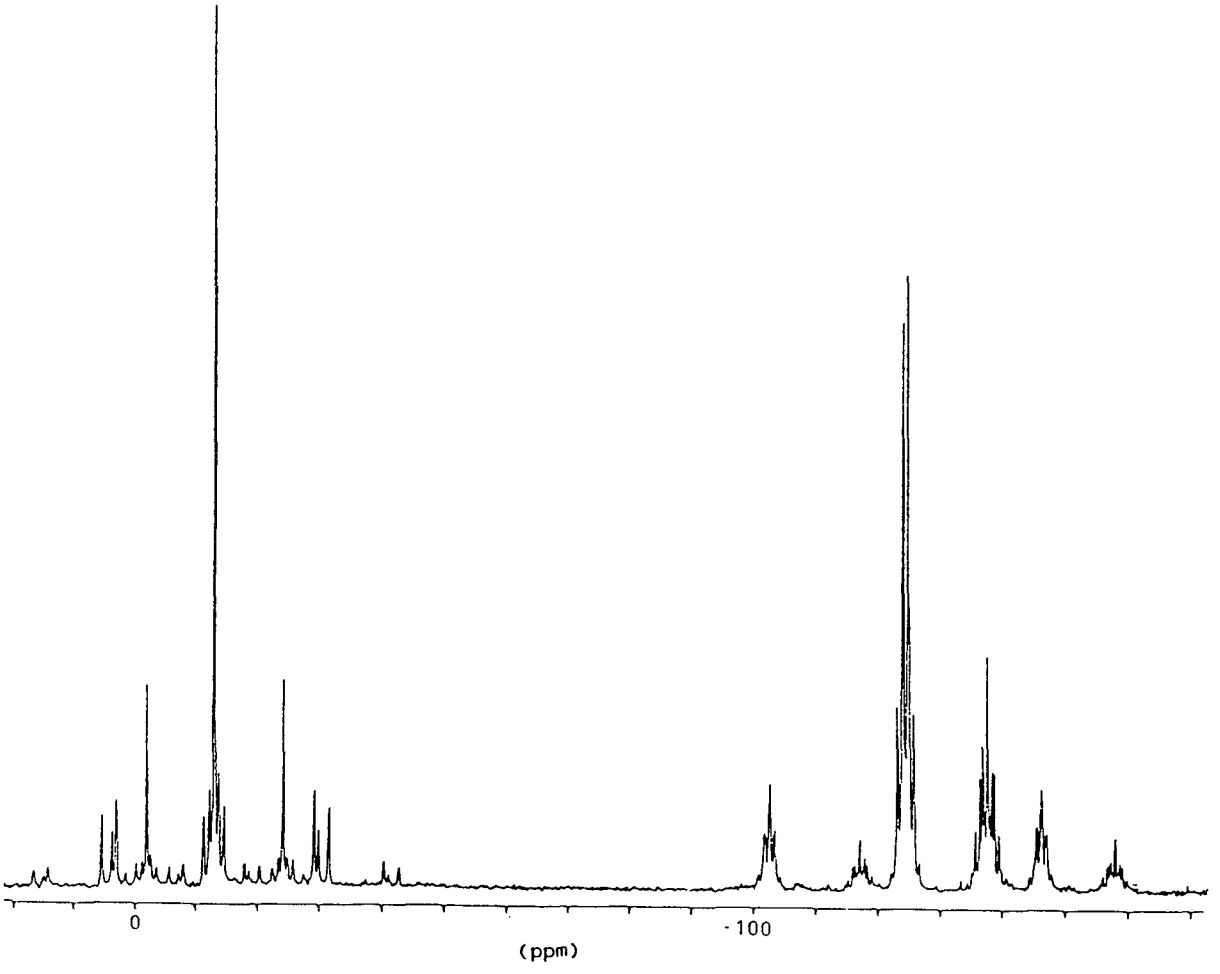

initial interpretation, only the isotopomers with zero and one ^{195}Pt are considered since they constitute about 75% of the total composition. For a complete analysis, however, all the isotopomers shown in figure **2-5** must be considered. In the case with no spin-active platinum (isotopomer A), the spectrum clearly shows the presence of three types of phosphorus. The peak at -13.1 ppm belongs to the μ-PPh_2 phosphorus. The doublet at -124.6 ppm and the triplet at -137.9 ppm belong to the two equivalent and one unique terminal phosphines respectively coupling to each other with a coupling constant of 76 Hz. The major sidebands in the low-field region of the spectrum may be explained as follows: coupling of the μ-PPh_2 phosphorus with the unique platinum in isotopomer C gives rise to a doublet with a coupling constant of 2265 Hz. When one of the other platinums is spin-active (as in isotopomer B), the two μ-PPh_2 phosphorus become different, leading to two sets of doublets (coupling between the now two different phosphido bridges with the coupling constant of 243 Hz) of doublets as sidebands. The one-bond and two-bond phosphorus-platinum coupling constants are 3523 Hz and 95 Hz respectively. For the peak at -124.6 ppm, isotopomer B gives the principal side-band with a one-bond platinum-phosphorus coupling constant of 4406 Hz. The three-bond phosphorus-phosphorus coupling constants between the unique PPh_3 and

Figure 2-5

Isotopomers of $[Pt_3(\mu\text{-}Cl)(\mu\text{-}PPh_2)_2(PPh_3)_3][BF_4]$ with Their Relative Abundances

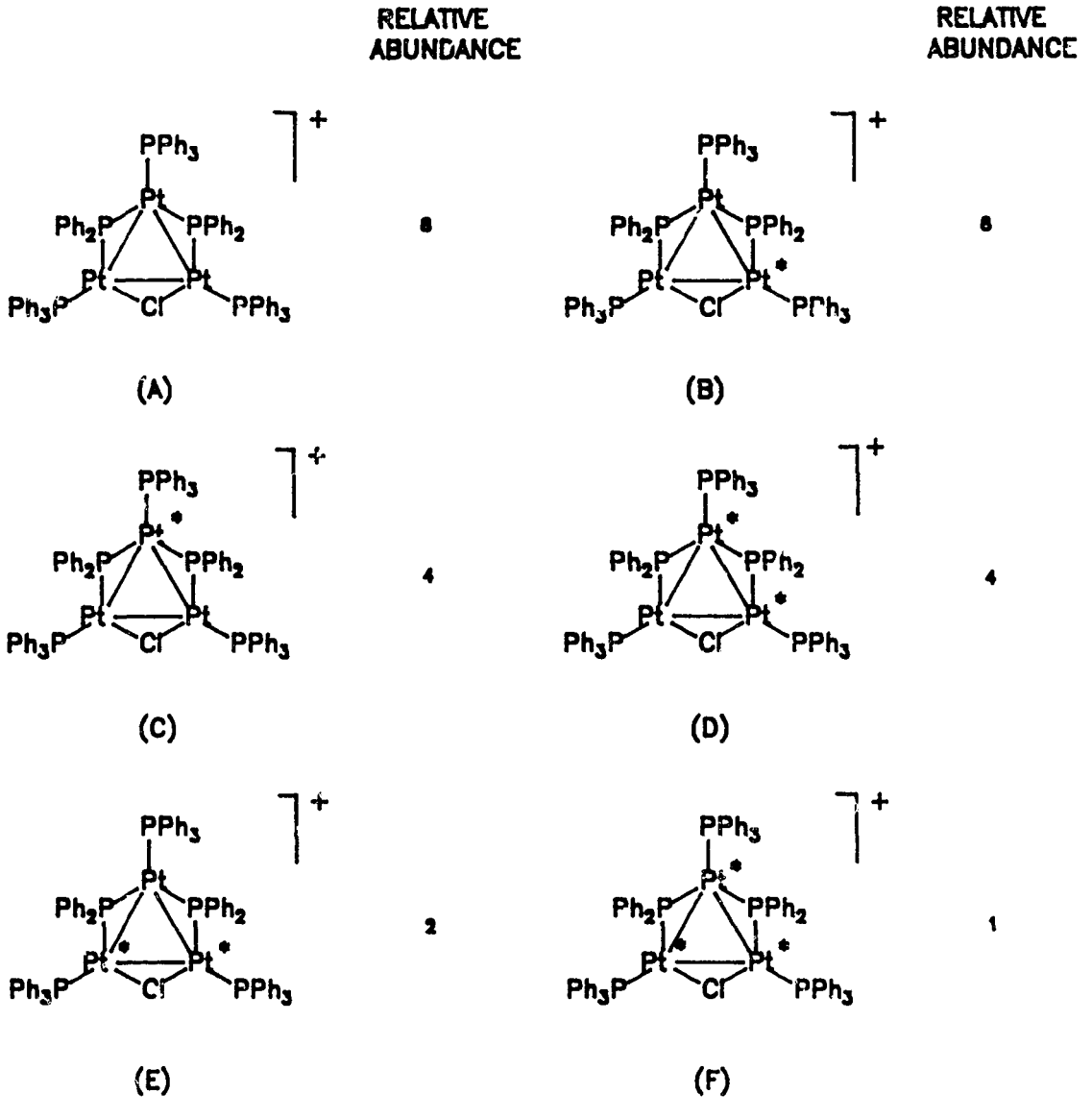

one of the equivalent PPh_3, and between the two equivalent terminal PPh_3 are similar in magnitude and in consequence the side-bands appear almost as triplets with poorly resolved fine structure. The side-bands for the triplet peak at -137.9 ppm are two sets of triplets (with the one-bond and two-bond phosphorus-platinum coupling constants of 4143 Hz and 233 Hz) from isotopomers B and C. The spectrum was simulated using the parameters summarized in chapter seven of this thesis. Isotopomer F was neglected because of its low abundance and complex spin system which leads to many very low intensity lines.

The $^{195}Pt\{^1H\}$ NMR spectrum of $[Pt_3(\mu\text{-}Cl)(\mu\text{-}PPh_2)_2(PPh_3)_3][BF_4]$ is shown in figure **2-6**. The major features of the spectrum may be assigned to the isotopomers with one spin-active platinum. The peak at higher field is a doublet of triplets of triplets arising from isotopomer C. Isotopomer D also contributes to this multiplet. In this isotopomer, the unique platinum, in addition to the three types of phosphorus present, is coupled to the other spin-active platinum with a coupling constant of 651 Hz which gives rise to a doublet of doublets of triplets of triplets. The low-field multiplet is a doublet of doublets of doublets of doublets of doublets belonging to the ^{195}Pt in isotopomer B coupling to five different phosphorus. The contribution

Figure 2-6

The $^{195}Pt\{^{1}H\}$ NMR spectrum of $[Pt_3(\mu\text{-}Cl)(\mu\text{-}PPh_2)_2(PPh_3)_3][BF_4]$

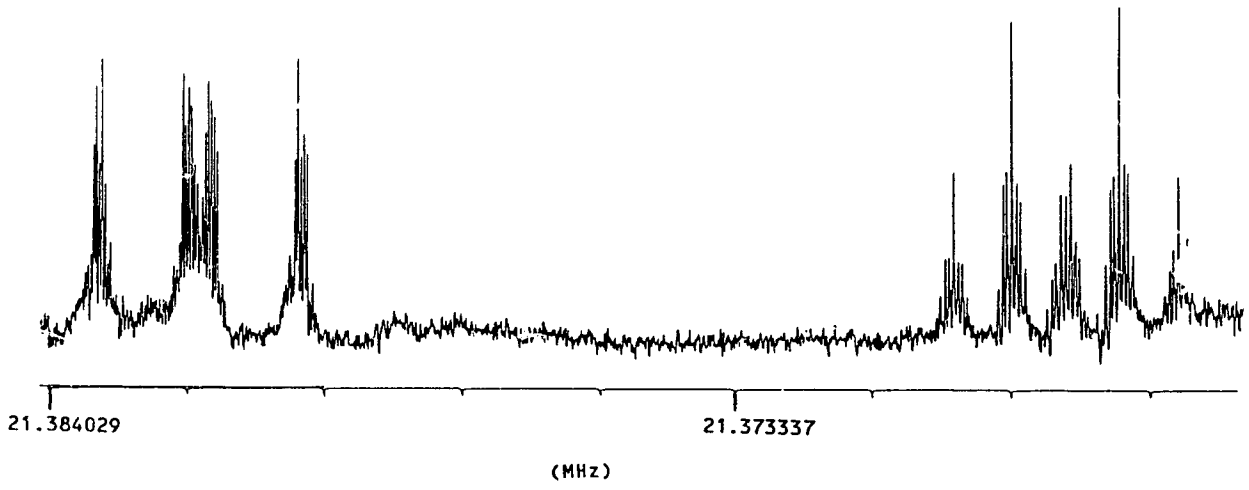

of isotopomer D to this multiplet is not intense enough to be clearly observed. The coupling constants agree well with the values obtained from the $^{31}P\{^{1}H\}$ NMR spectrum.

$[Pt_3(\mu\text{-}Cl)(\mu\text{-}PPh_2)_2(PPh_3)_3][BF_4]$ may be converted back to original μ-H cluster by its reaction with Zn/AcOH in methanol. An attempt to prepare the hydride-bridged palladium cluster in a similar fashion by reducing $[Pd_3(\mu\text{-}Cl)(\mu\text{-}PPh_2)_2(PPh_3)_3]^+$ with Zn/MeOH/AcOH failed. Of the many products formed, the only one isolated was the previously reported fully symmetrical $[Pd_3(\mu\text{-}PPh_2)_3(PPh_3)]^+$ cluster, as established by $^{31}P\{^{1}H\}$ NMR spectroscopy.

A suitable crystal of $[Pt_3(\mu\text{-}Cl)(\mu\text{-}PPh_2)_2(PPh_3)_3][BF_4]$ was obtained and its crystal structure was determined by Dr. Browning (figure **2-7**). Table **2-3** lists the relevant crystallographic parameters. Table **2-4** contains a list of selected bond lengths and angles. The structure is similar to the μ-H starting cluster and the μ-Cl palladium analogue. All the platinums and the other ligands lie in a plane with minor deviations from planarity. The platinum-platinum bond lengths are 2.914Å, 2.906Å, and 2.849Å. Since the trans influence of μ-PPh_2 is greater than μ-Cl to a larger extent than it is over μ-SCH_2Ph , the asymmetry in the μ-PPh_2 phosphorus-platinum bond lengths is more

Figure 2-7

The Molecular Structure of
$[Pt_3(\mu\text{-}Cl)(\mu\text{-}PPh_2)_2(PPh_3)_3][BF_4]$

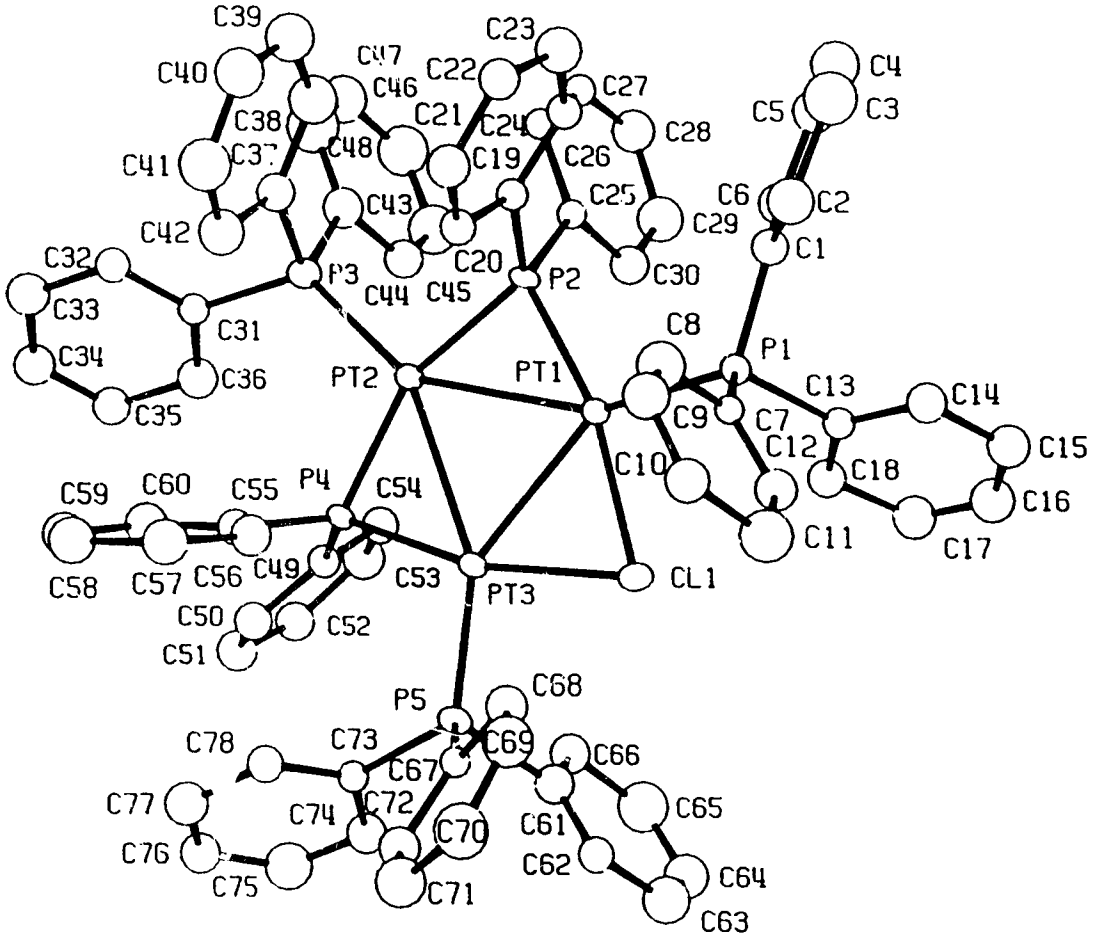

Table 2-3

Crystallographic Parameters for
$[Pt_3(\mu\text{-}Cl)(\mu\text{-}PPh_2)(PPh_3)_3[BF_4]$

formula	$C_{78}H_{65}BClF_4P_5Pt_3$
fw	1865
space group	$P2_1/c$
a (Å)	15.240
b (Å)	17.118
c (Å)	27.541
α (degrees)	90.0
β (degrees)	93.25
ϒ (degrees)	90.00
volume ($Å^3$)	7173
Z	4
calculated density (g/cm^3)	1.7267
μ (cm^{-1})	57.84
radiation (Å)	Mo 0.71069
temperature (K)	295
scan method	ω/2θ
total reflections collected	4577
parameters refined	376
R	0.0680
R_w	0.0667

Table 2-4

Selected Bond Lengths(Å) and Angles(°) for $[Pt_3(\mu\text{-}Cl)(\mu\text{-}PPh_2)_2(PPh_3)_3][BF_4]$

Atoms	Distance
Pt(2)-Pt(3)	2.914(1)
Pt(2)-Pt(1)	2.906(1)
Pt(3)-Pt(1)	2.849(1)
P(3)-Pt(2)	2.260(7)
P(5)-Pt(3)	2.243(7)
P(1)-Pt(1)	2.271(7)
P(4)-Pt(2)	2.266(6)
P(4)-Pt(3)	2.192(6)
P(2)-Pt(2)	2.279(6)
P(2)-Pt(1)	2.200(7)
Cl(1)-Pt(3)	2.420(7)
Cl(1)-Pt(1)	2.415(7)

Atoms	Angle
Pt(3)-Pt(2)-Pt(1)	58.6(1)
Pt(2)-Pt(3)-Pt(1)	60.5(1)
Pt(2)-Pt(1)-Pt(3)	60.8(1)
Pt(3)-Cl(1)-Pt(1)	72.2(2)
Pt(2)-P(4)-Pt(3)	81.6(2)
Pt(2)-P(2)-Pt(1)	80.9(2)
P(4)-Pt(2)-Pt(3)	48.1(2)
P(2)-Pt(2)-Pt(1)	48.4(2)
P(2)-Pt(1)-Pt(2)	50.7(2)
P(4)-Pt(3)-Pt(2)	50.3(2)
Pt(1)-Pt(3)-Cl(1)	53.8(2)
P(5)-Pt(1)-Cl(1)	54.0(2)
P(3)-Pt(2)-P(4)	105.8(2)
P(3)-Pt(2)-P(2)	99.2(3)
P(5)-Pt(3)-P(4)	104.4(2)
P(1)-Pt(1)-P(2)	104.2(2)
P(5)-Pt(3)-Cl(1)	91.5(2)
P(1)-Pt(1)-Cl(1)	90.4(1)

(Estimated standard deviations are given in parentheses.)

pronounced here than in the $[Pd_3(\mu\text{-}SCH_2Ph)(\mu\text{-}PPh_2)_2(PEt_3)_3][BF_4]$ cluster mentioned earlier (P(4)-Pt(2), 2.266Å; P(4)-Pt(3), 2.192Å). Later in this chapter, a more detailed comparison of the structural variations of these clusters will be presented.

The reactivity of the chloride bridge in $[Pt_3(\mu\text{-}Cl)(\mu\text{-}PPh_2)_2(PPh_3)_3][BF_4]$ now can be utilized to synthesize various platinum clusters with different bridging groups similar to $[Pd_3(\mu\text{-}Cl)(\mu\text{-}PPh_2)_2(PPh_3)_3]^+$. The μ-Cl in $[Pt_3(\mu\text{-}Cl)(\mu\text{-}PPh_2)_2(PPh_3)_3]^+$ can be replaced by other halides (Br, I) to give quantitavely $[Pt_3((\mu\text{-}Br)(\mu\text{-}PPh_2)_2(PPh_3)_3]^+$ and $[Pt_3(\mu\text{-}I)(\mu\text{-}PPh_2)_2(PPh_3)_3]^+$ by reacting the μ-Cl cluster with the corresponding salts (KBr, KI).

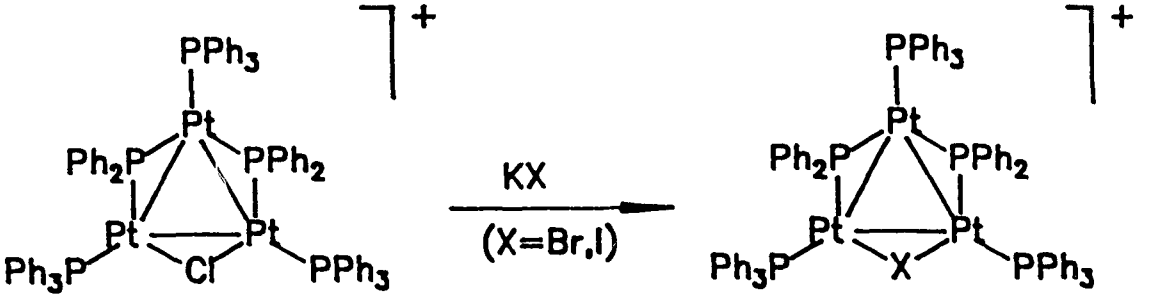

These complexes were characterized by $^{31}P\{^1H\}$ NMR spectroscopy and elemental analysis. $^{31}P\{^1H\}$ NMR spectra of these compounds have exactly the same pattern as the μ-Cl

case but with different chemical shifts and coupling constants (for values see chapter seven). $[Pt_3(\mu\text{-}I)(\mu\text{-}PPh_2)_2(PPh_3]^+$ may also be prepared from the reaction of $[Pt_3(\mu\text{-}H)(\mu\text{-}PPh_2)_2(PPh_3)_3]^+$ with excess CH_3I. This was confirmed by $^{31}P\{^1H\}$ NMR spectroscopy. $[Pt_3(\mu\text{-}H)(\mu\text{-}PPh_2)_2(PPh_3)_3]^+$ does not, however, react with other halohydrocarbons such as $PhCH_2Br$, CH_2I_2.

Reaction of $[Pt_3(\mu\text{-}Cl)(\mu\text{-}PPh_2)_2(PPh_3)]^+$ with excess Na_2S in methanol yields the neutral, benzene soluble cluster, $[Pt_3(\mu\text{-}S)(\mu\text{-}PPh_2)_2(PPh_3)_3]$. Similar to the μ-S in $[Pd_3(\mu\text{-}S)(\mu\text{-}PPh_2)_2(PPh_3)_3]$, the bridging sulphide in $[Pt_3(\mu\text{-}S)(\mu\text{-}PPh_2)_2(PPh_3)_3]$ is nucleophilic and susceptible to an electrophilic attack. This quality was exploited to prepare $[Pt_3(\mu\text{-}SR)(\mu\text{-}PPh_2)_2(PPh_3)_3]^+$ (R= H, CH_3, CH_2Ph), by reacting the μ-S cluster with $HBF_4 \cdot Et_2O$, CH_3I, and $BrCH_2Ph$ respectively. All of these reactions proceed cleanly and quantitatively.

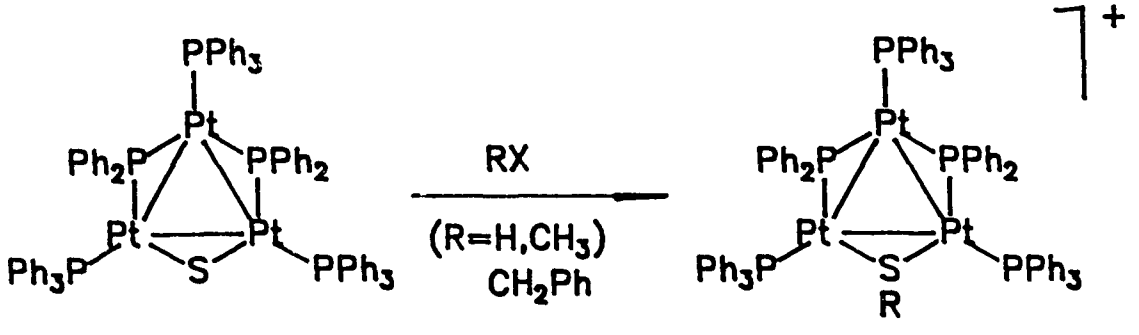

Again the $^{31}P\{^{1}H\}$ NMR spectra are similar to the previous cases but with different chemical shifts and coupling constants (for values see chapter seven). Other examples of this type of reaction were provided in the previous section.

The reaction of $[Pt_3(\mu\text{-}Cl)(\mu\text{-}PPh_2)_2(PR_3)_3]^+$ (R= Ph, Et) with one equivalent of PPh_2H in the presence of a base (p-toluidine) affords the symmetrical clusters, $[Pt_3(\mu\text{-}PPh_2)_3(PR_3)_3]^+$ (R= Ph, Et), in quantitative yields. In the reaction of the triphenylphosphine analogue stoichiometry is very important as addition of excess PPh_2H leads to the substitution of triphenylphosphines.

The $^{31}P\{^{1}H\}$ NMR spectrum of the PEt_3 derivative, $[Pt_3(\mu\text{-}PPh_2)_3(PEt_3)_3]^+$, is shown in figure 2-8. The isotopomers with no, and one spin-active platinum account for the major features of the spectrum. In the case of the isotopomer with no ^{195}Pt, the singlet peak at -56.8 ppm corresponds to the three equivalent phosphido bridges, and the singlet peak

Figure 2-8

The $^{31}P\{^{1}H\}$ NMR Spectrum of
$[Pt_3(\mu\text{-}PPh_2)_3(PEt_3)_3][BF_4]$

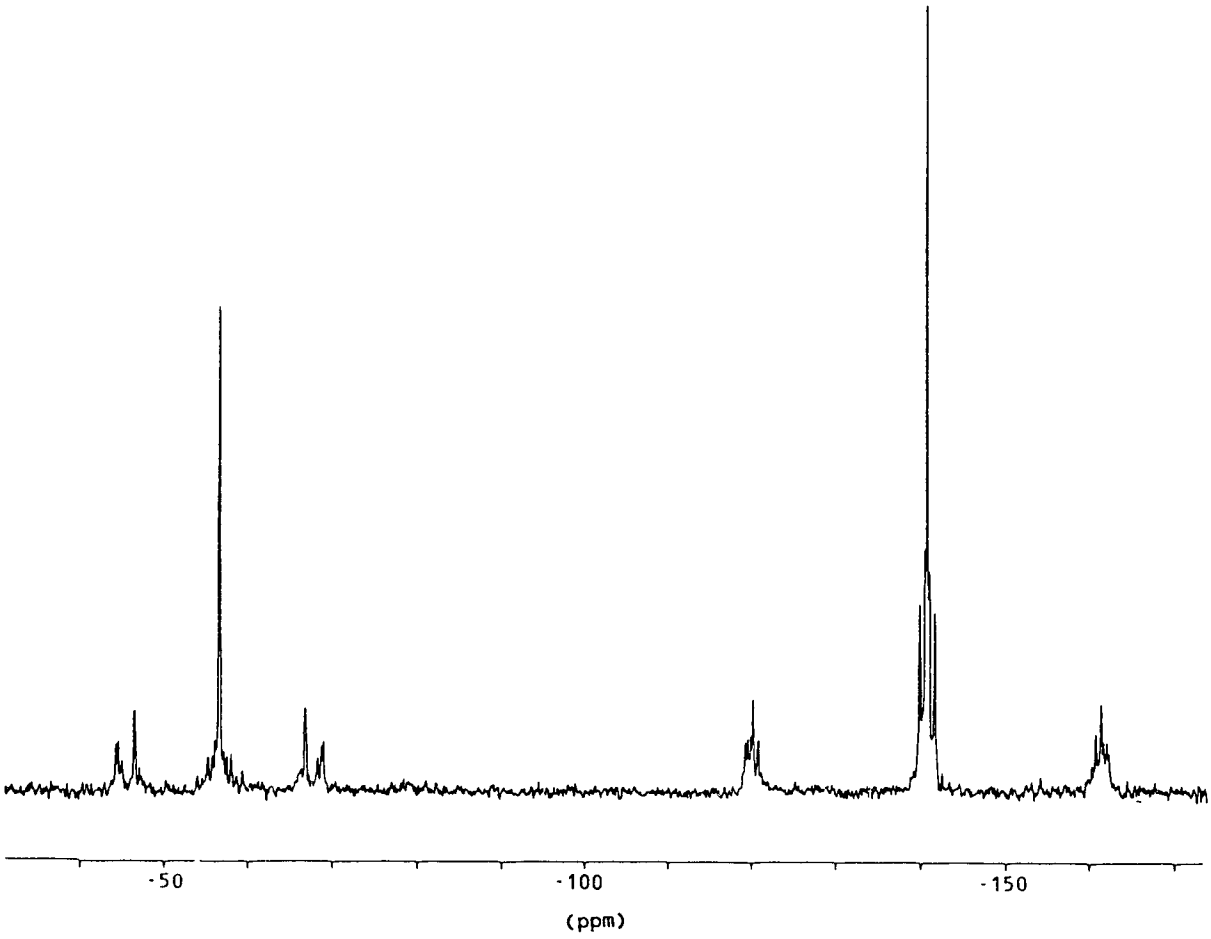

at -141.1 ppm belongs to the three terminal phosphines. The major sideband for the low-field peak is a doublet of doublets arising from the isotopomer with one spin-active platinum. The platinum-phosphorus coupling constant is 2057 Hz. The sidebands for the peak at -141.1 ppm are two sets of peaks. The first is a doublet of triplets from coupling of the the now unique terminal phosphine with the spin-active platinum and the equivalent terminal triethylphosphines. The coupling constants are 4178 Hz and 64 Hz. The two-bond coupling of the equivalent terminal phosphines with platinum and their coupling to the unique phosphine gives rise to the other sideband as a doublet of doublets. The two-bond platinum-phosphorus coupling constant is 115 Hz.

Figure **2-9** shows the $^{195}Pt\{^{1}H\}$ NMR spectrum of $[Pt_3(\mu\text{-}PPh_2)_3(PEt_3)_3]^+$. The spectrum is a doublet of triplets of doublets of triplets corresponding to the isotopomer with one spin-active platinum. The two-bond platinum-phosphorus coupling between the two equivalent terminal phosphines and the unique phosphido bridge with the spin-active platinum are similar in magnitude which causes one of the doublet of triplets to appear almost as a quartet.

In all cases, the terminal triphenylphosphines are labile

Figure 2-9

The $^{195}Pt\{^{1}H\}$ NMR Spectrum of
$[Pt_3(\mu\text{-}PPh_2)_3(PEt_3)_3][BF_4]$

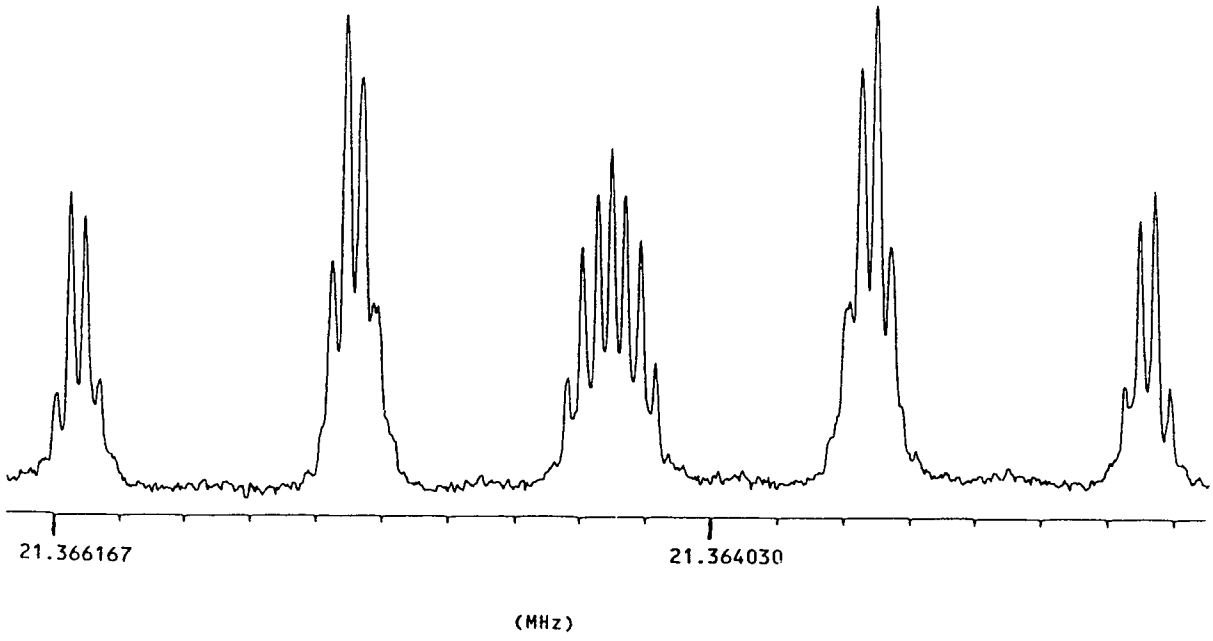

and may be substituted by more basic phosphines.

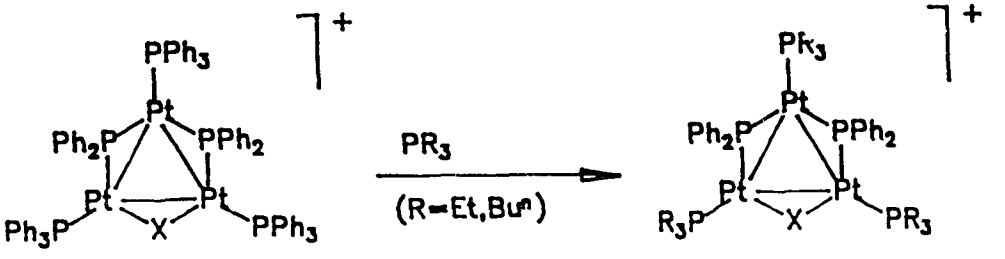

The PEt_3 and $PBu^n{}_3$ analogues of some of the clusters were prepared (see chapter seven). In these phosphine substitution reactions, stoichiometry appears to be very important especially to clusters with weak bridges (e.g. H, Cl). For example, addition of excess PEt_3 to $[Pt_3(\mu\text{-}X)(\mu\text{-}PPh_2)_2(PPh_3)_3]^+$ (X= H, Cl) affords principally $[Pt_3(\mu\text{-}PPh_2)_3(PEt_3)_3]^+$, rather than the simple substitution product. This is in contrast to $[Pd_3(\mu\text{-}Cl)(\mu\text{-}PPh_2)_2(PPh_3)_3]^+$, where addition of excess PEt_3 yields only the substituted product, $[Pd_3(\mu\text{-}Cl)(\mu\text{-}PPh_2)_2(PEt_3)_3]^+$. In the case of the μ-Cl platinum cluster, the mechanism of the reaction probably involves fragmentation of the cluster with the subsequent rearrangement of one of the terminal triphenylphosphines to the bridging position. The other products were not identified. In the case of clusters with stronger bridging units such as $\mu\text{-}PPh_2$ in $[Pt_3(\mu\text{-}$

$PPh_2)_3(PPh_3)_3]^+$ and μ-SCH_3 in $[Pt_3(\mu\text{-}SCH_3)(\mu\text{-}PPh_2)_2(PPh_3)_3]^+$, addition of excess PEt_3 only produces the trisubstituted product in quantitative yield.

A suitable crystal of the PEt_3 analogue of the μ-Cl cluster, $[Pt_3(\mu\text{-}Cl)(\mu\text{-}PPh_2)_2(PEt_3)_3][BF_4]$, was obtained and its crystal structure was solved by Dr. J. Browning. An ORTEP diagram of the structure is shown in figure **2-10**. Table **2-5** contains the relevant crystallographic parameters. A list of selected bond lengths and angles may be found in table **2-6**. The structure is essentially the same as $[Pt_3(\mu\text{-}Cl)(\mu\text{-}PPh_2)_2(PPh_3)_3][BF_4]$. The platinum-phosphorus bond lengths are slightly shorter which reflect the stronger bonding of the PEt_3 groups to the platinums. Out of plane distortions in this cluster are less than the PPh_3 analogue, and are presumably due to the lesser steric requirements of the ethyl group compared to those of a phenyl group.

The most notable and characteristic feature of the $^{31}P\{^1H\}$ NMR spectra of the clusters discussed in this chapter is the chemical shift of the μ-PPh_2 group. This shift is very sensitive to the electron donating ability of the μ-X ligand and the terminal phosphines. The more electron donating the μ-X or the terminal phosphine the lower the chemical shift of the phosphido bridge. For example, the μ-PPh_2 chemical

Figure 2-10

The Molecular Structure of
$[Pt_3(\mu\text{-}Cl)(\mu\text{-}PPh_2)_2(PEt_3)_3][BF_4]$

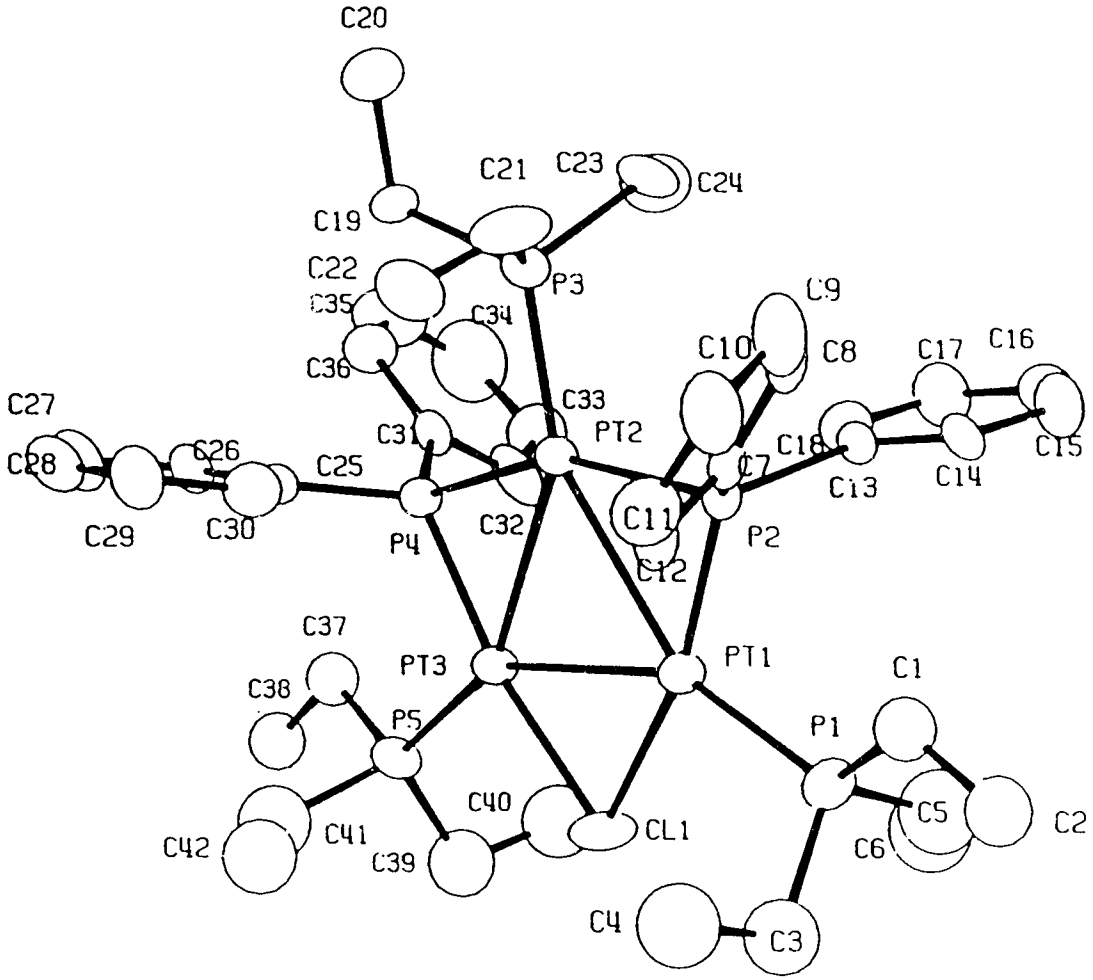

Table 2-5

Crystallographic Parameters for
$[Pt_3(\mu\text{-}Cl)(\mu\text{-}PPh_2)_2(PEt_3)_3][BF_4]$

formula	$C_{42}H_{65}BClF_4P_5Pt_3$
fw	1432
space group	$P2_1/c$
a (Å)	15.390(5)
b (Å)	14.808(3)
c (Å)	24.764(5)
α (degrees)	90.00
β (degrees)	103.32(2)
ϒ (degrees)	90.00
volume ($Å^3$)	5492
Z	4
calculated density (g/cm^3)	1.820
μ (cm^{-1})	79.35
radiation (Å)	Mo 0.71009
temperature (K)	295
scan method	ω/2θ
total reflections collected	4105
parameters refined	500
R	0.0502
R_w	0.0521

Table 2-6

Selected Bond Lengths(Å) and Angles(°) for $[Pt_3(\mu\text{-}Cl)(\mu\text{-}PPh_2)_2(PEt_3)_3][BF_4]$

Atoms	Distance
Pt(2)-Pt(3)	2.921(1)
Pt(2)-Pt(1)	2.916(1)
Pt(3)-Pt(1)	2.860(1)
P(3)-Pt(2)	2.258(5)
P(5)-Pt(3)	2.264(5)
P(1)-Pt(1)	2.264(6)
P(4)-Pt(2)	2.259(4)
P(4)-Pt(3)	2.186(5)
P(2)-Pt(2)	2.263(5)
P(2)-Pt(1)	2.186(5)
Cl(1)-Pt(3)	2.401(6)
Cl(1)-Pt(1)	2.406(6)

Atoms	Angle
Pt(3)-Pt(2)-Pt(1)	58.7(1)
Pt(2)-Pt(3)-Pt(1)	60.6(1)
Pt(2)-Pt(1)-Pt(3)	60.7(1)
Pt(3)-Cl(1)-Pt(1)	73.0(2)
Pt(2)-P(4)-Pt(3)	82.2(2)
Pt(2)-P(2)-Pt(1)	81.9(1)
P(4)-Pt(2)-Pt(3)	47.8(1)
P(2)-Pt(2)-Pt(1)	47.9(1)
P(2)-Pt(1)-Pt(2)	50.2(1)
P(4)-Pt(3)-Pt(2)	50.0(1)
Pt(1)-Pt(3)-Cl(1)	53.6(1)
P(5)-Pt(1)-Cl(1)	53.4(1)
P(3)-Pt(2)-P(4)	104.7(2)
P(3)-Pt(2)-P(2)	101.4(2)
P(5)-Pt(3)-P(4)	102.3(2)
P(1)-Pt(1)-P(2)	102.6(2)
P(5)-Pt(3)-Cl(1)	93.7(2)
P(1)-Pt(1)-Cl(1)	93.3(2)

(Estimated standard deviations are given in parentheses.)

shifts in $[Pt_3(\mu\text{-}X)(\mu\text{-}PPh_2)_2(PPh_3)_3]^{n+}$ vary from 14.2 ppm for X=I to -47.8 ppm for X= S (X= Br, -2.0 ppm; X= Cl, -13.2 ppm; X= SMe, -28.4 ppm). The effect of the terminal phosphines may be observed in the following set of complexes: $[Pt_3(\mu\text{-}SMe)(\mu\text{-}PPh_2)_2(PR_3)_3]^+$ (R= Ph, -28.4 ppm; R= Et, -45.9 ppm; R= Bu^n, -46.5 ppm). Even though theoretical treatments of $^{31}P\{^1H\}$ chemical shifts are not yet sophisticated enough to explain these trends, a simple qualitative argument may be used to explain them. The more electron donating ligands increase the electron density at the metal centers which in turn perturb the metal-phosphido bridge interaction. This causes an increase in the diamagnetic contribution to the shielding of the phosphorus which causes the resonance to move to higher field.

The chemical shift of the $\mu\text{-}PPh_2$ also decreases upon an increase in the atomic number of the metal. This effect is readily observable by comparing the $\mu\text{-}PPh_2$ shifts in $[Pd_3(\mu\text{-}Cl)(\mu\text{-}PPh_2)_2(PPh_3)_3]^+$ (80.7 ppm), $[PtPd_2(\mu\text{-}Cl)(\mu\text{-}PPh_2)_2(PPh_3)_3]^+$ (61.7 ppm), and $[Pt_3(\mu\text{-}Cl)(\mu\text{-}PPh_2)_2(PPh_3)_3]^+$ (-13.2 ppm). The crystal structures for these compounds indicate that there are no major differences in their bond lengths and angles. Therefore, any change in the phosphido bridge chemical shift is solely due to the changing of the metal. The more electron rich metal, platinum, increases

the diamagnetic contributions to the chemical shift which has a shielding effect on the phosphorus nucleus.

Structural considerations:

Although currently there is no detailed understanding of the electronic structure and bonding in metal clusters, some simple theories based on symmetry arguments and semi-empirical molecular orbital calculations have been developed to rationalize and predict cluster structures. The polyhedral skeletal electron pair theory has been the most successful to date.[60-63] Its name is derived from the correspondence between the number of electron pairs available and the number of metal-metal bonds formed. The polyhedral skeletal electron pair approach is by no means a replacement for accurate molecular orbital calculations, but it provides a simple way to explain and understand the different structures of polynuclear compounds.

This theory is based on the idea that the total electron count in a cluster is decided by the number of antibonding skeletal molecular orbitals derived from the atomic orbitals of metal atoms in the cluster unit. These antibonding molecular orbitals are unavailable for either metal-ligand or metal-metal skeletal bonding because of their high-lying

nature; consequently, setting an upper limit on the total electron count for a particular polyhedral arrangement. In other words, it is possible for many cluster compounds to relate the geometry to the number of electron pairs required to fill all the bonding metal-metal molecular orbitals.

The most convenient way to determine the number of orbitals and electrons available for metal-metal skeletal bonding is first to break up the cluster into suitable fragments. The orbital requirements for bonding within the fragments are determined and the remaining orbitals, frontier orbitals, are used for metal-metal bonding. This method is called fragment analysis.[64] For polynuclear complexes with up to four metals, it is possible to consider each metal-metal bond, a polyhedral edge, as a two-electron/two-center bond. Each cluster fragment, therefore, contributes the same number of atomic orbitals and electrons as the number of bonds it forms. Based on the polyhedral skeletal electron pair theory, a triangle of metal atoms would require 48 electrons to be stable.

All the clusters presented in this chapter, however, with the exception of $[Pt_3(\mu\text{-}H)(\mu\text{-}PPh_2)_2(PPh_3)_3]^+$ which has 42 electrons, have 44 electrons. A qualitative explanation for this discrepancy is as follows: for palladium and platinum

metals, the s(d)-p orbital separation becomes important. One of the p orbitals becomes too high in energy to be available for bonding within the fragment. On this basis, one would expect a triangle of palladium or platinum atoms to require 42 electrons to be stable. That p-orbital however, must be considered when the different fragments are brought together to form the cluster. The three p-orbitals on each metal interact to generate one bonding and two antibonding orbitals. Therefore, two additional electrons are required to fill this bonding molecular orbital and to stabilize the cluster.

Molecular orbital calculations on model compounds support the qualitative explanation and show that for triangular phosphido-bridged platinum clusters, there are 22 low lying orbitals.[65-66] The first nine have their wavefunctions located on the ligands and the next eleven are mainly platinum d in character. The twenty first molecular orbital has its wavefunction mainly localized on the metals and lies in the plane of the triangle making it metal-metal bonding. The last orbital is a combination of μ-PR_2 p-orbitals and in-plane metal d-orbitals. This orbital places most of the electron density on the bridging μ-PR_2 and is slightly metal-metal antibonding. The last two orbitals are of approximately the same energy. In 42-electron clusters only

up to the last orbital is filled which leaves a very small gap between HOMO and LUMO. Addition of two electrons fills the last orbital and leaves a large gap between filled and unfilled levels.

Only in a very few cases has it been possible to isolate and structurally characterize both the 42-electron and 44-electron species of a cluster. One good example is the $[Pt_3(\mu\text{-}SO_2)_3(PCy_3)_3]$ and $[Pt_3(\mu\text{-}Br)(\mu\text{-}SO_2)_2(PCy_3)_3]^-$ clusters reprted by Mingos and co-workers.[67] $[Pt_3(\mu\text{-}H)(\mu\text{-}PPh_2)_2(PPh_3)_3]^+$ (42-electron) and $[Pt_3(\mu\text{-}Cl)(\mu\text{-}PPh_2)_2(PPh_3)_3]^+$ (44-electrons) provide another good example. The easy interconversion of the two supports molecular orbital calculations in suggesting that the last two molecular orbitals are close in energy. The increase in the Pt-Pt bond length which is observed by replacing μ-H with μ-Cl (2.796Å, 2.705Å, and 2.638Å to 2.914Å, 2.906Å, and 2.849Å) provides further proof for the correctness of the calculations as the addition of two electrons is into an orbital which is slightly metal-metal anti-bonding.

In all the 44-electron clusters, $[M_3(\mu\text{-}X)(\mu\text{-}PPh_2)_2(PR_3)_3]^+$ (M= Pd, Pt; R= Ph, Et), the non-phosphido edge is always the shortest. This is probably due to the smaller steric requirement of the μ-X (X= Cl, SCH_2Ph) ligands with respect

to the phosphido bridge. There is no major change in bond lengths and angles as palladium is replaced by platinum which is expected as they have relatively the same size. Replacement of PPh_3 by PEt_3 also does not cause any major changes in the arrangement of the atoms.

CHAPTER THREE

FRAGMENTATION REACTIONS OF $[M_3(\mu\text{-}X)(\mu\text{-}PPh_2)_2(PR_3)_3][Y]$ (M= Pt, Pd) CLUSTERS

INTRODUCTION

As was mentioned in chapter one, cluster fragmentation is often the limiting factor in catalytic systems, making an understanding of such fragmentation processes of interest. Recently a few examples of cluster fragmentation have appeared in the literature.

$[Pt_3(\mu\text{-}CO)_3(PBu^t{}_2Ph)_3]$ fragments immediately when reacted with molecules such as CS_2, OCS, and S_8 to yield $[Pt_2(\mu\text{-}S)(CO)_2(PBu^t{}_2Ph)_2]$. The cluster also reacts with SO_2 to yield the fragmented product $[Pt_2(\mu\text{-}SO_2)(CO)_2(PBu^t{}_2Ph)_2]$. The μ-S dimer can be converted to the $\mu\text{-}SO_2$ dimer through its reaction with m-chloroperbenzoic acid.[68]

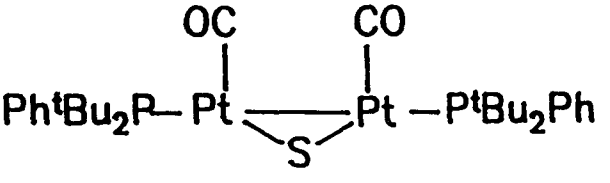

Reaction of $[Pt_3(\mu\text{-}SO_2)_3(PCy_3)_3]$ with CO leads to immediate formation of $[Pt_2(\mu\text{-}SO_2)(CO)_2(PCy_3)_2]$.[69] $[Pt_3(\mu\text{-}RNC)_3(RNC)_3]$ (R= $Bu^t{}_3C_6H_2$) reacts with olefins, actylenes, or alkyl halides to undergo fragmentation to mainly give mononuclear species.[70-71] $[Pt_3(\mu\text{-}RNC)_3(RNC)_3]$ (R= $Bu^t{}_3C_6H_2$) also fragments with CS_2 or S_8 to afford $[Pt_2(\mu\text{-}CS_2)(RNC)_4]$, and $[Pt_2(\mu\text{-}S)(RNC)_4]$ respectively.[71]

Mingos and coworkers reported that the reaction of 2,6-xylyl isocyanide with $[Pt_3(\mu\text{-}SO_2)_3(PCy_3)_3]$ results in the fragmentation of that cluster to produce $[Pt_2(\mu\text{-}SO_2)(CNC_8H_9)_2(PCy_3)_2]$.[72]

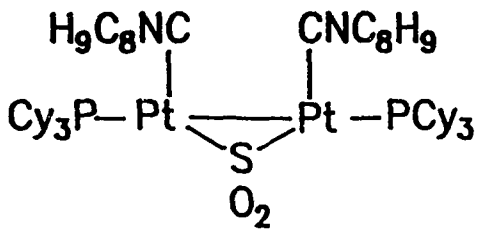

All these dinuclear platinum compounds contain a core Pt_2S triangle with the other ligands lying approximately in the same plane. The Pt-Pt distances range from 2.60Å to 2.69Å; and are within the range for Pt-Pt single bonds.

In contrast to platinum clusters, examples of fragmentation among palladium clusters are limited to one reported case. $[Pd_3(\mu\text{-}PBu^t_2)_3(CO)_2Cl]$ is fragmented by PMe_3 to yield $[Pd_2(\mu\text{-}PBu^t_2)_2(PMe_3)_2]$.[73] This reaction, however, is not very clear since the starting material was not pure. It was a mixture which included the trinuclear cluster.

In the context of utilizing ligands to prevent compound fragmentation, diphosphine ligands in general, and bis(diphenylphosphino)methane (dppm) and its analogues in

particular have been the subject of extensive studies in recent years.[74] The ability of dppm to form strong bonds with a variety of transition metals, ranging from molybdenum and tungsten to mercury, in low oxidation states, and to act as bridges between two or more metal centers has been of special importance.[75-78] These qualities, combined with the relative inertness of the diphosphine, allow reactions involving metal-metal bond cleavage and formation to take place without complex disintegration. The reduction of sulphur dioxide to sulphur monoxide and sulphur by $[Ir_2(\mu\text{-dppm})_2(CO)_2(H)_4]$, where the reaction steps involve metal-metal bond cleavage and reformation, is a good example.[79] A point to note, however, is that some recent reports show that diphosphine ligands are not always inert and are sometimes involved in the reactions occurring at the metal centers. For example, Knox and coworkers recently reported that at room temperature dppm was not involved in the reactions occurring at the metal centers in $[Fe_2(\mu\text{-CHCHCO})(\mu\text{-dppm})(CO)_5]$, but at higher temperatures participated in a variety of unique transformations.[80-81]

Another useful aspect of these ligands is that their steric and electronic nature can easily be modified by varying the substituents on the phosphorus; thus altering the activity or selectivity of the metal complex. For example,

$[Pt_2(\mu\text{-}R_2PCH_2PR_2)_2Me_4]$ (R= Ph) is not reactive towards CH_3I, but when R= Me, it oxidatively adds CH_3I.[82]

The interesting properties of diphosphine ligands combined with the cluster fragmentation reactions mentioned earlier encouraged us to investigate the reactions of the phosphido-bridged clusters discussed in chapter two with similar molecules. In the first sections of this chapter, the reactions of the triangular palladium and platinum clusters, $[M_3(\mu\text{-}X)(\mu\text{-}PPh_2)_2(PR_3)_3]^{n+}$ (M= Pd, Pt; X= H, Cl, PPh_2, SR, S; R= Ph, Et; n= 0, 1), with various diphosphine ligands, especially dppm, are discussed. The last part deals with the reaction of $[Pt_3(\mu\text{-}X)(\mu\text{-}PPh_2)_2(PR_3)_3]^+$(X= H, Cl) with Bu^tNC.

RESULTS AND DISCUSSION

Reactions of $[Pd_3(\mu\text{-}Cl)(\mu\text{-}PPh_2)_2(PR_3)_3[BF_4]$ (R= Ph, Et) with R_2PYPR_2 (R= Ph, Pr^i, OEt; Y= CH_2, O):

The addition of dppm to a solution of $[Pd_3(\mu\text{-}Cl)(PPh_2)_2(PPh_3)_3]^+$ in CH_2Cl_2 at room temperature proceeds with a series of color changes to yield two products: yellow, relatively insoluble crystals of $[Pd_2(\mu\text{-}PPh_2)(\mu\text{-}dppm)_2Cl_2]^+$; and soluble, red crystals of $[Pd_2(\mu\text{-}PPh_2)(\mu\text{-}dppm)(PPh_3)_2]^+$.

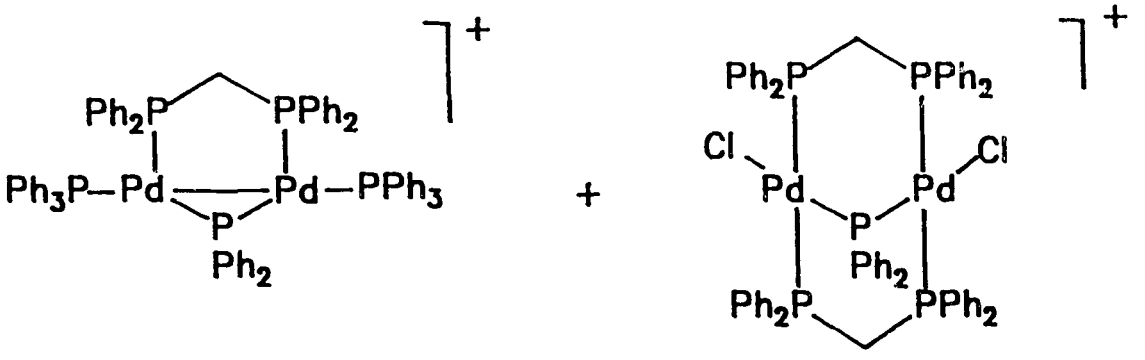

This reaction was first carried out by Nasim Hadj-Bagheri in this laboratory.[83] $[Pd_2(\mu\text{-}PPh_2)(\mu\text{-}dppm)(PPh_3)_2]^+$ is the first example of of a Pd(I) complex in which a metal-metal bond is supported by both dppm and phosphido bridges. Complexes with both these structural features are rare. Only three previous examples exist: $[Co_2(\mu\text{-}PPh_2)(\mu\text{-}dppm)(\mu\text{-}H)(CO)_4]$[84-85] and $Ru_2(\mu\text{-}PPh_2)(\mu\text{-}dppm)(\mu\text{-}Cl)(CO)_4]$.[86] The

$^{31}P\{^{1}H\}$ NMR spectrum of $[Pd_2(\mu\text{-}PPh_2)(\mu\text{-}dppm)(PPh_3)_2]^+$ is shown in figure **3-1**. It consists of three sets of signals due to the three types of phosphorus nuclei present. The highly deshielded triplet of triplets signal at 96.7 ppm is assigned to $\mu\text{-}PPh_2$ phosphorus coupling to the two terminal phosphines and the dppm ligand. The coupling constants are 32 Hz and 207 Hz. This low chemical shift indicates that the two palladium centers are bonded together. The dppm and PPh_3 resonances appear at -135.0 and -125.4 ppm respectively as deceptively simple doublet of doublets which are further split by coupling to $\mu\text{-}PPh_2$.

$[Pd_2(\mu\text{-}PPh_2)(\mu\text{-}dppm)_2Cl_2]^+$ is a rare example of a common class of compounds known as "A-frames".[87] The only other example of an "A-frame" complex with a phosphido bridge is $[Pt_2(\mu\text{-}PPh_2)(\mu\text{-}dppm)_2(H)_2]^+$, prepared previously by the reaction of $[Pt_2H_3(\mu\text{-}dppm)_2]^+$ with diphenylphosphine.[88] The $^{31}P\{^{1}H\}$ NMR spectrum of $[Pd_2(\mu\text{-}PPh_2)(\mu\text{-}dppm)_2Cl_2][BF_4]$ (figure **3-2**) consists of a quintet at -67.6 ppm ($\mu\text{-}PPh_2$) and a doublet at -129.3 ppm (dppm). The coupling constant is 11.5 Hz which is consistent with two bond phosphorus-phosphorus coupling. The highly shielded chemical shift of the $\mu\text{-}PPh_2$ signal indicates that this group is bridging two palladium centers which are not bonded. This contrasts with

Figure 3-1

The $^{31}P\{^{1}H\}$ NMR Spectrum of
$[Pd_2(\mu\text{-}PPh_2)(\mu\text{-}dppm)(PPh_3)_2][BF_4]$

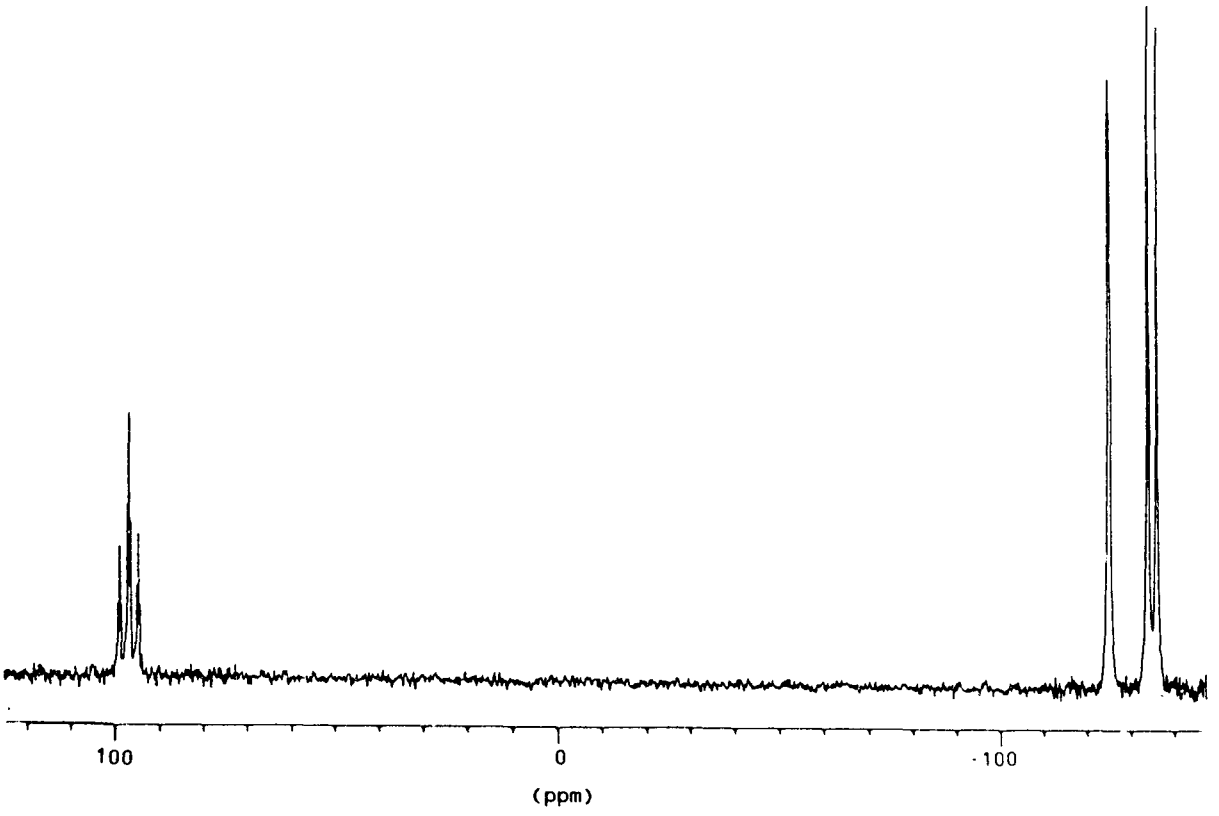

Figure 3-2

The $^{31}P\{^{1}H\}$ NMR Spectrum of
$[Pd_2(\mu\text{-}PPh_2)(\mu\text{-}dppm)_2Cl_2][BF_4]$

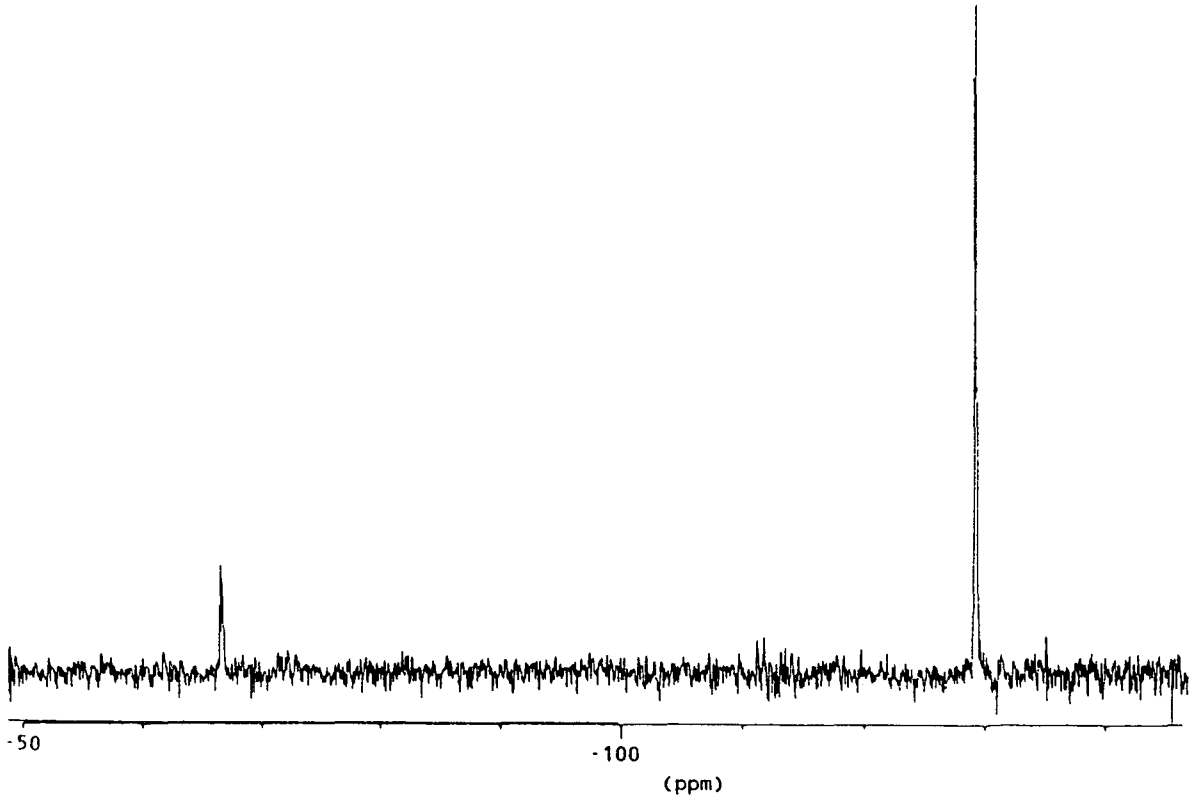

the situation in $[Pd_2(\mu\text{-}PPh_2)(\mu\text{-}dppm)(PPh_3)_2]^+$, where the peak for $\mu\text{-}PPh_2$ appears at 97.1 ppm, which clearly indicates the presence of a metal-metal bond. A tentative structure of this compound was obtained by Dr. J. Browning through X-ray crystallography (figure **3-3**). Table **3-1** lists the relevant crystallographic parameters for this structure. The palladium-palladium separation is 3.413Å which supports the $^{31}P\{^1H\}$ NMR evidence for the lack of a single metal-metal bond.

$[Pd_3(\mu\text{-}Cl)(PPh_2)_2(PPh_3)_3]^+$ reacts with $Ph_2PCH_2PPr^i_2$ to give $[Pd_2(\mu\text{-}PPh_2)(\mu\text{-}Ph_2PCH_2PPr^i_2)(PPh_3)_2]^+$.

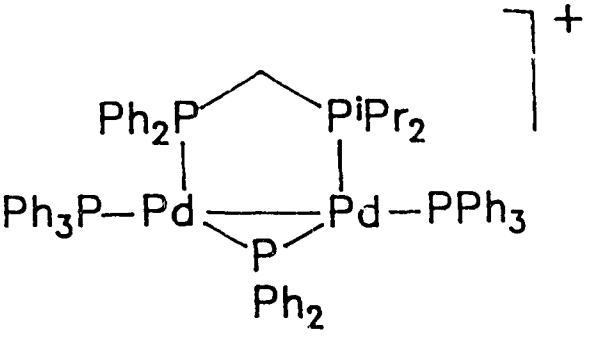

The $^{31}P\{^1H\}$ NMR spectrum of $[Pd_2(\mu\text{-}PPh_2)(\mu\text{-}Ph_2PCH_2PPr^i_2)(PPh_3)_2]$ is depicted in diagram **3-4**. The spectrum consists of five sets of signals due to the five types of phosphorus nuclei. The highly deshielded peak at 95.8 ppm belongs to the $\mu\text{-}PPh_2$ group coupling to the other four types of phosphorus present. The two cis couplings and

Figure 3-3

The Molecular Structure of
$[Pd_2(\mu\text{-}PPh_2)(\mu\text{-}dppm)_2Cl_2][BF_4]$

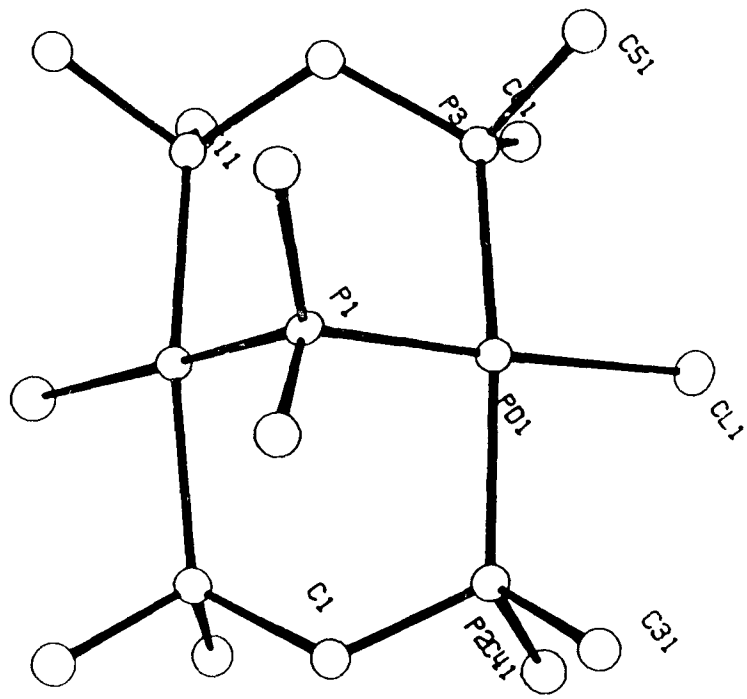

N.B. The phenyl groups are not shown for clarity.

Table 3-1

Crystallographic Parameters for
$[Pd_2(\mu\text{-}PPh_2)(\mu\text{-dppm})_2Cl_2]BF_4$

formula	$C_{62}H_{54}BCl_2F_4P_5Pd_2$
fw	1324
space group	C2/c
a (Å)	29.123
b (Å)	16.343
c (Å)	21.366
α (degrees)	90.0
β (degrees)	125.31
ϒ (degrees)	90.0
volume ($Å^3$)	8298.5
Z	4
calculated density (g/cm^3)	
μ (cm^{-1})	5.99
radiation (Å)	Mo 0.71069
temperature (K)	295
scan method	$\omega/2\theta$
total reflections collected	6517
parameters refined	166
R	not converged
R_w	not converged

Figure 3-4

The $^{31}P\{^{1}H\}$ NMR Spectrum of
$[Pd_2(\mu\text{-}PPh_2)(\mu\text{-}Pr^{i}{}_2PCH_2PPh_2)(PPh_3)_2][BF_4]$

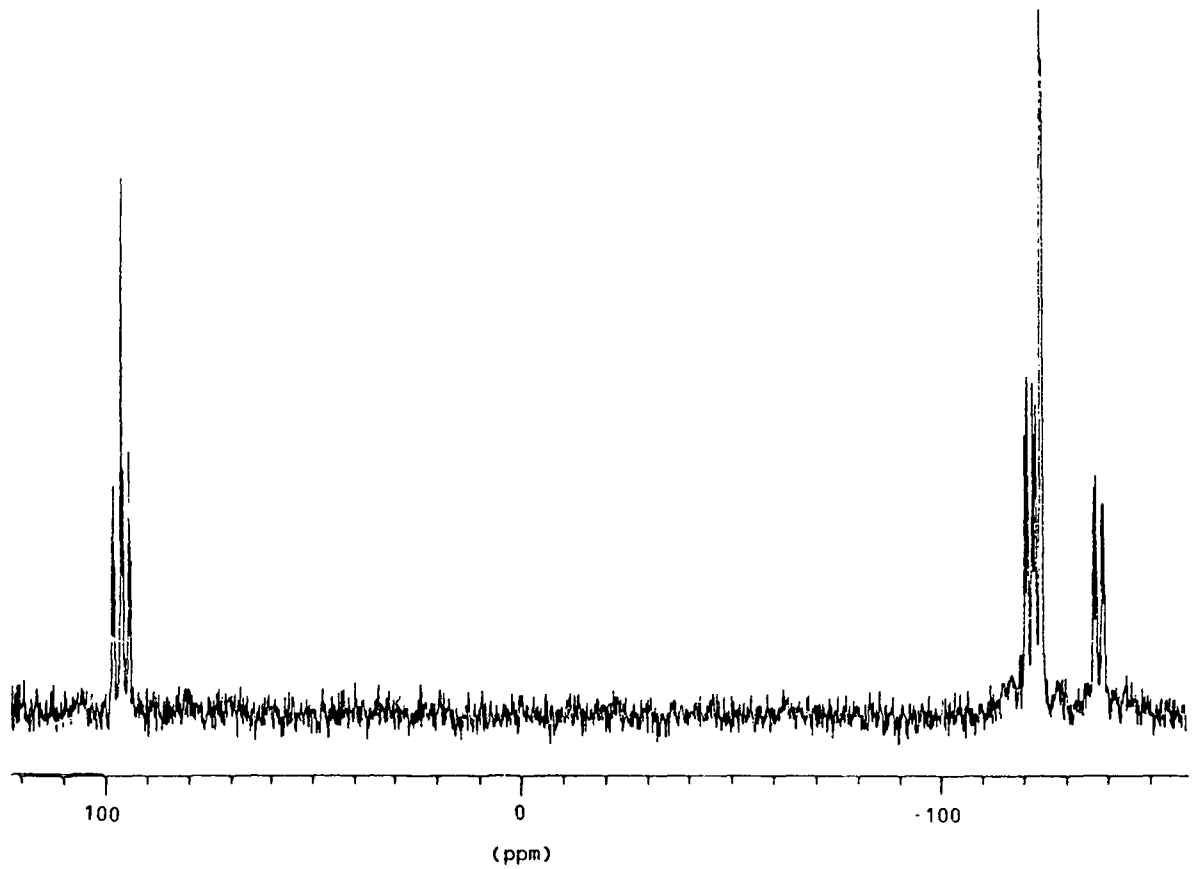

the two trans couplings are similar in magnitude, therefore, the multiplet appears almost as a triplet of triplets. The multiplets at -121.5 ppm and -138.2 ppm correspond to the diphenyl-end and the isopropyl-end of the unsymmetrical bidentate ligand respectively. These peaks are deceptively simple doublets of doublets. The resonances at -124.4 ppm belong to the two different triphenylphosphines.

Suitable crystals of $[Pd_2(\mu\text{-}PPh_2)(\mu\text{-}Ph_2PCH_2PPr^i{}_2)(PPh_3)_2]^+$ were obtained and the crystal structure was determined by Dr. Browning. An ORTEP drawing of the crystal structure is shown in figure **3-5**. The relevant crystallographic parameters may be found in tables **3-2**. A list of selected bond lengths and bond angles are presented in table **3-3**. The coordination about both palladium atoms is non-planar. Relative to the plane formed by the two palladiums and μ-PPh_2 phosphorus, one of the triphenylphosphines is approximately in the plane, the other is 0.43Å above the plane, and the $Pr^i{}_2PCH_2PPh_2$ ligand lies in a twisted conformation such that the plane formed by the diphosphine is at 32.78° relative to the palladium-palladium-phosphido bridge plane. This non-planar geometry is similar to that of $[Pd_2(\mu\text{-}PPh_2)(\mu\text{-dppm})(PPh_3)_2]^+$ (figure **3-6**).[89] The Pd-Pd bond length in $[Pd_2(\mu\text{-}PPh_2)(\mu\text{-}Ph_2PCH_2PPr^i{}_2)(PPh_3)_2]^+$ is 2.688Å (as compared to 2.715Å in $[Pd_2(\mu\text{-}PPh_2)(\mu\text{-}$

Figure 3-5

The Molecular Structure of
$[Pd_2(\mu\text{-}PPh_2)(\mu\text{-}Pr^i{}_2PCH_2PPh_2)(PPh_3)_2][BF_4]$

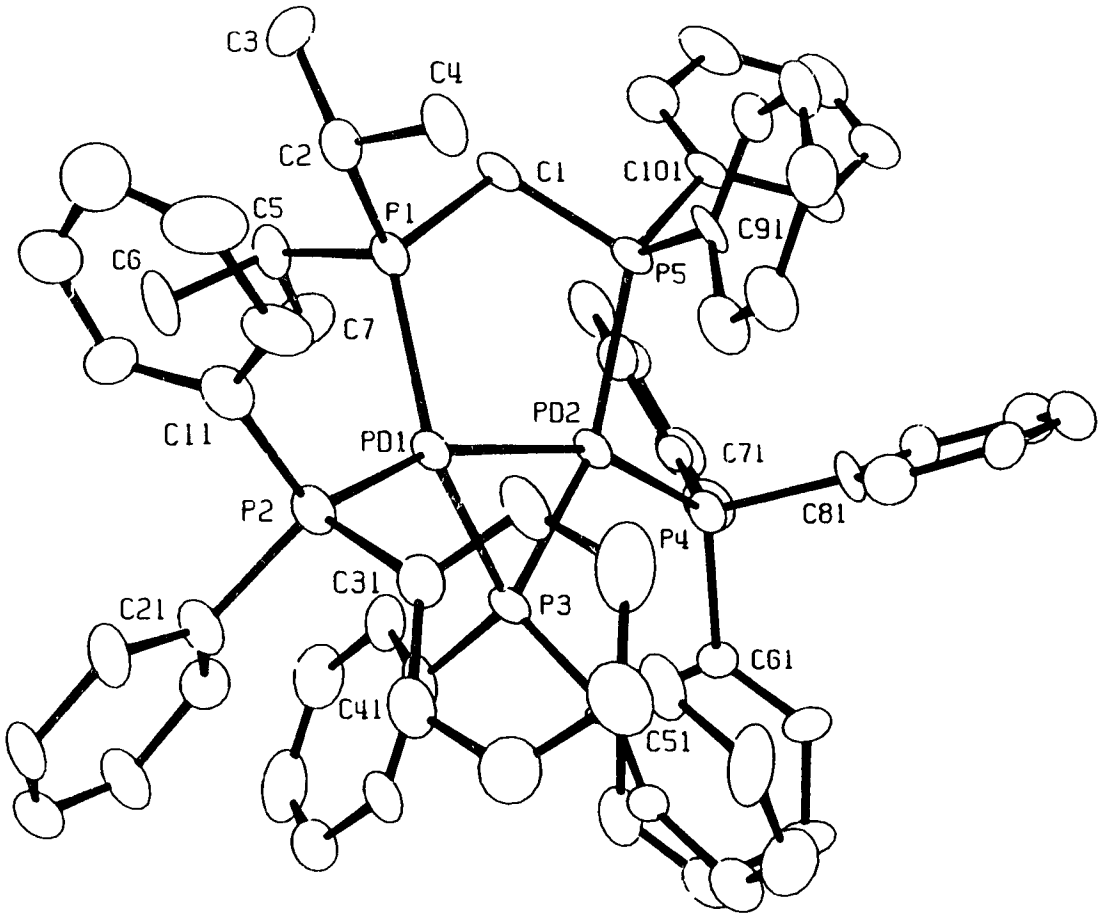

Table 3-2

Crystallographic Parameters for
$[Pd_2(\mu\text{-}PPh_2)(\mu\text{-}Pr^i{}_2PCH_2PPh_2)(PPh_3)_2][BF_4]$

formula	$C_{67}H_{66}BF_4P_5Pd_2$
fw	1326
space group	$P\bar{1}$
a (Å)	12.361(5)
b (Å)	22.362(8)
c (Å)	12.215(5)
α (degrees)	103.34(4)
β (degrees)	89.75(3)
ϒ (degrees)	99.17(3)
volume ($Å^3$)	3241(2)
Z	2
calculated density (g/cm^3)	1.356
μ (cm^{-1})	7.19
radiation (Å)	Mo 0.71069
temperature (K)	295
scan method	$\omega/2\theta$
total reflections collected	6039
parameters refined	712
R	0.0880
R_w	0.0744

Table 3-3

Selected Bond Lengths(Å) and Angles(°) for
$[Pd_2(\mu\text{-}PPh_2)(\mu\text{-}Pr^i{}_2PCH_2PPh_2)(PPh_3)_2][BF_4]$

Atoms	Distance
Pd(1)-Pd(2)	2.688(2)
Pd(1)-P(1)	2.336(4)
Pd(1)-P(2)	2.354(5)
Pd(1)-P(3)	2.266(4)
Pd(2)-P(5)	2.337(4)
Pd(2)-P(4)	2.314(5)
Pd(2)-P(3)	2.249(4)

Atoms	Angle
P(1)-Pd(1)-Pd(2)	90.5(1)
P(2)-Pd(1)-Pd(2)	161.4(1)
P(3)-Pd(1)-Pd(2)	53.2(1)
P(2)-Pd(1)-P(1)	107.4(2)
P(3)-Pd(1)-P(1)	139.7(2)
P(3)-Pd(1)-P(2)	110.9(2)
P(3)-Pd(2)-Pd(1	53.8(1)
P(4)-Pd(2)-Pd(1)	160.1(1)
P(4)-Pd(2)-P(3)	106.4(2)
Pd(1)-P(3)-Pd(2)	73.1(1)

(Estimated standard deviations are given in parentheses.)

Figure 3-6

The Molecular Structure of
$[Pd_2(\mu\text{-}PPh_2)(\mu\text{-dppm})(PPh_3)_2][BF_4]$

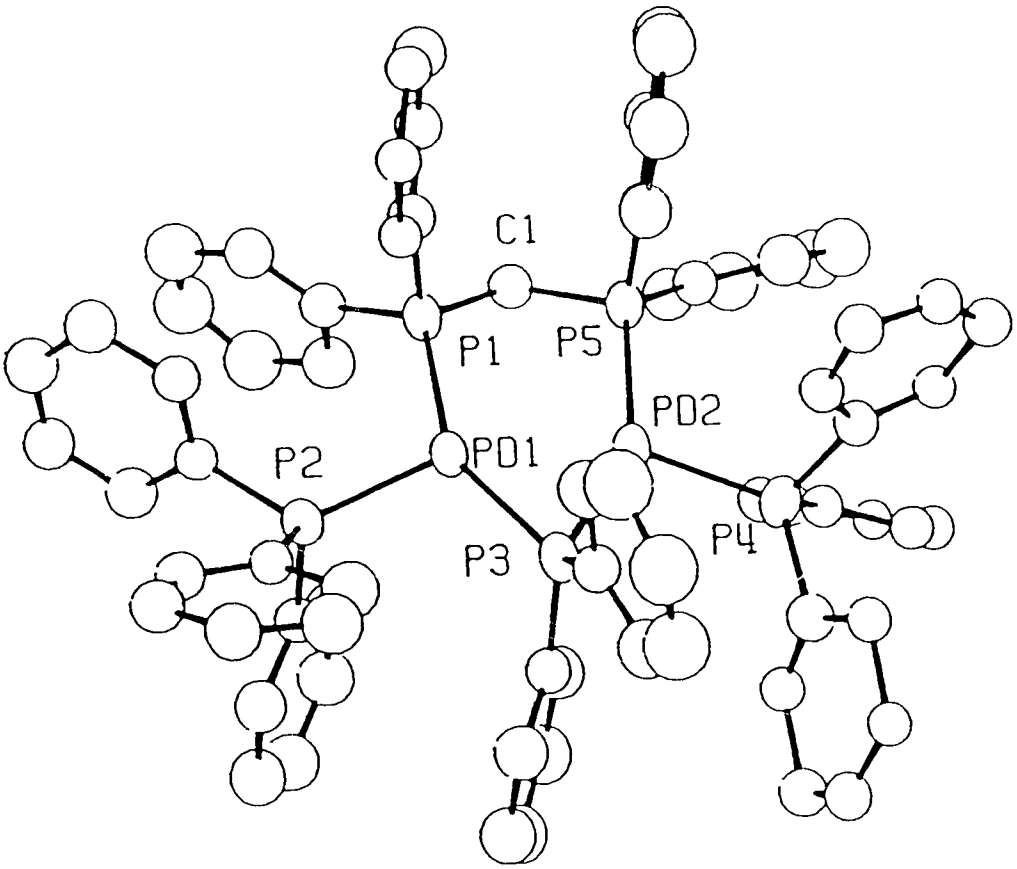

dppm)$(PPh_3)_2]^+$, and 2.89Å and 2.93Å in $[Pd_3(\mu$-Cl)$(PPh_2)_2(PPh_3)_3]^+$), and is within the range 2.531Å- 2.694Å reported previously for binuclear Pd(I) complexes.[90] Examples are $[Pd_2(\mu\text{-}I)(\mu\text{-}C_3H_5)(PPh_3)_2]$ (Pd-Pd= 2.686Å), and $[Pd_2(\mu\text{-}C_5H_5)(\mu\text{-}C_4H_7)(PPh_3)_2]$ (Pd-Pd= 2.679Å).

The reaction of $[Pd_3(\mu\text{-}Cl)(PPh_2)_2(PPh_3)_3]^+$ with tetraethylpyrophosphite $[(EtO)_2POP(OEt)_2)]$, POP, results in the formation of $[Pd_2(\mu\text{-}PPh_2)(\mu\text{-}POP)(PPh_3)_2]^+$.

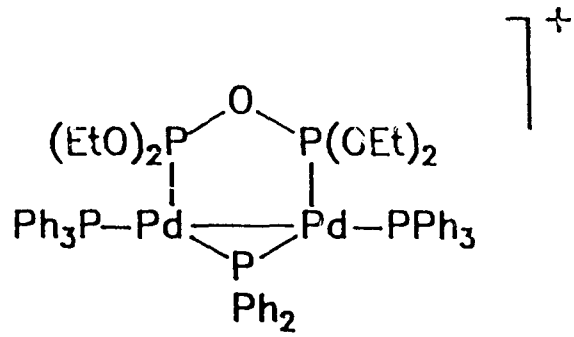

The structure was assigned on the basis of $^{31}P\{^1H\}$ NMR data and elemental analysis. Figure 3-7 depicts the $^{31}P\{^1H\}$ NMR spectrum of this compound. The multiplet at 85.2 ppm belongs to the μ-PPh_2 group coupling to the μ-POP and the terminal triphenylphosphine ligands. The coupling constants are 330 Hz and 25 Hz. The peaks at -15.2 ppm and -123.3 ppm correspond to the μ-POP and the terminal phosphines respectively. Only two of the coupling constants can be

Figure 3-7

The $^{31}P\{^{1}H\}$ NMR Spectrum of
$[Pd_2(\mu\text{-}PPh_2)(\mu\text{-}POP)(PPh_3)_2][BF_4]$

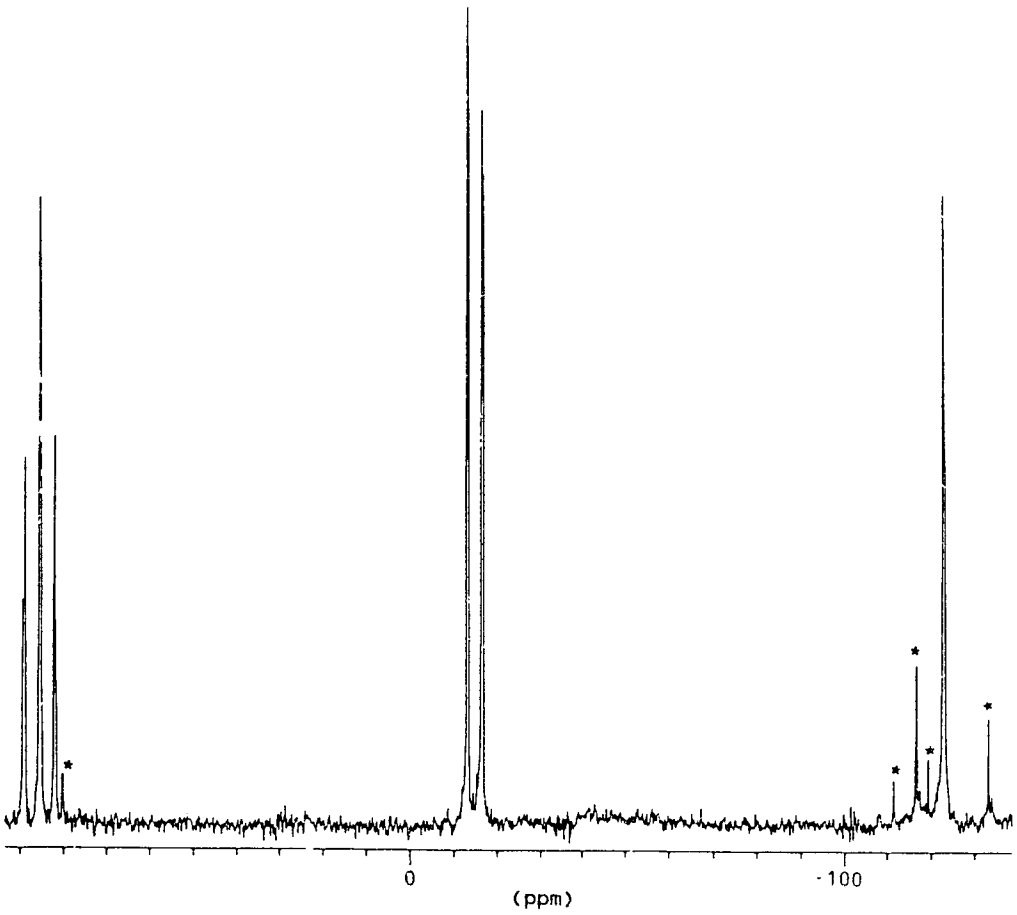

*= Impurity

directly determined from the spectrum. Computer simulation provides the rest of the spectral parameters (for values see chapter seven). $[Pd_2(\mu\text{-}PPh_2)(\mu\text{-}POP)(PPh_3)_2]^+$ reacts with one equivalent of dppm to replace μ-POP to afford the previously characterized $[Pd_2(\mu\text{-}PPh_2)(\mu\text{-}dppm)(PPh_3)_2]^+$, providing further support for the correctness of the structure assigned.

Reactions of $[Pt_3(\mu\text{-}X)(\mu\text{-}PPh_2)_2(PR_3)_3][Y]$ with $R_2PCH_2PR_2$ (R= Ph, Me):

$[Pt_3(\mu\text{-}H)(\mu\text{-}PPh_2)_2(PPh_3)_3]^+$ reacts with dppm to yield the Pt(I) dinuclear species, $[Pt_2(\mu\text{-}PPh_2)(\mu\text{-}dppm)(PPh_3)_2]^+$.

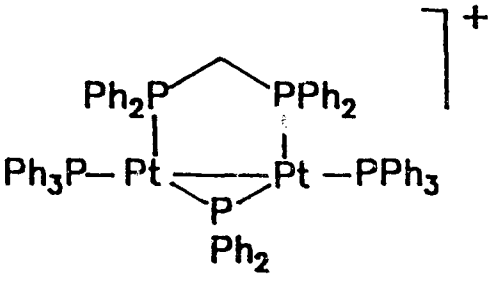

The $^{31}P\{^1H\}$ NMR spectrum of the dimer and a computer simulation are provided in figure **3-8**. An interpretation of the spectrum requires the consideration of the three different isotopomers (zero, one, and two ^{195}Pt) present. The spectrum is completely first order once it is realized that some peaks are hidden by overlap. The low-field

Figure 3-8

The $^{31}P\{^{1}H\}$ NMR Spectrum of
$[Pt_2(\mu\text{-}PPh_2)(\mu\text{-}dppm)(PPh_3)_2]_2[C_2O_4]$

a) simulated b) observed

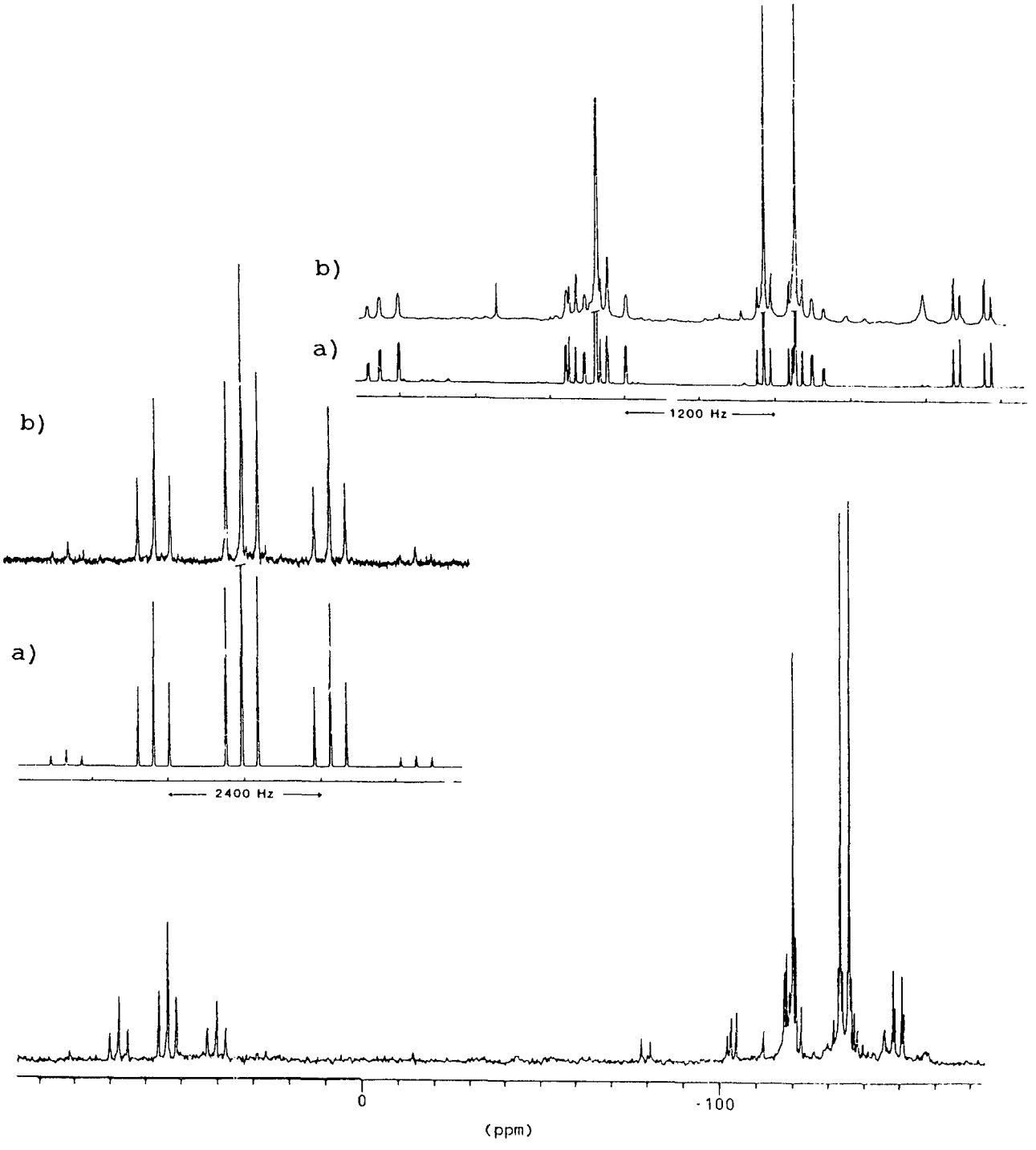

resonance (μ-PPh_2) is a triplet (J= 11 Hz) of triplets (J= 251 Hz) from coupling to the two terminal phosphines and the dppm ligand respectively. The major sideband is a doublet of triplets of triplets arising from the one spin-active platinum case. The phosphorus-platinum coupling constant is 2781 Hz. The isotopomer with two spin-active platinums gives rise to the less intense triplet of triplets of triplets as sidebands. The upfield resonances consist of the expected doublets at -120.3 ppm (J= 11 Hz) and -134.7 ppm (J= 251 Hz) with the corresponding platinum satellites and belong to the PPh_3 and dppm phosphorus atoms respectively. The major outer sidebands of the peak at -135 ppm consist of a doublet of doublets of doublets of doublets due to the isotopomer with one spin-active platinum. The one bond phosphorus-platinum coupling is 3066 Hz. The presence of one ^{195}Pt in this isotopomer makes the two ends of the dppm ligand different which allows their coupling constant to be determined directly from the spectrum (55 Hz). This is not the case with the palladium dimers where only two of the coupling constants (two bond cis and trans P-P coupling to μ-PPh_2) can be extracted directly from the spectrum. The major sidebands for the PPh_3 resonance at -120.3 ppm consist of a doublet of doublets of doublets of doublets as well. The one bond phosphorus-platinum coupling is 3293 Hz. The coupling between the two terminal

phosphines is 149 Hz. The inner sidebands of μ-dppm and PPh_3 resonances are similar to the outer sidebands except that two-bond phosphorus-platinum coupling (53 Hz, and 343 Hz respectively) replaces the one bond phosphorus-platinum coupling. The $^{195}Pt\{^1H\}$ NMR spectrum (figure **3-9**) consists of a doublet of doublets of doublets of doublets. The coupling constants agree within the experimental error with those derived from the $^{31}P\{^1H\}$ NMR spectrum.

Bis-dimethylphosphinomethane (dmpm) reacts in a similar manner to dppm with $[Pt_3(\mu\text{-}H)(PPh_2)_2(PPh_3)_3]^+$ to afford $[Pt_2(\mu\text{-}PPh_2)(\mu\text{-}dmpm)(PPh_3)_2]^+$. The $^{31}P\{^1H\}$ and $^{195}Pt\{^1H\}$ NMR spectra are similar to the previous case (for values see chapter seven). An X-ray crystallographic structure determination of a suitable crystal of $[Pt_2(\mu\text{-}PPh_2)(\mu\text{-}dmpm)(PPh_3)_2]^+$ was carried out by Dr. Browning and the result is shown in figure **3-10**. Crystallographic parameters for this structure are summarized in table **3-4**. Table **3-5** contains a list of selected bond lengths and angles. Unfortunately, with this structure the oxalato counter-ion was disordered and could not be located. Therefore, the bond lengths and angles data should be used cautiously. Currently attempts are being made to synthesize the PF_6^- and BPh_4^- analogues of this complex to solve that problem. Nevertheless, the crystallographic data in conjunction with

Figure 3-9

The $^{195}Pt\{^{1}H\}$ NMR Spectrum of
$[Pt_2(\mu\text{-}PPh_2)(\mu\text{-}dppm)(PPh_3)_2]_2[C_2O_4]$

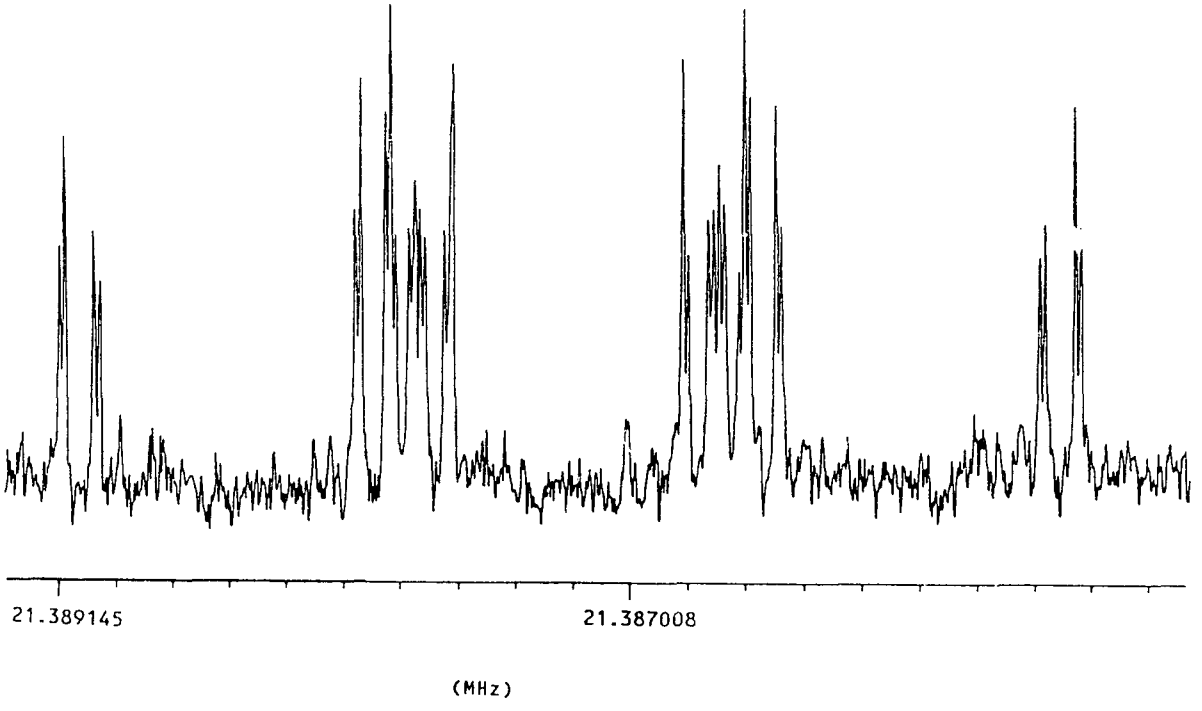

Figure 3-10

The Molecular Structure of
$[Pt_2(\mu\text{-}PPh_2)(\mu\text{-dmpm})(PPh_3)_2]_2[C_2O_4]$

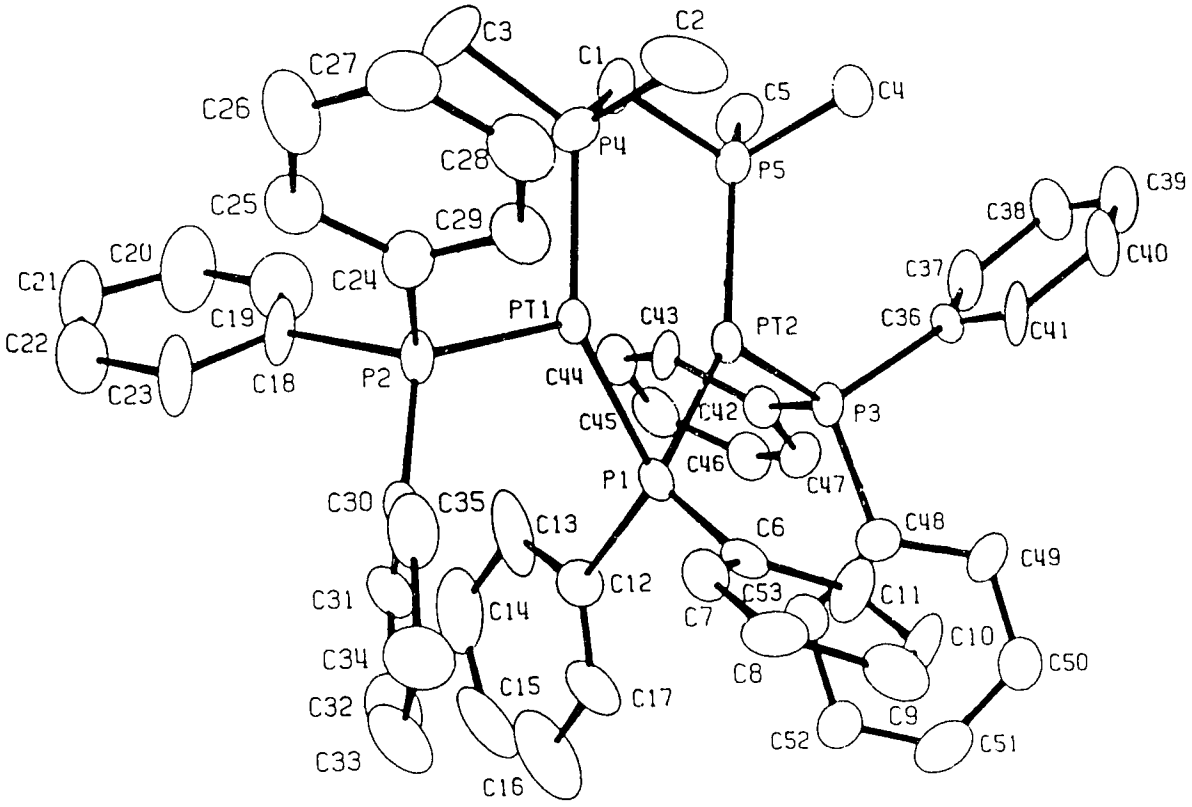

Table 3-4

Crystallographic Parameters for
$[Pt_2(\mu\text{-}PPh_2)(\mu\text{-dmpm})(PPh_3)_2]_2[C_2O_4]$

formula	$C_{108}H_{108}O_4P_{10}Pt_4$
fw	2560
space group	$P2_1/c$
a (Å)	13.214(2)
b (Å)	14.422(4)
c (Å)	29.914(6)
α (degrees)	90.0
β (degrees)	111.69(2)
ϒ (degrees)	90.00
volume (Å^3)	5297
Z	4
calculated density (g/cm^3)	1.605
μ (cm^{-1})	57.47
radiation (Å)	Mo 0.71069
temperature (K)	295
scan method	ω/2θ
total reflections collected	4927
parameters refined	540
R	not converged
R_w	not converged

Table 3-5

Selected Bond Lengths(Å) and Angles(°) for $[Pt_2(\mu\text{-}PPh_2)(\mu\text{-}dmpm)(PPh_3)_2]_2[C_2O_4]$

Atoms	Distance
Pt(1)-Pt(2)	2.678(2)
Pt(1)-P(1)	2.260(8)
Pt(1)-P(2)	2.27(1)
Pt(1)-P(4)	2.285(8)
Pt(2)-P(1)	2.257(8)
Pt(2)-P(3)	2.278(9)
Pt(2)-P(5)	2.291(8)

Atoms	Angle
P(1)-Pt(1)-Pt(2)	53.6(2)
P(2)-Pt(1)-Pt(2)	162.2(2)
P(3)-Pt(2)-Pt(1)	163.9(2)
P(2)-Pt(1)-P(1)	111.3(3)
P(4)-Pt(1)-P(1)	146.4(4)
P(3)-Pt(2)-P(5)	100.2(3)
P(5)-Pt(2)-Pt(1)	94.1(3)
P(4)-Pt(1)-Pt(2)	93.6(3)
P(5)-Pt(2)-P(1)	147.8(3)
Pt(1)-P(1)-Pt(2)	72.7(2)

(Estimated standard deviations are given in parentheses.)

other spectroscopic data clearly support the determined structure. The platinum-platinum bond length is 2.678Å, and is comparable to the metal-metal bond lengths in $[Pd_2(\mu\text{-}PPh_2)(\mu\text{-dppm})(PPh_3)_2]^+$(2.715Å), and $[Pd_2(\mu\text{-}PPh_2)(\mu\text{-}Ph_2PCH_2PPr^i{}_2)(PPh_3)_2]^+$ (2.688Å). The rest of the structure is similar to the palladium case discussed before.

$[Pt_3(\mu\text{-}Cl)(PPh_2)_2(PPh_3)_3]^+$ cluster also reacts with dppm to produce the dimer $[Pt_2(\mu\text{-}PPh_2)(\mu\text{-dppm})(PPh_3)_2]^+$. This reaction, however, proceeds much slower (24-48 h) than the comparable hydrido-bridged cluster (one minute). This may be explained by the fact $[Pt_3(\mu\text{-}H)(\mu\text{-}PPh_2)_2(PPh_3)_3]^+$ is a 42-electron cluster, whereas, $[Pt_3(\mu\text{-}Cl)(\mu\text{-}PPh_2)_2(PPh_3)_3]^+$ has 44 electrons. As described in the last chapter, molecular orbital calculations on model triangular phosphido-bridged platinum clusters have shown that the last two low lying orbitals are close in energy. 42-electron clusters only fill up to the last one of these molecular orbitals leaving a small gap between the HOMO and the LUMO. Addition of two electrons fills the last orbital leading a large gap between filled and unfilled levels. Any type nucleophilic attack, therefore, would be more facile with a 42-electron cluster than a 44-electron one. $[Pt_3(\mu\text{-}H)(\mu\text{-}PPh_2)_2(PPh_3)]^+$ was also reacted with the unsymmetrical ligands $Bu^t{}_2PCH_2PPh_2$. The resulting complex had an

extremely complicated $^{31}P\{^{1}H\}$ NMR spectrum. Based on previous results the expected product was $[Pt_2(\mu\text{-}PPh_2)(\mu\text{-}Bu^t{}_2PCH_2PPh_2)(PPh_3)_2]^+$. To simplify the $^{31}P\{^{1}H\}$ NMR spectrum, $[Pt_2(\mu\text{-}PPh_2)(\mu\text{-}Bu^t{}_2PCH_2PPh_2)(PPh_3)_2]^+$ was reacted with Bu^tNC to replace the terminal triphenylphosphines to obtain $[Pt_2(\mu\text{-}PPh_2)(\mu\text{-}Bu^t{}_2PCH_2PPh_2)(Bu^tNC)_2]^+$.

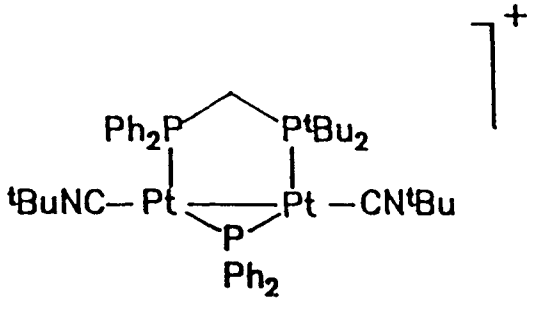

The $^{31}P\{^{1}H\}$ NMR spectrum of this complex (figure **3-11**) consists of three sets of peaks. The $\mu\text{-}PPh_2$ resonance at low field, 53.5 ppm, is a doublet (J= 233 Hz) of doublets (J = 254 Hz) due to coupling with two different phosphorus of the unsymmetrical diphosphine ligand. The sidebands are two sets of doublets of doublets of doublets due to the two isotopomers with one spin-active platinum. The platinum-phosphorus coupling constants are 3011 Hz and 2546 Hz. The doublet of doublets at -95 ppm and -138.7 ppm belong to $Bu^t{}_2P$- and Ph_2P- ends of the diphosphine ligand respectively, coupling to $\mu\text{-}PPh_2$ and to each other. The coupling constant between them is 55 Hz. The sidebands in

Figure 3-11

The $^{31}P\{^{1}H\}$ NMR Spectrum of
$[Pt_2(\mu\text{-}PPh_2)(\mu\text{-}Bu^t{}_2PCH_2PPh_2)(Bu^tNC)_2]_2[C_2O_4]$

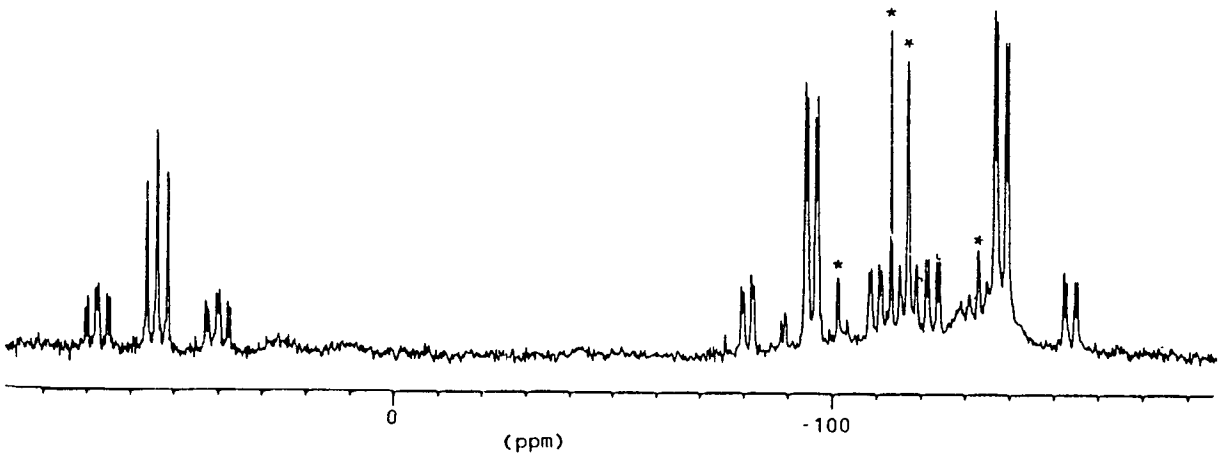

*= Impurity

both cases are doublets of doublets of doublets. The platinum-phosphorus coupling constant are 2924 Hz and 3149 Hz. The resonances at -114 ppm and -117 ppm belong to some impurities present. This product was not isolated because in solution over time (during crystallization), it decomposes to afford $[Pt_2(\mu\text{-}PPh_2)(PPh_3)_3(Bu^tNC)]^+$ as established by $^{31}P\{^1H\}$ NMR spectroscopy. $[Pt_2(\mu\text{-}PPh_2)(PPh_3)_3(Bu^tNC)]^+$ was also synthesized by another method which shall be discussed later in this chapter.

Reaction of $[Pd_2Pt(\mu\text{-}Cl)(\mu\text{-}PPh_2)_2(PPh_3)_3][BF_4]$ with $Ph_2PCH_2PPh_2$:

$[Pd_2Pt(\mu\text{-}Cl)(PPh_2)_2(PPh_3)_3]^+$ reacts with one equivalent of dppm to afford two complexes: $[PtPd(\mu\text{-}PPh_2)(\mu\text{-}dppm)(PPh_3)_2]^+$ and $[Pt_2(\mu\text{-}PPh_2)(\mu\text{-}dppm)_2Cl_2]^+$.

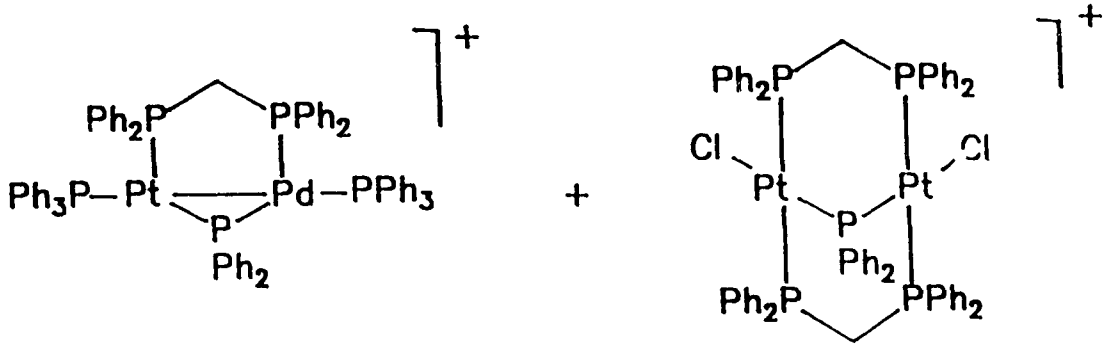

Due to the synthetic method used to prepare $[Pd_2Pt(\mu\text{-}Cl)(PPh_2)_2(PPh_3)_3]^+$ some $[Pd_3(\mu\text{-}Cl)(PPh_2)_2(PPh_3)_3]^+$ contaminant is always present. Therefore, reaction with

dppm also yields $[Pd_2(\mu\text{-}PPh_2)(\mu\text{-}dppm)(PPh_3)_2]^+$ and $[Pd_2(\mu\text{-}PPh_2)(\mu\text{-}dppm)_2Cl_2]^+$ as evident by $^{31}P\{^1H\}$ NMR spectroscopy. The structures of these products were assigned on the basis of their $^{31}P\{^1H\}$ and $^{195}Pt\{^1H\}$ NMR spectra.

$^{31}P\{^1H\}$ NMR spectrum of $[Pt_2(\mu\text{-}PPh_2)(\mu\text{-}dppm)_2Cl_2]^+$ (figure **3-12**) consists of a doublet at -134.1 ppm (μ-dppm) and a quintet at -94.3 ppm (μ-PPh_2) with the corresponding platinum sidebands. The platinum-phosphorus coupling constants are 2715 Hz, and 2552 Hz. The peak at -129 ppm belongs to $[Pd_2(\mu\text{-}PPh_2)(\mu\text{-}dppm)_2Cl_2]^+$. The $^{195}Pt\{^1H\}$ NMR spectrum of $[Pt_2(\mu\text{-}PPh_2)(\mu\text{-}dppm)_2Cl_2]$ (figure **3-13**) consists of a doublet of triplets of triplets due to the isotopomer with one spin-active platinum. The two bond platinum-phosphorus coupling is 132 Hz. The other coupling constants agree with the values obtained from the $^{31}P\{^1H\}$ NMR spectrum within the experimental error. The peaks due to the second isotopomer (i.e. two ^{195}Pt) are not intense enough to be clearly observed.

The low field portion of the $^{31}P\{^1H\}$ NMR spectrum of $[PtPd(\mu\text{-}PPh_2)(\mu\text{-}dppm)(PPh_3)_2][BF_4]$ (figure **3-14**) is composed of a doublet of doublets of doublets of doublets at 78.3 ppm and belongs to the μ-PPh_2 group coupling to the four different types of phosphorus present. The coupling

Figure 3-12

The $^{31}P\{^{1}H\}$ NMR Spectrum of
$[Pt_2(\mu\text{-}PPh_2)(\mu\text{-}dppm)_2Cl_2][BF_4]$

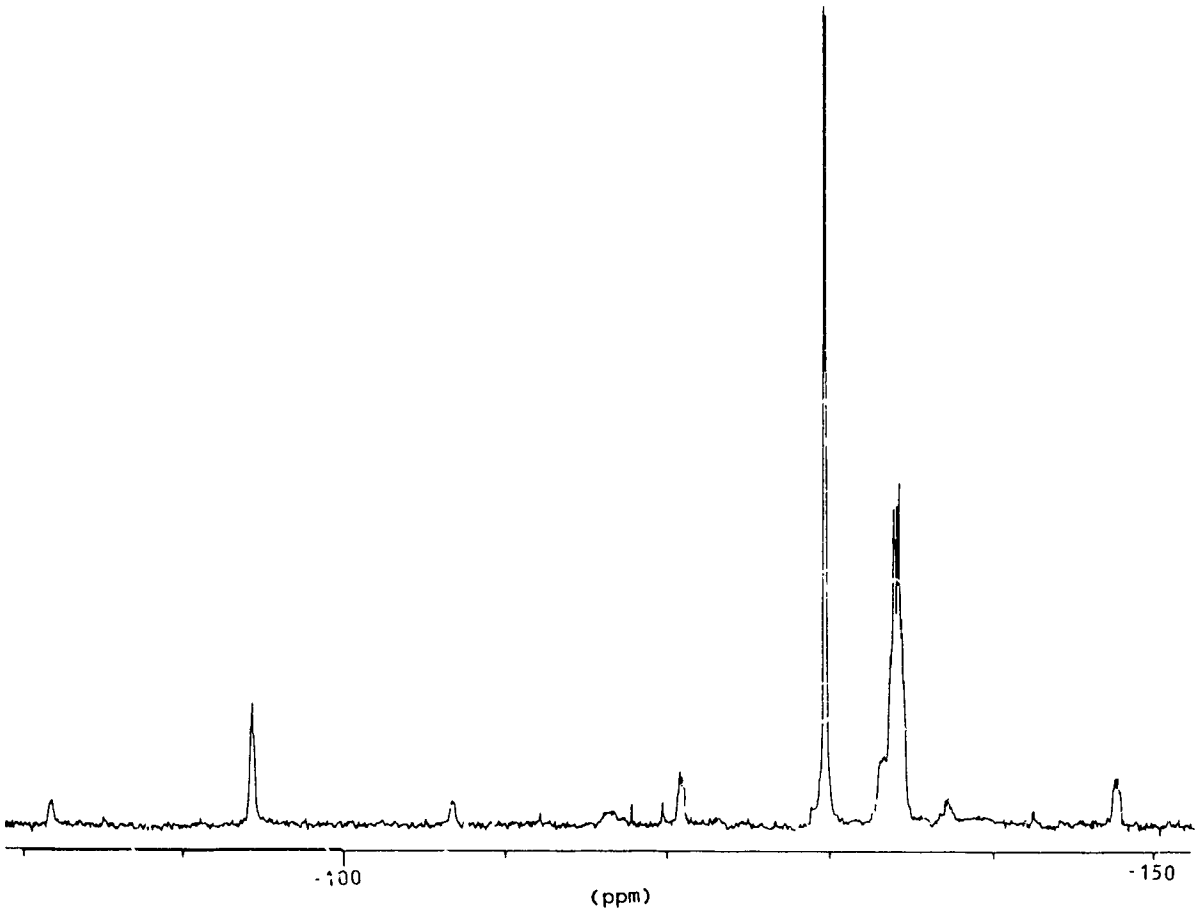

Figure 3-13

The $^{195}Pt\{^{1}H\}$ NMR Spectrum of $[Pt_2(\mu\text{-}PPh_2)(\mu\text{-}dppm)_2Cl_2][BF_4]$

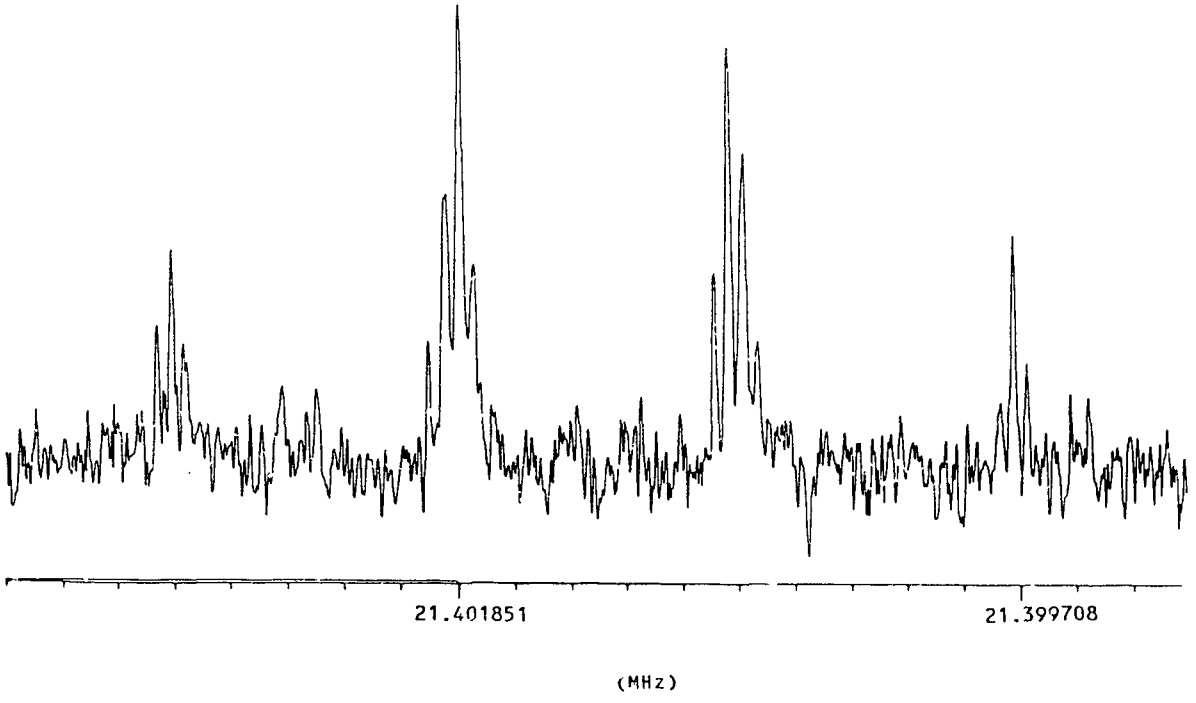

Figure 3-14

The Low-Field Portion of the $^{31}P\{^{1}H\}$ NMR Spectrum of $[PtPd(\mu\text{-}PPh_2)(\mu\text{-}dppm)(PPh_3)_2][BF_4]$

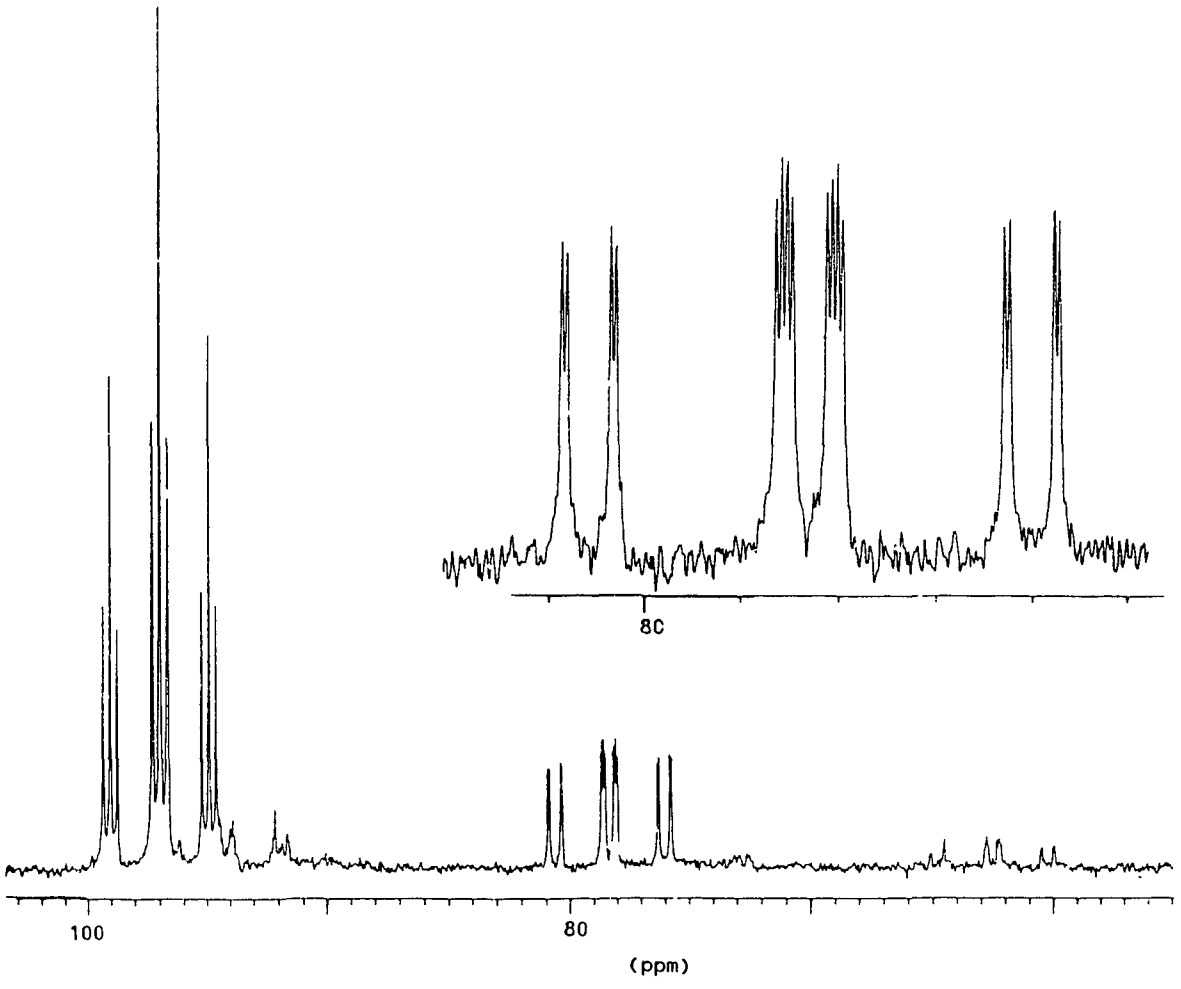

constants are: 6 Hz, and 52 Hz for the cis; and 227 Hz and 238 Hz for the trans phosphorus-phosphorus coupling. The peak at 97 ppm belongs to the $[Pd_2(\mu\text{-}PPh_2)(\mu\text{-}dppm)(PPh_3)_2][BF_4]$ contaminant present. The high-field resonances are two sets of doublets of doublets at -130.3 ppm and -132.6 ppm for the two terminal triphenylphosphines; and two sets of doublets of doublets of doublets at -137.8 ppm and -140.0 ppm for the two ends of the dppm ligand. This portion of the spectrum, however, is not as clearly resolved due to overlap with the peaks belonging to the $[Pd_2(\mu\text{-}PPh_2)(\mu\text{-}dppm)(PPh_3)_2][BF_4]$ contaminant present. $^{195}Pt\{^1H\}$ NMR spectrum of $[PtPd(\mu\text{-}PPh_2)(\mu\text{-}dppm)(PPh_3)_2]^+$ (figure 3-15) is a doublet of doublets of doublets. The coupling constants agree well with values extracted from the $^{31}P\{^1H\}$ spectrum.

No other work was done on this system due to the difficulty in separating the products. Nevertheless, this system offers a wide area for research for future workers. The primary concern, however, would be to achieve successful separation of the mixed palladium/platinum cluster and the tripalladium complex.

Figure 3-15

The $^{195}Pt\{^{1}H\}$ NMR Spectrum of
$[PtPd(\mu\text{-}PPh_2)(\mu\text{-dppm})(PPh_3)_2][BF_4]$

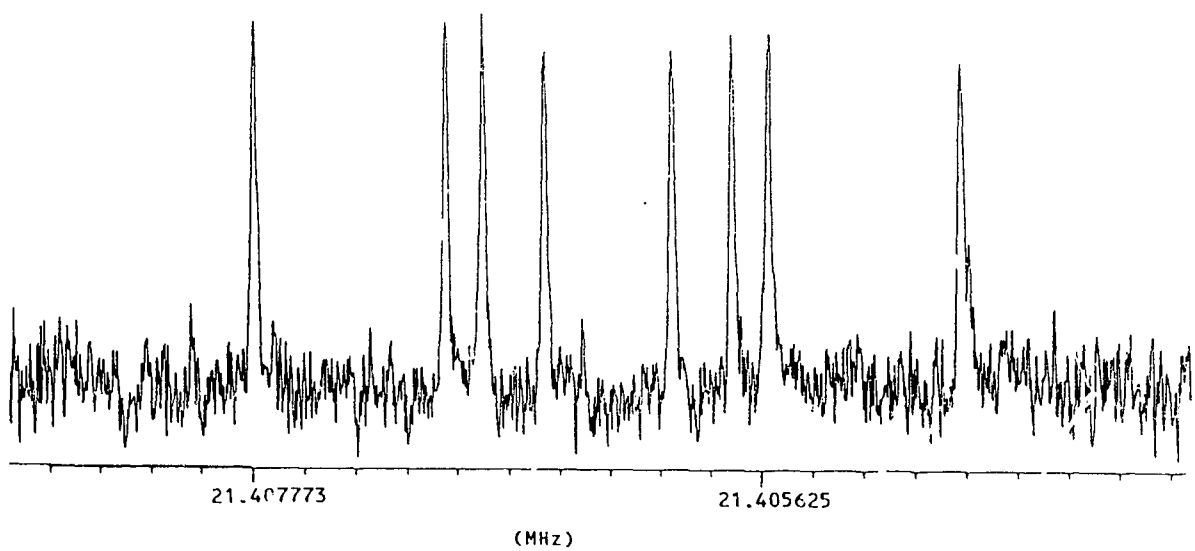

Reaction of $[Pt_3(\mu\text{-}X)(\mu\text{-}PPh_2)_2(PPh_3)_3]^+$ (X= Cl, H) with Bu^tNC:

$[Pt_3(\mu\text{-}H)(\mu\text{-}PPh_2)_2(PPh_3)_3]^+$ immediately reacts with one equivalent of Bu^tNC to give the dinuclear species $[Pt_2(\mu\text{-}PPh_2)(PPh_3)_3(Bu^tNC)]^+$.

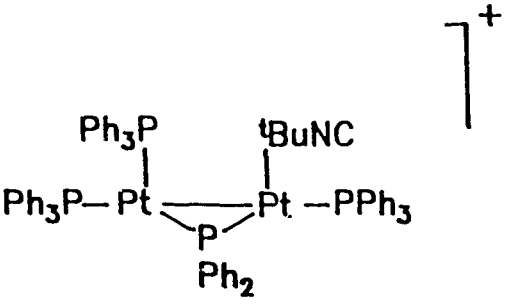

The $^{31}P\{^1H\}$ spectrum of $[Pt_2(\mu\text{-}PPh_2)(Bu^tNC)(PPh_3)_3]^+$ (figure **3-16**) consists of four sets of peaks. The center doublet at 26.6 ppm belongs to the $\mu\text{-}PPh_2$ group coupling to the triphenylphosphine trans to it (J= 250 Hz). The side-bands are two sets of doublets of doublets arising from the two different isotopomers with one spin-active platinum. The phosphorus-platinum coupling constants are 2754 Hz and 3101 Hz. The doublet (J= 250 Hz) at -110.0 ppm belongs to the terminal triphenylphosphine trans to the $\mu\text{-}PPh_2$ group. The sideband is a doublet of doublets with a phosphorus-platinum coupling constant of 3004 Hz. The resonances at -121.9 and -128.3 ppm correspond to the other two terminal triphenylphosphines coupled to each other with a coupling

Figure 3-16

The $^{31}P\{^{1}H\}$ NMR Spectrum of
$[Pt_2(\mu\text{-}PPh_2)(Bu^tNC)(PPh_3)_3][BF_4]$

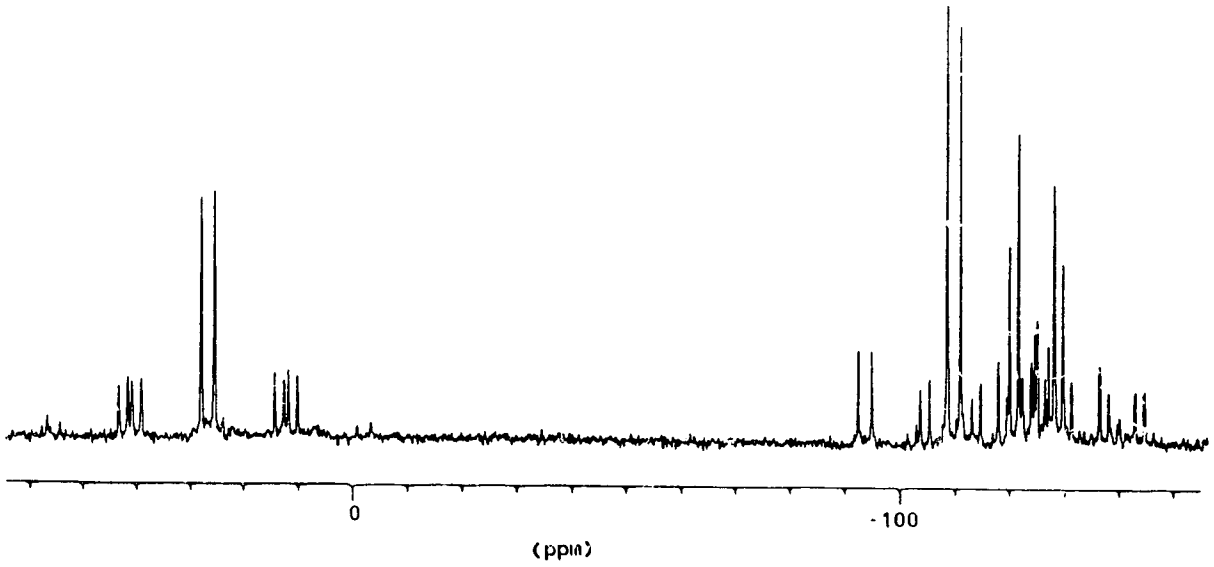

constant of 162 Hz, with one-bond and two-bond phosphorus-platinum coupling giving rise to the inner and outer sidebands.

The crystal structure of $[Pt_2(\mu\text{-}PPh_2)(Bu^tNC)(PPh_3)_3]^+$ which is illustrated in figure **3-17** confirms the spectroscopic data collected for it. Crystallographic parameters are listed in table **3-6**. Table **3-7** lists a number of selected bond lengths and angles. Due to a large disorder the oxalato counter-ion could not be located. Efforts are under way to prepare this complex with different counter-ions such as PF_6 or BPh_4. The Bu^tNC ligand and one of the terminal phosphine groups are almost trans to the phosphido bridge. The other two terminal phosphines are in cis positions with respect to the phosphido bridge. All ligands and the two platinum atoms are approximately in the same plane. The slight asymmetry in the bond lengths of the μ-PPh_2 phosphorus to the two platinums is probably due to the stronger trans influence of PPh_3 with respect to Bu^tNC. The Pt-Pt bond distance is 2.716Å which is comparable to those in the isoelectronic sulphur-bridged dimers $[Pt_2(\mu\text{-}SO_2)(CNC_8H_9)_2(PCy_3)_2]$ (2.693Å),[91] $[Pt_2(\mu\text{-}S)(PPh_3)_3CO]$ (2.647Å),[92] and $[Pt_2(\mu\text{-}S)(RNC)_4]$ (R= $Bu^t{}_3C_6H_2$) (2.604(2)Å.[93] With the formalism of a single Pt-Pt bond, each platinum atom achieves a sixteen electron environment. The IR

Figure 3-17

The Molecular Structure of
$[Pt_2(\mu\text{-}PPh_2)(Bu^tNC)(PPh_3)_3]_2[C_2C_4]$

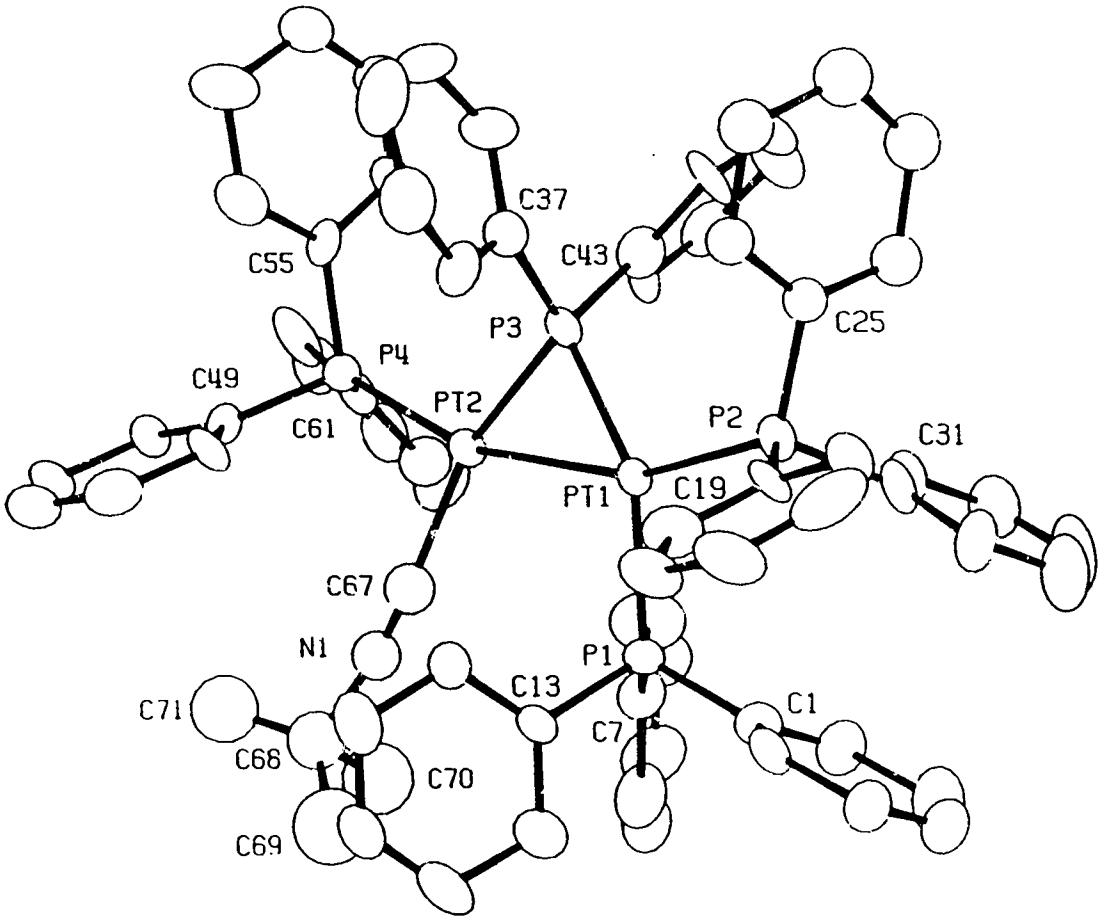

Table 3-6

Crystallographic Parameters for
$[Pt_2(\mu\text{-}PPh_2)(PPh_3)_3(Bu^tNC)]_2[C_2O_4]$

formula	$C_{144}H_{128}N_2O_4P_8Pt_4$
fw	2979
space group	$P\bar{1}$
a (Å)	14.641(4)
b (Å)	20.538(5)
c (Å)	12.254(3)
α (degrees)	88.34(4)
β (degrees)	88.35(3)
ϒ (degrees)	100.44(2)
volume ($Å^3$)	3620
Z	2
calculated density (g/cm^3)	1.41
μ (cm^{-1})	40.29
radiation (Å)	Mo 0.71067
temperature (K)	295
scan method	$\omega/2\theta$
total reflections collected	6755
parameters refined	565
R	0.0817
R_w	0.0817

Table 3-7

Selected Bond Lengths(Å) and Angles(°) for $[Pt_2(\mu\text{-}PPh_2)(PPh_3)_3(Bu^tNC)]_2[C_2O_4]$

Atoms	Distance
Pt(1)-Pt(2)	2.716(2)
Pt(1)-P(1)	2.323(8)
Pt(1)-P(2)	2.289(8)
Pt(1)-P(3)	2.270(7)
Pt(2)-P(5)	2.03(4)
Pt(2)-P(4)	2.254(7)
Pt(2)-P(3)	2.217(9)
C(67)-N(1)	1.09(5)

Atoms	Angle
P(1)-Pt(1)-Pt(2)	97.9(2)
P(2)-Pt(1)-Pt(2)	160.2(2)
P(3)-Pt(1)-Pt(2)	51.9(2)
P(2)-Pt(1)-P(1)	101.9(3)
P(3)-Pt(1)-P(1)	149.2(3)
P(3)-Pt(1)-P(2)	108.4(3)
P(3)-Pt(2)-Pt(1)	53.6(2)
P(4)-Pt(2)-Pt(1)	161.1(2)
P(4)-Pt(2)-P(3)	107.6(3)
Pt(1)-P(3)-Pt(2)	74.5(3)
C(67)-Pt(2)-P(4)	94(1)
C(67)-Pt(2)-Pt(1)	105(1)
C(67)-Pt(2)-P(3)	159(1)

(Estimated standard deviations are given in parentheses.)

spectrum of the product further supports the presence of terminal isocyanide (2160 cm^{-1}).

Addition of dppm to a CH_2Cl_2 solution of $[Pt_2(\mu\text{-}PPh_2)(Bu^tNC)(PPh_3)_3]^+$ produces the substituted product $[Pt_2(\mu\text{-}PPh_2)(\mu\text{-dppm})(PPh_3)_2]^+$ the identical compound to the dppm fragmentation product. This reaction is similar to the reaction of $[Pt_2(\mu\text{-}S)(CO)(PPh_3)_3]$ with dppm which yielded $[Pt_2(\mu\text{-}S)(\mu\text{-dppm})(PPh_3)_2]$.[94]

Since the terminal triphenylphosphines in $[Pt_2(\mu\text{-}PPh_2)(\mu\text{-dppm})(PPh_3)_2]^+$ are labile the Bu^tNC present in the solution can easily replace them. There is a dynamic exchange between the PPh_3 and Bu^tNC as evident by $^{31}P\{^1H\}$ NMR spectroscopy. Crystallization, however, yields pure $[Pt_2(\mu\text{-}PPh_2)(\mu\text{-dppm})(PPh_3)_2]^+$. $[Pt_3(\mu\text{-}Cl)(\mu\text{-}PPh_2)_2(PPh_3)_3]^+$ reacts with Bu^tNC to produce a similar product. This reaction however proceeds slower than the hydride-bridged analogue. The reason for the slower rate was explained earlier in this chapter.

Comments on the Mechanisms of Fragmentation of $[M_3(\mu\text{-}X)(\mu\text{-}PPh_2)_2(PR_3)_3]^{n+}$ by $R_2PCH_2PR_2$:

A summary of all the fragmentation reactions with dppm is

depicted in figure **3-18**. A number of these fragmentation reactions was carried out to observe whether there is any preference for the different bridging units in the resulting dimers. In all cases, the μ-PPh_2-bridged dimer was produced. Based on this series of reactions it appears that fragmentation depends on two factors: the lability of the terminal phosphines, and the strength of the bridging X ligand. If the terminal phosphines are labile (e.g. PPh_3), then fragmentation proceeds as described. If the terminal phosphines are less labile (e.g. PEt_3), then fragmentation depends on the strength of the bridging ligand X. Clusters with strong bridges do not react with dppm (strength of bridges: Ph_2P, S> SR> H, Cl). For example, $[Pd_3(\mu\text{-}SCH_2PH)(\mu\text{-}PPh_2)_2(PEt_3)_3]^+$ which has a basic ligand and a relatively strong bridge does not react with dppm; whereas, $[Pd_3(\mu\text{-}Cl)(\mu\text{-}PPh_2)_2(PEt_3)_3]^+$ does to yield the dimer $[Pd_2(\mu\text{-}PPh_2)(\mu\text{-dppm})(PEt_3)_2]^+$. Another example is provided by $[Pt_3(\mu\text{-}PPh_2)_3(PEt_3)_3]^+$ which does not react with dppm because it contains a strong μ-PPh_2 bridge and a basic ligand. Whereas, $[Pt_3(\mu\text{-}PPh_2)_3(PPh_3)_3]^+$, which has terminal triphenylphosphines, reacts with dppm to form a dimer. Another clue to the mechanism is given by the reaction of $[PtPd_2(\mu\text{-}Cl)(\mu\text{-}PPh_2)_2(PPh_3)_3]^+$ cluster with dppm which yields $[PtPd(\mu\text{-}PPh_2)(\mu\text{-dppm})(PPh_3)_2]^+$. Based on the information presented the following mechanism may be

Figure 3-18

Summary of All the Fragmentation Reactions with $Ph_2PCH_2PPh_2$

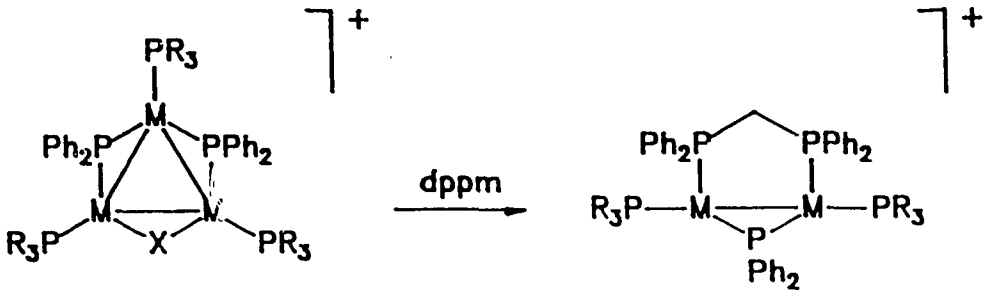

M=Pd,R=Ph,X=Cl,SH
M=Pd,R=Et,X=Cl

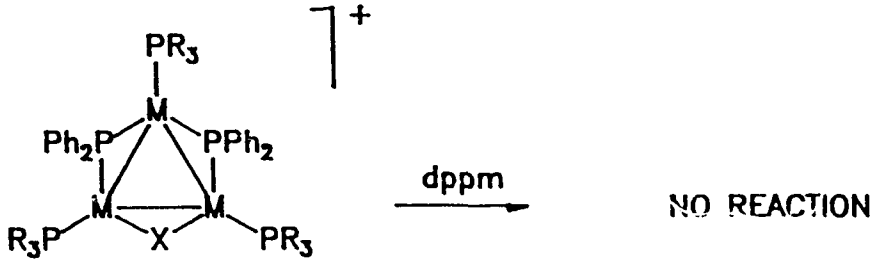

M=Pd,R=Et,X=S,SCH_2Ph,PPh_2
M=Pt,R=Et,X=PPh_2

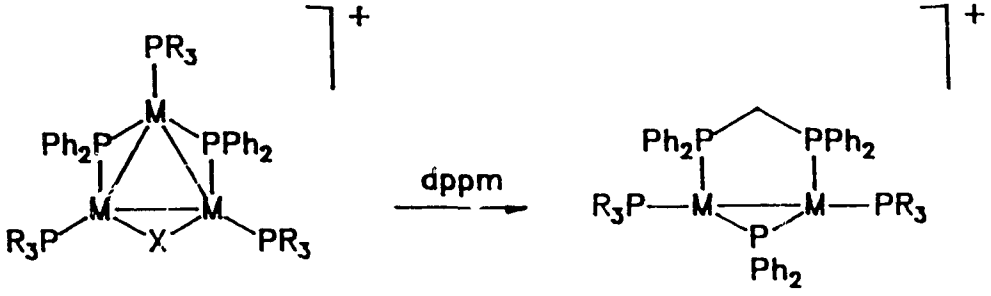

M=Pt,R=Ph,X=H,Cl,PPh_2,SCH_3,SCH_2Ph
M=Pt,R=Et,X=H,Cl

suggested:

1. initial coordination of one end of dppm to either M(2) of M(3) center with cleavage of the M-X bond.

2. cleavage of M(2)-M(3) and M(1)-M(2) (or M(1)-M(3)).

3. coordination of the other end of the dppm molecule to M(1).

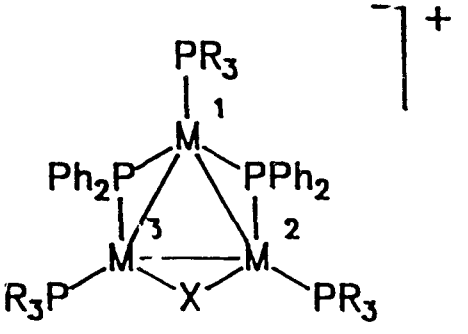

This mechanism is by no means conclusive and further detailed mechanistic studies are required to unequivocally establish pathways.

CHAPTER FOUR

REACTIVITY OF Pd(I) AND Pt(I) DIMERS FORMED FROM THE FRAGMENTATION OF TRINUCLEAR CLUSTERS

INTRODUCTION

The ability of a compound to activate small molecules such as CO and H_2 has been correlated with its catalytic potential.[95-96] The major reaction type for activating a molecule by a metal center is termed oxidative addition.

Oxidative addition is the term used to describe reactions in which a molecule A-B, adds to a metal complex during which the metal is oxidized and the incoming molecule is reduced. It can either be a one-electron or two-electron oxidation.[95]

$$L_nM + A{-}B \rightleftharpoons L_n\overset{A}{\underset{|}{M}}{-}B \text{ or } [L_n\overset{A}{\underset{|}{M}}]^+[B]^-$$

In all oxidative addition reactions, therefore, there is an increase in both the coordination number and the formal oxidation state of the metal. The reverse of the oxidative-addition reaction is termed reductive elimination. A number of different molecules may be oxidatively added to a metal complex. A few examples are: H_2, X_2(X= Cl, Br, I), HX (X= Cl, Br, I, SH, , OCH_3, CCR, CN), CH_3I, PhI, CH_2Cl_2, RCN, Ph_3PAuCl, $HgCl_2$, R_3MCl (M= Sn, Si), and RCCR.[96] It is important to note that these terms only refer to classes of reactions and not particular mechanisms. For example, in oxidative addition reactions, ionic, radical,

and concerted mechanisms are known.[96]

There are many examples of oxidative addition reactions on mononuclear metal centers. The classic example is provided by the Ir^{I} complex, [trans-$Ir(Cl)(CO)(PPh_3)_2$], known as "Vaska's complex".[96] This complex undergoes reactions with molecules such as CH_3I, HCl, H_2, and O_2 to yield six-coordinate Ir^{III} complexes: $[Ir(Cl)(CO)(PPh_3)_2(CH_3)(I)]$, $[Ir(Cl)_2(CO)(PPh_3)_2(H)]$, and $[Ir(Cl)(CO)(PPh_3)_2(Y)_2]$ (Y= H, O) respectively.

In the case of bimetallic complexes, examples are much less common. Three routes have been observed for the addition of a group A-B to a dimeric species: cleavage of a metal-metal bond with concurrent one-electron oxidation of each metal; formation of a metal-metal bond with the concurrent one-electron oxidation of each metal; or oxidative addition at only one metal center resulting in a mixed-valence dimer.[97]

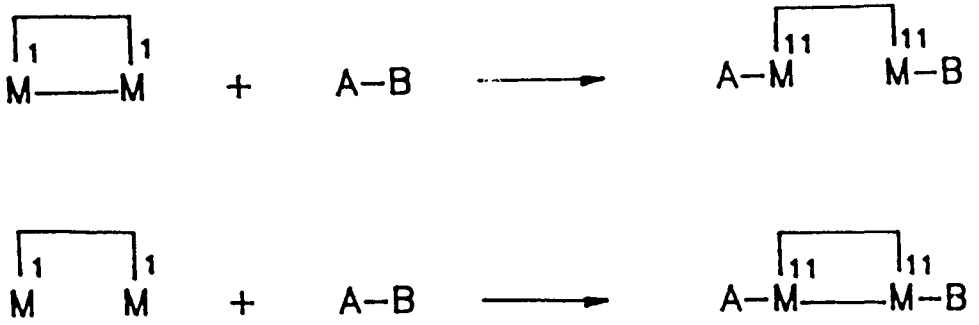

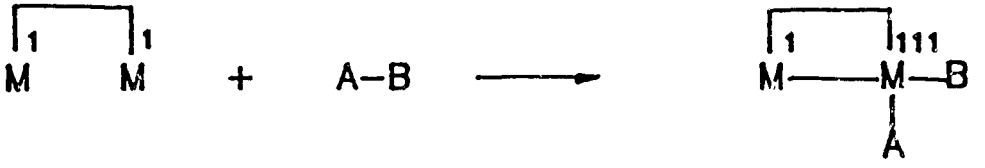

Examples of each type are: reaction of X_2 (X= Cl, Br, I) with $[Mo_2(O^iPr)_6]$ (Mo-Mo triple bond) to give $[Mo_2(O^iPr)_6(X)_4]$ in which the two molybdenum atoms are linked by a single bond;[98] reactions of CH_2X_2 (X= Cl, Br), X_2 (X= Br, I), RI (R= Me, Et) with gold(I) ylide complexes $[Au_2(\mu\text{-}CH_2PR_2CH_2)_2]$ (R= Me, Ph) to afford $[Au_2(\mu\text{-}CH_2PR_2CH_2)_2(X)(Y)]$, gold(II) dimers with single Au-Au bonds,[99-102] oxidative addition of halogens and alkyl halides to pyrazolyl-diiridium complexes such as $[Ir_2(\mu\text{-}C_3N_2H_4)(COD)_2]$;[103-105] and the addition of CH_3I to $[Rh_2(\mu\text{-}{}^tBuS)_2(CO)(PMe_2Ph)_2]$[106] and $[Pt_2(\mu\text{-dmpm})(Me)_4]$[107] which occurs only at one metal center. In the second case the mixed-valent compound, $[Pt_2(\mu\text{-dmpm})(Me)_4(Me)(I)]$, is only an intermediate.

Another type of reaction common to organometallic species is the insertion reaction.[108] In insertion reactions, an atom or a molecule inserts itself between two atoms initially bound together. There is no increase in the oxidation number of metal centers. As with oxidative addition the

term insertion has no mechanistic implications. The reverse of the insertion reaction is termed extrusion.

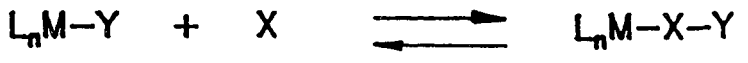

In terms of bimetallic systems, in insertion reactions, a small molecule is inserted into a metal-metal bond. Insertions of CS_2, SO_2, $MeO_2CC{\equiv}CCO_2Me$ into the metal-metal bonds of $[Pt_2(\mu\text{-dppm})_2(C{\equiv}CR)_2]$ provide good examples of this type of reaction.[109]

Previously reported Pd(I) and Pt(I) dimers with bridging phosphine ligands, for example $[M_2(\mu\text{-}R_2PCH_2PR_2)_2Cl_2]$ (M= Pd, Pt; R= Me, Ph), have been shown to contain unusually reactive metal-metal bonds. They oxidatively add and insert a variety of reagents to produce a number of interesting compounds. Oxidative addition of CH_3I, I_2, and insertions of carbon monoxide, isocyanides, sulphur, sulphur dioxide and diazonium cations have all been reported.[110-115] The reason for this reactivity was attributed to the coordinative unsaturation of the M(1) centers (two directly bonded 16 electron centers). One of these dimers, $[Pt_2(\mu\text{-}H)(H)_2(dppm)_2]^+$,[116] was also shown to catalyze hydrogenation and water-gas shift reactions.

Recently, a few research groups have shown that the usually inert three-electron donor phosphido bridge is susceptible to several reactions. Two examples of reactions that lead to the cleavage of the μ-PPh_2 group are: the reaction of $[M_2(\mu\text{-}PPh_2)_2(CO)_8]$ (M= Mo, W) with one equivalent of $LiBEt_3H$ to yield $[M_2(\mu\text{-}PPh_2)(CO)_8(PPh_2H)]^-$ (M= Mo, W),[117-119] and the reaction of $[WRh(\mu\text{-}PPh_2)_2(CO)_5(H)(PPh_3)]$ with C_2H_4 to afford $[WRh(\mu\text{-}PPh_2)(CO)_5(PPh_3)(PPh_2Et)]$.[120]

The Pd(I) and Pt(I) dimers formed from the fragmentation of the trinuclear clusters, $[M_3(\mu\text{-}X)(\mu\text{-}PPh_2)_2(PR_3)_3]^+$ (M= Pd, Pt), contain two metal centers that are held in close proximity by two flexible and strongly binding bridges; therefore, they should, in principle, exhibit similar reaction chemistry to the palladium and platinum examples cited. The reactions of $[M_2(\mu\text{-}PPh_2)(\mu\text{-}R_2PCH_2PR_2)(PPh_3)_2]^+$ (M= Pd, Pt; R= Ph, Me) dimers, discussed in this chapter, were concentrated on three areas:

1) Reaction chemistry of the metal-metal bonds

2) Reaction chemistry of the phosphido-bridges

3) Substitution chemistry of the terminal phosphine ligands

Unfortunately, these dimers were not as reactive as their previously reported analogues.

RESULTS AND DISCUSSION

$[M_2(\mu\text{-}PPh_2)(\mu\text{-}R_2PCH_2PR_2)(PPh_3)_2]^+$ (M= Pd, Pt) complexes proved to contain a very unreactive metal-metal bond. The M(I)-M(I) bond is stable towards oxidative addition as well as insertion reactions. $[Pd_2(\mu\text{-}PPh_2)(\mu\text{-}dppm)(PPh_3)_2]^+$ does not react with C_4H_6, $HCCCO_2Me$, CH_2N_2, CO, CH_3I, CH_2I_2, proton or hydride sources. $[Pd_2(\mu\text{-}PPh_2)(\mu\text{-}dppm)(PPh_3)_2]^+$ is also not susceptible to oxidation by H_2O_2. Similarly $[Pt_2(\mu\text{-}PPh_2)(\mu\text{-}dppm)(PPh_3)_2]^+$ does not react with a host of reagents, among them: CH_2I_2, Bu^tOOH, $PhCH_2Br$, H_2, CO, HCl, $LiBEt_3H$, $NOBF_4$, $MeO_2CC{\equiv}CCO_2Me$.

At first, this lack of reactivity was thought to be due to the steric bulk of the ligands. This was supported by studies done on other dinuclear systems which had shown that using a ligand with a smaller steric effect such as $Me_2PCH_2PMe_2$ (dmpm) can lead to different and in some ways enhanced reactivity compared to similar dppm complexes. But this proved not to be the case as the less sterically hindered analogue of the platinum dimer, $[Pt_2(\mu\text{-}PPh_2)(\mu\text{-}dmpm)(PPh_3)_2]^+$, was as unreactive towards small molecules. For example, no reaction occurs with CO and H_2 even at very high temperatures and pressures.

Other compounds with similar structures: $[Pt_2(\mu$-

S)$(PPh_3)_3(CO)]$, $[Pt_2(\mu\text{-}S)(\mu\text{-}dppm)(PPh_3)_2,]$and $[Pt_2(\mu\text{-}SMe)(\mu\text{-}dppm)(PPh_3)_2]^+$ are reported to be very inert towards oxidative addition of CH_3I and insertion reaction of CO as well.[121] This lack of reactivity was unexpected since the isoelectronic dimer $[Ir_2(\mu\text{-}O)(NO)_2(PPh_3)_2]$ was shown to react with halogens and mercuric halides to break the metal-metal bond.[122-123] Also, it has been shown that $[Ir_2(\mu\text{-}PBu^t_2)(\mu\text{-}H)(CO)_2(PBu^t_2H)_2]$ reacts reversibly with H_2 to give the unsymmetrical trihydride $[Ir_2(\mu\text{-}PBu^t_2)(\mu\text{-}H)_2(CO)_2(PBu^t_2H)_2(H)]$.[124]

The phosphido bridges in $[M_2(\mu\text{-}PPh_2)(\mu\text{-}dppm)(PPh_3)_2]^+$ (M= Pd, Pt) are also inert failing to react with reagents such as $LiBEt_3H$ which caused $\mu\text{-}PPh_2$ opening as reported by Wojcicki.[125] The results for the platinum μ-S dimers mentioned, in conjuction with our results suggest that the $Pt_2(\mu\text{-}X)$ (X= S, PPh_2) core is remarkably stable. The reasons for this stability are not clearly understood.

The only reactive portion in $[M_2(\mu\text{-}PPh_2)(\mu\text{-}dppm)(PPh_3)_2]^+$ (M= Pd, Pt) dimers is the terminal phosphines which may be easily replaced by other ligands such as phosphines, CN, I, and Bu^tNC. $[M_2(\mu\text{-}PPh_2)(\mu\text{-}dppm)(PPh_3)_2]^+$ (M= Pt, Pd) reacts with excess PEt_3 and PBu^n_3 to yield $[M_2(\mu\text{-}PPh_2)(\mu\text{-}dppm)(PR_3)_2]^+$ (R= Et, Bu^n respectively).

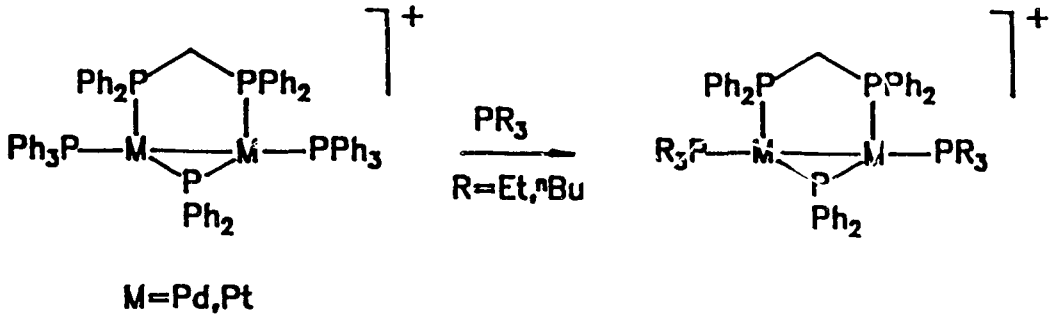

These compounds were characterized by $^{31}P\{^{1}H\}$ NMR spectroscopy. The NMR peak patterns are similar to the starting material but with different shifts and coupling constants (see chapter seven for values).

$[Pd_2(\mu\text{-}PPh_2)(\mu\text{-dppm})(PPh_3)_2]^+$ reacts with KCN under reflux conditions to afford $[Pd_2(\mu\text{-}PPh_2)(\mu\text{-dppm})(PPh_3)(CN)]$.

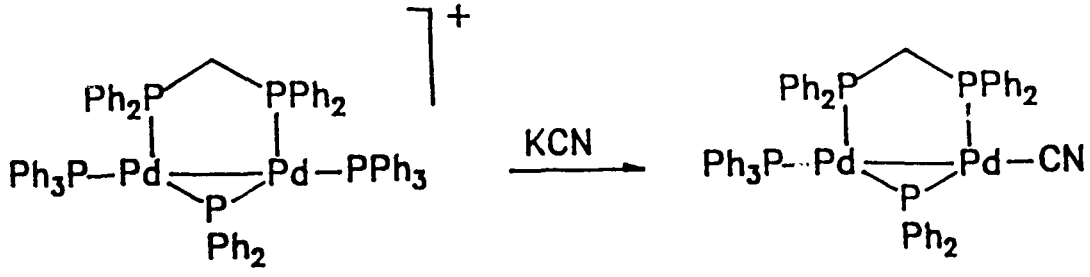

This reaction is very slow and even after long periods of reflux does not go to completion. The presence of the monosubstituted product is evident from the changes in the

distinctive, low-field, bridging μ-PPh_2 resonances (figure **4-1**). In this case it becomes a doublet of doublets of doublets from coupling to three different phosphorus nuclei. The coupling constants range from 15 Hz for the phosphorus-phosphorus cis coupling to 204 Hz and 255 Hz for trans coupling to the two ends of the dppm ligand. The multiplet at 97 ppm belongs to μ-PPh_2 in the starting material, $[Pd_2(\mu\text{-}PPh_2)(\mu\text{-}dppm)(PPh_3)_2]^+$. The high-field peaks could not be clearly distinguished due to overlap with the starting dimer peaks. In contrast to $[Pd_2(\mu\text{-}PPh_2)(\mu\text{-}dppm)(PPh_3)_2]^+$, $[Pt_2(\mu\text{-}PPh_2)(\mu\text{-}dppm)(PPh_3)_2]^+$ does not react with CN^- even under very severe conditions.

Excess CH_3I reacts with $[Pt_2(\mu\text{-}PPh_2)(\mu\text{-}dppm)(PPh_3)_2]^+$ to yield $[Pt_2(\mu\text{-}PPh_2)(\mu\text{-}dppm)(PPh_3)(I)]$. Some $[PPh_3CH_3I]$ is also formed.

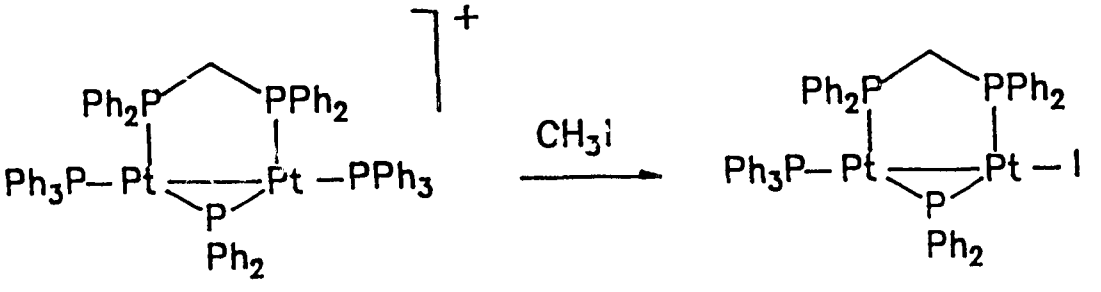

This compound was characterized by its $^{31}P\{^1H\}$ NMR spectrum. The $^{31}P\{^1H\}$ spectrum of the complex and a computer simulation

Figure 4-1

The Low-Field Portion of the $^{31}P\{^{1}H\}$ NMR spectrum of $[Pd_2(\mu\text{-}PPh_2)(\mu\text{-}dppm)(PPh_3)(CN)]$

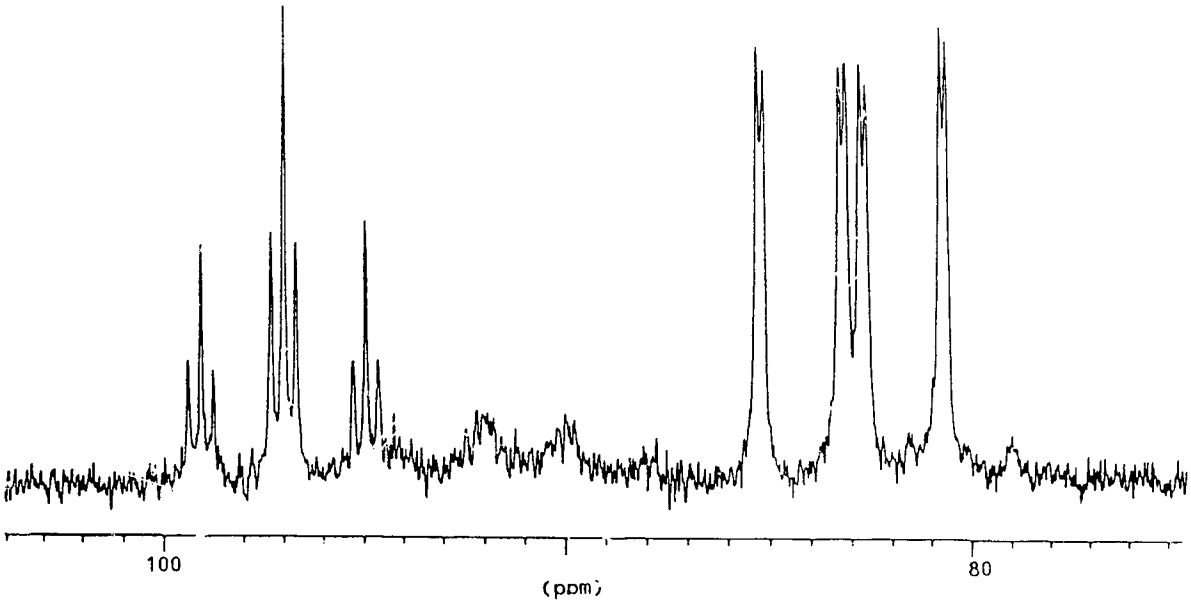

are shown in figure 4-2. The spectrum is essentially first order and most of the parameters may be extracted directly from the spectrum. For the analysis of the spectrum the three different isotopomers of the complex have to be considered. The center peak at 16.2 ppm (μ-PPh_2) is a doublet of doublets from coupling to the two different ends of the dppm molecule. The coupling constants are 376 Hz and 270 Hz respectively. The major side-bands are two sets of doublets of doublets of doublets because of the two different types of the one spin-active platinum present. The platinum-phosphorus coupling constants are 2036 Hz and 2863 Hz. The isotopomer with two spin-active platinums gives rise to a triplet of doublets of doublets. The center peak at -131.5 ppm (PPh_3) is a doublet (coupled to one end of dppm) with a coupling constant of 8 Hz. The side-bands are again two sets of doublets of doublets with one and two bond platinum-phosphorus coupling constants of 3688 Hz and 614 Hz. The peak at -134.5 ppm corresponds to that end of the dppm ligand cis to the terminal triphenylphosphine. The center peak is a doublet of doublets of doublets from coupling to the terminal phosphine, the phosphido bridge and the other end of the dppm ligand. The coupling constants are 8 Hz, 270 Hz, and 59 Hz respectively. Again, the side-bands are two sets of doublets of doublets of doublets of doublets arising from the the two different isotopomers with

Figure 4-2

The $^{31}P\{^{1}H\}$ NMR Spectrum of
$[Pt_2(\mu\text{-}PPh_2)(\mu\text{-}dppm)(PPh_3)(I)]$

a) simulated b) observed

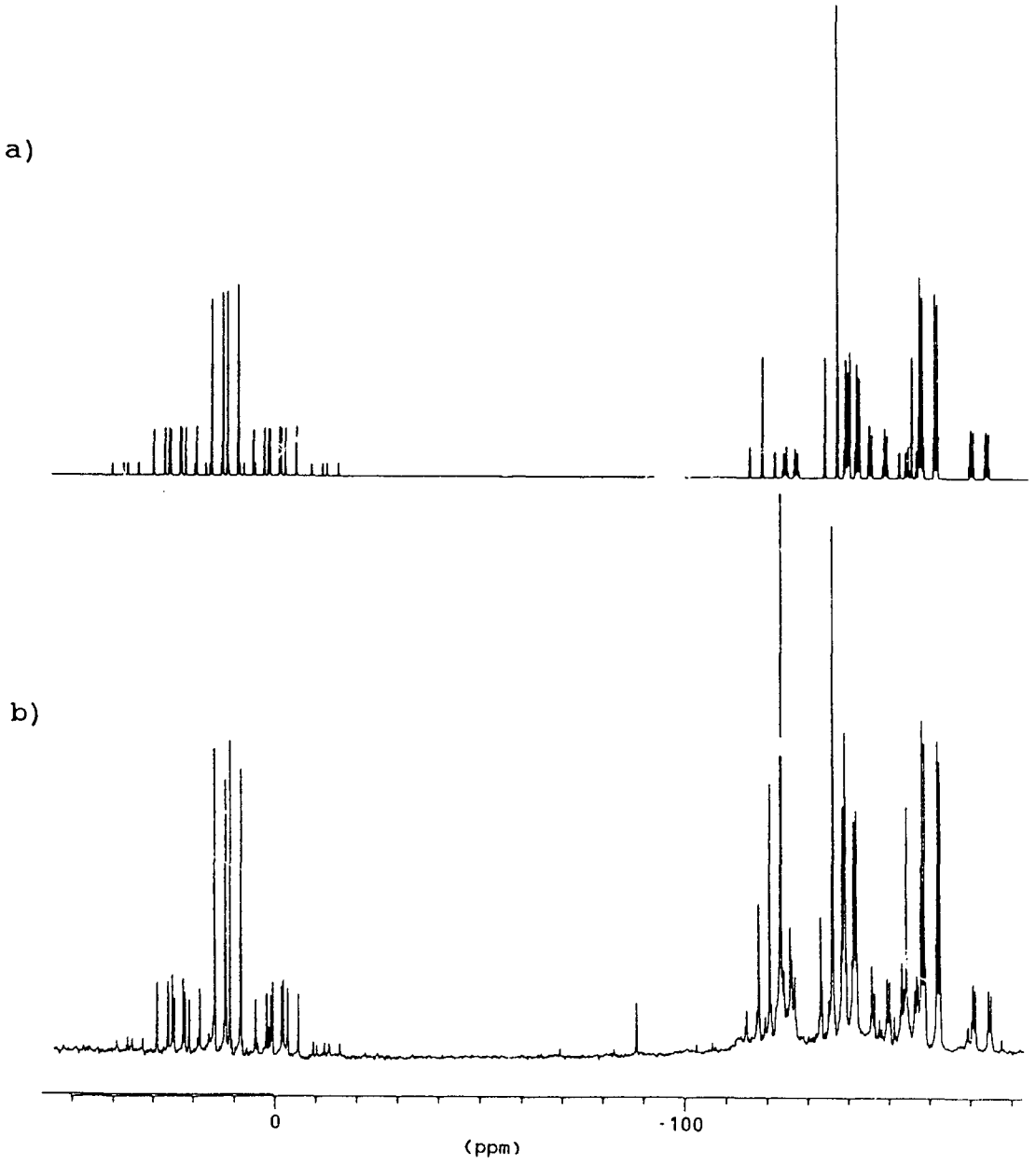

one spin-active platinum. The one-bond and two-bond coupling constants are 3020 Hz and 59 Hz respectively. The phosphorus-phosphorus coupling constant between the ends of the dppm ligand and two-bond phosphorus-platinum coupling constant are similar in magnitude; therefore, the multiplets appear almost as doublets of doublets of triplets. The same explanation can be used for the peak at -153.1 ppm which belongs to that end of dppm ligand cis to the iodide. The peak at -119 ppm belongs to $[PPh_3CH_3][I]$ contaminant present. $[Pt_2(\mu\text{-}PPh_2)(\mu\text{-dppm})(PPh_3)I]$ could not be isolated because in solution it decomposes to $[PPh_3CH_3][I]$ and $[PtI_2(dppm)]$. $[PtI_2(dppm)]$ was identified by its identical NMR parameters to reported values.[126] At the early stages of the reaction not much side products are formed, but upon sitting in solution in the presence of CH_3I, the product, over a period of hours, decomposes to primarily yield $[PtI_2(dppm)]$. $[Pt_2(\mu\text{-}PPh_2)(\mu\text{-dppm})(PPh_3)I]$ in solution, in the absence of CH_3I, reverts back to $[Pt_2(\mu\text{-}PPh_2)(\mu\text{-dppm})(PPh_3)_2]^+$ which implies the existence of an equilibrium between the two compounds. $[Pt_2(\mu\text{-}PPh_2)(\mu\text{-dppm})(PEt_3)_2]^+$ also reacts with excess CH_3I to produce the monosubstituted product. This reaction, however, proceeds much slower than the PPh_3 analogue (twenty four hours in contrast to six hours) as followed by $^{31}P\{^1H\}$ NMR spectroscopy. This is not surprising since PEt_3 is a more

basic ligand and more strongly bound to the metal, making its substitution more difficult. $[Pt_2(\mu\text{-}PPh_2)(\mu\text{-}dmpm)(PPh_3)_2]^+$ reacts with excess CH_3I in less than one hour to produce a similar product. The smaller steric bulk of the dmpm ligand with respect to dppm is probably the reason for the faster rate of substitution.

Reaction of $[Pt_2(\mu\text{-}PPh_2)(\mu\text{-}dppm)(PPh_3)_2]^+$ with I_2 leads to the break up of the dimer to form $[PtI_2(dppm)]$ as indicated by $^{31}P\{^1H\}$ NMR spectroscopy. This behaviour is similar to the reported reaction of $[Pt_2(\mu\text{-}S)(PPh_3)_3(CO)]$ with I_2 which breaks up the Pt-Pt bond to form $[PtI_2(PPh_3)_2]$.[127]

The terminal triphenylphosphines in $[M_2(\mu\text{-}PPh_2)(\mu\text{-}dppm)(PPh_3)_2]^+$ (M= Pd, Pt) may also be replaced with Bu^tNC. This is clearly indicated by $^{31}P\{^1H\}$ NMR spectroscopy where the resonance due to the terminal phosphines disappears and its coupling with other resonances is lost. The $^{31}P\{^1H\}$ NMR spectrum of $[Pt_2(\mu\text{-}PPh_2)(\mu\text{-}dppm)(Bu^tNC)_2]^+$ is shown in figure **4-3** as an example. This substitution is, however, reversible and upon recrystallization the starting material is isolated. This dynamic behaviour was not further investigated.

Figure 4-3

The $^{31}P\{^{1}H\}$ NMR Spectrum of
$[Pt_2(\mu\text{-}PPh_2)(\mu\text{-dppm})(Bu^tNC)_2]_2[C_2O_4]$

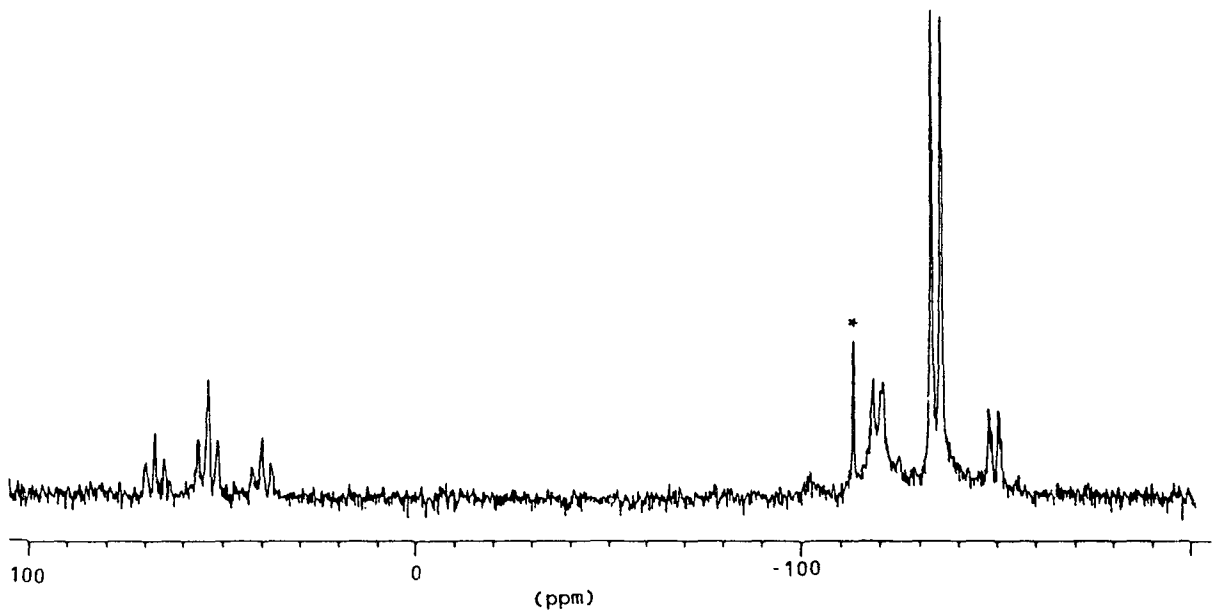

*= Impurity

CHAPTER FIVE

PHOSPHIDO-BRIDGED TRINUCLEAR RHODIUM AND IRIDIUM CLUSTERS AND THEIR REACTIONS

Introduction

Similar to the palladium and platinum clusters discussed previously, the number of triangular rhodium and iridium clusters in general, and phosphido-bridged ones in particular, is limited. Examples of non-phosphido bridged clusters include: $[M_3(\mu^3\text{-}X)_2(CO)_6]^-$ (M= Rh, Ir; X= S, Se),[128-129] $[M_3(C_5H_5)_3(CO)_3]$ (M= Rh, Ir),[130-131] $[M_3(\mu\text{-}CH)_2(C_5H_5)_3]$ (M= Rh, Ir),[132-133] $[Rh_3(\mu\text{-}CH)(C_5H_5)_3(\mu\text{-}CO)_2]$,[134] $[Ir_3(CO)_6(Ph)(\mu^3\text{-}PPh)(\mu\text{-dppm})]$,[135] and $[Ir_3(Ph_2P(CH_2)_3PPh_2)_3(H)_7(CO)][BF_4]_2$.[136]

Haines and co-workers have shown that the thermal decomposition of $[Rh(H)(CO)(PPh_3)_3]$ in nonane at 120°C affords green crystals of $[Rh_3(\mu\text{-}PPh_2)_3(CO)_3(PPh_3)_2]$ in high yield.[137]

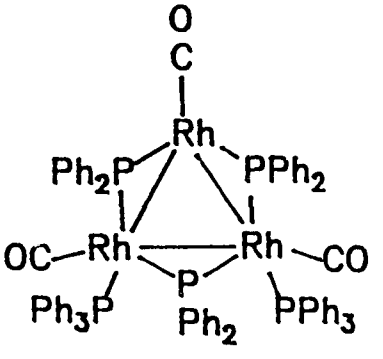

The crystal structure of $[Rh_3(\mu\text{-}PPh_2)_3(CO)_3(PPh_3)_2]$ is based on a triangle of rhodium atoms where the unique rhodium, as implied by the eighteen electron rule, is coordinatively

unsaturated. Two of the phosphido-bridges and the CO on the unique rhodium are essentially co-planar with the trirhodium plane, whereas, the unique phosphido-bridge is almost orthogonal to it. The dihedral angle between the planes is 97.2°. The rhodium-rhodium bond distances are 2.79Å, 2.82Å, and 2.74Å. The coordinative unsaturation of one of the rhodiums was attributed to the phenyl group on the orthogonal phosphido-bridge blocking a coordination site. Despite the interesting nature of $[Rh_3(\mu\text{-}PPh_2)_3(CO)_3(PPh_3)_2]$, no reactivity studies of this complex have been reported to date.

The reaction of $[Rh_2(CO)_4Cl_2]$ with two equivalents of $[PPh_2H]$ in benzene in the presence of a base such as diethyl amine affords the trinuclear species $[Rh_3(\mu\text{-}PPh_2)_3(CO)_5]$.[138] The crystal structure is similar to that of $[Rh_3(\mu\text{-}PPh_2)_3(CO)_3(PPh_3)_2]$. The Rh-Rh bond lengths are, however, slightly longer. The reaction of $[Rh_2(CO)_4Cl_2]$ with two equivalents of PPh_2H in the absence of a base yields $[Rh_3(\mu\text{-}PPh_2)_3(\mu\text{-}Cl)_2(\mu\text{-}CO)(CO)_3]$.[139] This cluster has the same framework as $[Rh_3(\mu\text{-}PPh_2)_3(CO)_5]$ except that two of the Rh-Rh bonds are also bridged by chloro-groups while the third is additionally bridged by a CO group. The chlorides may be easily abstracted with a base in the presence of CO to produce $[Rh_3(\mu\text{-}PPh_2)_3(CO)_5]$, which in turn reacts with

CCl_4 to regenerate the original compound. Later investigation has shown that the reaction of $[Rh(CO)_4Cl_2]$ with $[PPh_2H]$ is far more complex than originally reported. Depending on the reaction conditions used any one of a number of trinuclear rhodium clusters differing in the number of carbon monoxide ligands will form.[140] $[Rh_2(CO)_4Cl_2]$ also reacts with one equivalent of $[Bu^t_2PLi]$ in THF at -78°C to yield $[Rh_3(\mu\text{-}Bu^t_2P)_3(CO)_3]$.[141] The structure of this cluster, as revealed by X-ray crystallography, differs from the other phosphido-bridged rhodium trimers in two ways. The central Rh_3P_3 core is virtually planar, and the rhodium metal centers are all coordinatively unsaturated with each having only one terminal CO bonded to it. Steric factors were proposed to account for the structural differences. The tertiary butyl groups allow room for coordination of only one CO on each rhodium and also prevent major distortions of the Rh_3P_3 framework from planarity. Bubbling CO through a solution of $[Rh_3(\mu\text{-}Bu^t_2P)_3(CO)_3]$ in THF or hexane results in the reversible addition of two moles of CO to produce $[Rh_3(\mu\text{-}Bu^t_2P)_3(\mu\text{-}CO)(CO)_4]$.[142] This compound slowly loses CO under N_2 atmosphere and more rapidly under vacuum.

The only example of a trinuclear phosphido-bridged iridium cluster in the literature to date was reported by Arif et

al. in 1987.[143] $[Ir_4(CO)_{12}]$ was reacted with $[Bu^t_2PH]$ in refluxing toluene to give two compounds: the dark red-purple $[Ir_3(\mu\text{-}Bu^t_2P)_3(CO)_5]$ and orange $[Ir_2(\mu\text{-}H)(\mu\text{-}Bu^t_2P)(Bu^t_2Ph)_2(CO)_2]$.

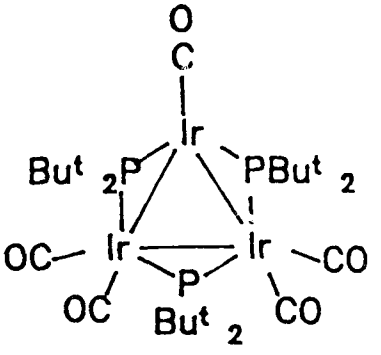

The structure of the cluster is similar to its rhodium analogue. The Ir-Ir bond distances are 2.729Å, 2.812Å, and 2.705Å.

In previous chapters the reactions of phosphido-bridged trinuclear palladium and platinum clusters with ligands such as dppm and Bu^tNC were discussed. This chapter describes the synthesis of a novel triiridium cluster, $[Ir_3(\mu\text{-}PPh_2)_3(CO)_5]$, and discusses the reactions of that cluster and its rhodium analogue, $[Rh_3(\mu\text{-}PPh_2)_3(CO)_3(PPh_3)_2]$, with similar ligands.

RESULTS AND DISCUSSION

$[Rh_3(\mu\text{-}PPh_2)_3(CO)_3(PPh_3)_2]$, which was prepared by refluxing $[Rh(H)(CO)(PPh_3)_3]$ in nonane, reacts with dppm to give the substitution product $[Rh_3(\mu\text{-}PPh_2)_3(\mu\text{-dppm})(CO)_3]$.

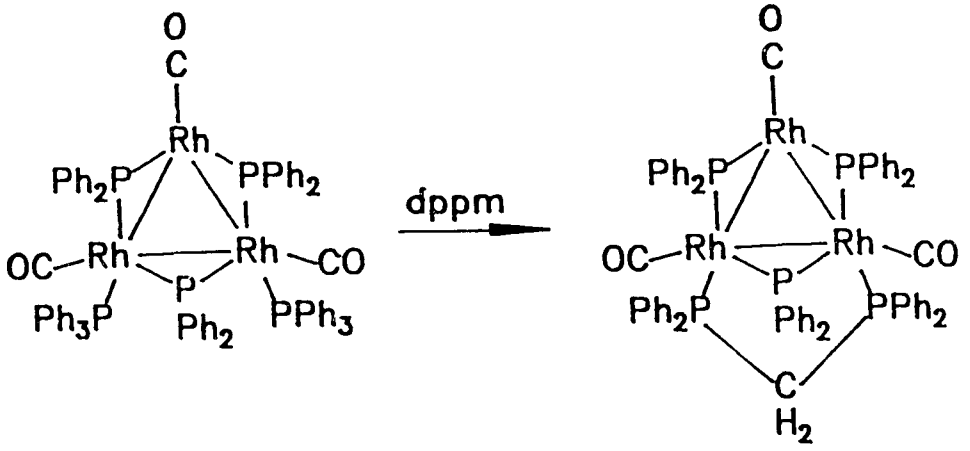

This is in contrast to the palladium and platinum phosphido-bridged clusters, $[M_3(\mu\text{-}X)(\mu\text{-}PPh_2)_2(PPh_3)_3]^+$, which upon reaction with dppm fragment to yield dimeric species as was described in chapter three. This difference could be explained as follows: the stable electron count for the triangular palladium and platinum clusters is 44; therefore, addition of two electrons would be into a strongly antibonding molecular orbital which leads to fragmentation. In the case of the the rhodium cluster, the accepted stable electron count is 48; thus the addition of an extra two electrons to the 46-electron $[Rh_3(\mu\text{-}PPh_2)_3(CO)_3(PPh_3)_2]$ would be into a bonding molecular orbital which does not lead to fragmentation.

The $^{31}P\{^{1}H\}$ NMR spectrum of $[Rh_3(\mu\text{-}PPh_2)_3(\mu\text{-}dppm)(CO)_3]$ and a computer simulation are shown in figure **5-1**. This complex second order spectrum consists of three sets of peaks. The two equivalent phosphido bridges give rise to the multiplet at 152.1 ppm. The resonance at 74.0 ppm belongs to the unique phosphido bridge coupling to the trans dppm ligand, the two cis phosphido bridges, and two rhodiums. The size of the phosphorus-phosphorus coupling constants (151 Hz, and 26 Hz) reflects the corresponding orientations of the groups to each other. The multiplet at -127.1 ppm belongs to the dppm ligand. Only a few of the coupling constants may be directly extracted from the spectrum. Computer simulation provides the rest of the parameters (for values see chapter seven). A suitable crystal of $[Rh_3(\mu\text{-}PPh_2)_3(\mu\text{-}dppm)(CO)_3]$ was obtained and its crystal structure was determined by Dr. Browning (figure **5-2**). The crystallographic parameters are listed in table **5-1**. Table **5-2** lists a number of selected bonds and angles. The structure of this compound is similar to the structure of the starting material. There is a plane of symmetry going through the unique rhodium, the CO ligand bound to it, the unique phosphido-bridge, and the methylene carbon of the dppm ligand. The Rh-Rh bond distances are 2.716Å and 2.765Å, well within the accepted metal-metal bond distances. The dppm ligand and the unique phosphido-bridge are essentially trans to each other and the planes formed by

Figure 5-1

The $^{31}P\{^{1}H\}$ NMR Spectrum of
$[Rh_3(\mu\text{-}PPh_2)_3(\mu\text{-}dppm)(CO)_3]$

a) simulated b) observed

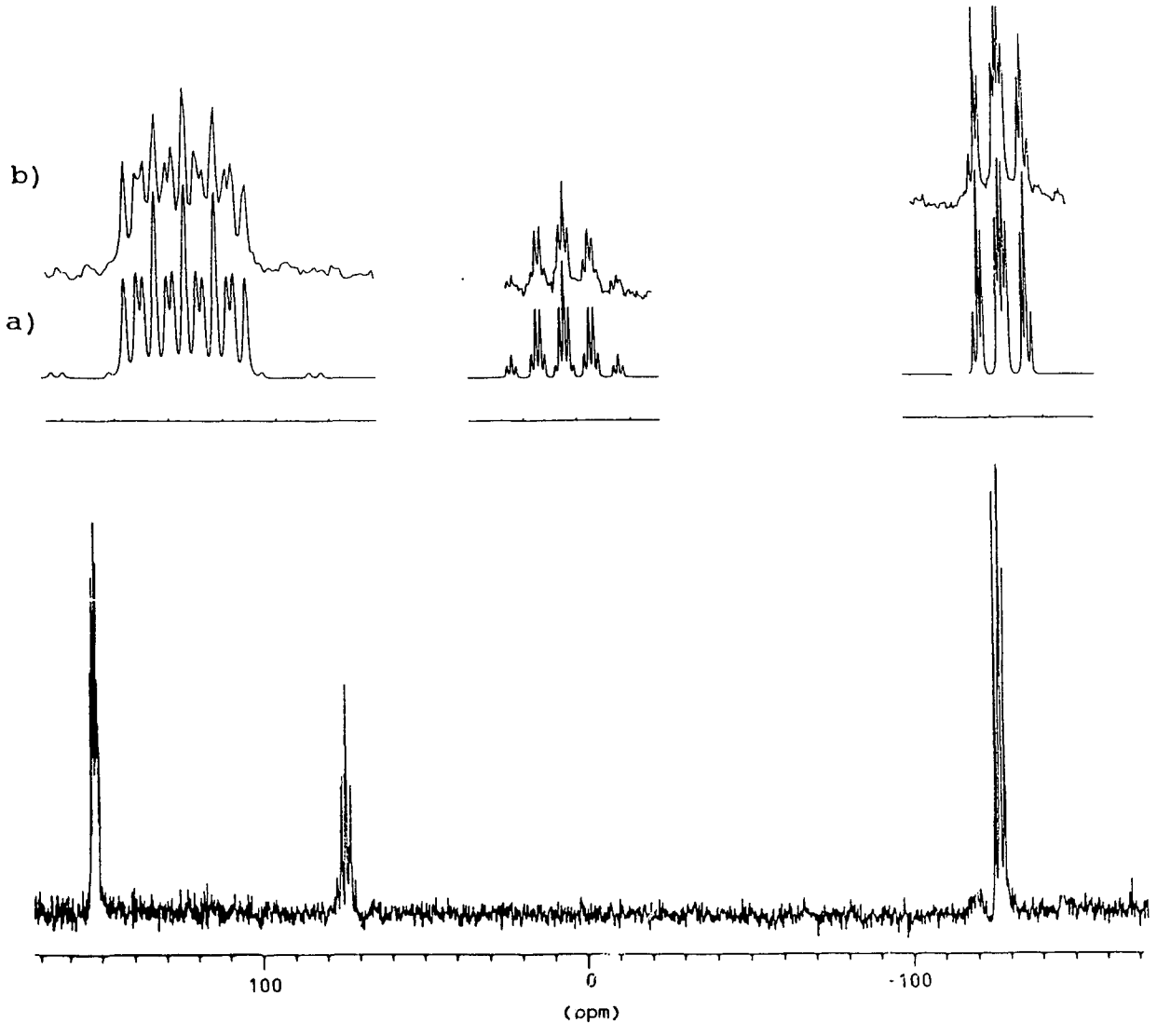

Figure 5-2

The Molecular Structure of
$[Rh_3(\mu\text{-}PPh_2)_3(\mu\text{-dppm})(CO)_3]$

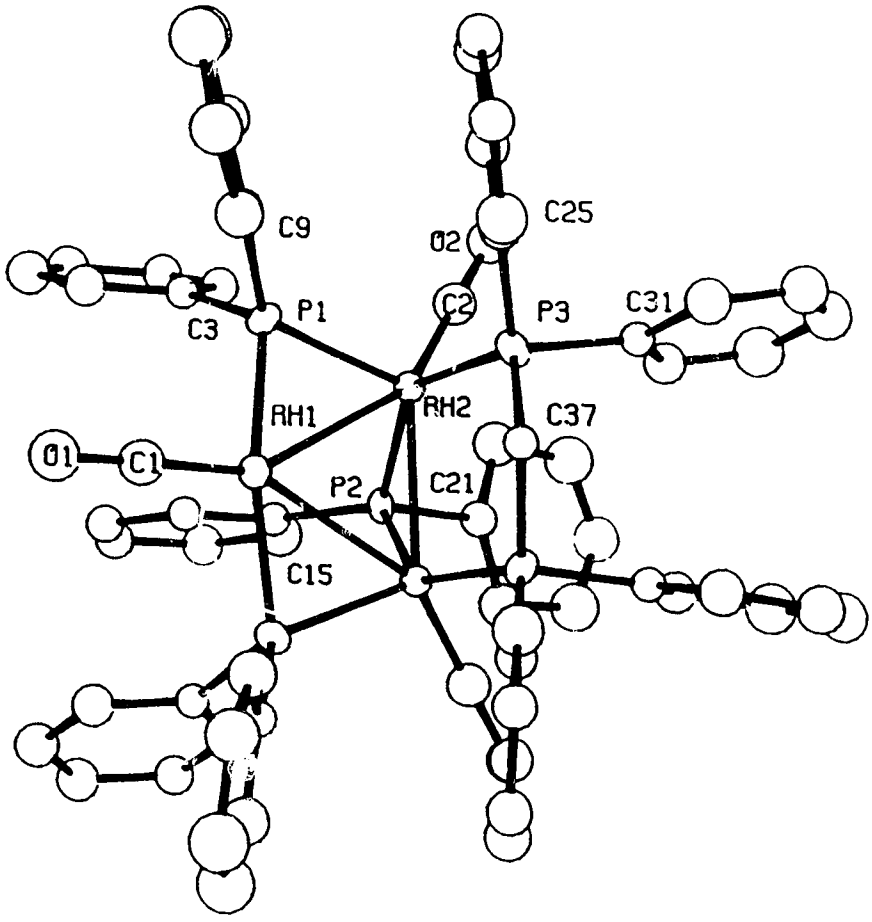

Table 5-1

Crystallographic Parameters for
$[Rh_3(\mu\text{-}PPh_2)_3(\mu\text{-dppm})(CO)_3]$

formula	$C_{64}H_{52}O_3P_5Rh_3$
fw	1333
space group	Pnma
a (Å)	24.031(6)
b (Å)	25.069(9)
c (Å)	11.117(4)
α (degrees)	90.00
β (degrees)	90.00
ϒ (degrees)	90.00
volume ($Å^3$)	6697
Z	4
calculated density (g/cm^3)	1.3108
μ (cm^{-1})	8.74
radiation (Å)	Mo 0.71069
temperature (K)	295
scan method	ω/2θ
total reflections collected	2579
parameters refined	113
R	0.106
R_w	0.107

Table 5-2

Selected Bond Lengths(Å) and Angles(°) for $[Rh_3(\mu\text{-}PPh_2)_3(\mu\text{-dppm})(CO)_3]$

Atoms	Distance
Rh(2)-Rh(1)	2.716(2)
Rh(2)-Rh(2')	2.765(4)
P(1)-Rh(1)	2.265(8)
C(1)-Rh(1)	1.78(4)
P(1)-Rh(2)	2.286(7)
P(2)-Rh(2)	2.291(7)
P(3)-Rh(2)	2.344(6)
C(2)-Rh(2)	1.742(9)
C(1)-O(1)	1.18(4)
C(2)-O(2)	1.23(2)

Atoms	Angle
Rh(2)-Rh(1)-Rh(2')	59.3(1)
Rh(1)-Rh(2)-Rh(2')	60.4(5)
Rh(1)-P(1)-Rh(2)	75.8(2)
C(1)-Rh(1)-Rh(2)	150.3(1)
P(1)-Rh(2)-Rh(1)	51.7(2)
P(1)-Rh(1)-Rh(2)	52.4(2)
C(1)-Rh(1)-P(1)	98.5(2)
C(2)-Rh(2)-P(1)	103.5(3)
C(2)-Rh(2)-P(2)	99.6(3)
C(2)-Rh(2)-P(3)	95.6(3)
P(2)-Rh(2)-P(3)	139.4(3)
P(2)-Rh(2)-Rh(1)	81.8(2)
P(3)-C(37)-P(3')	109(2)

(Estimated standard deviations are given in parentheses.)

them and the two equivalent rhodium atoms are orthogonal to the tri-rhodium plane (the dihedral angles are 102.95° and 80.04° respectively). The trans arrangement of these ligands is in contrast to the cis configuration of the PPh_3 groups and the unique phosphido-bridge in $[Rh_3(\mu\text{-}PPh_2)_3(CO)_3(PPh_3)_2]$. The reason for this difference is that the cis positions on the equivalent rhodiums, with respect to the phosphido-bridge, point away from each other making bridging by the bidentate ligand (dppm) impossible.

As was mentioned in the introduction there is only one example of a trinuclear phosphido-bridged iridium cluster in the literature. The main reasons for this have been the lack of suitable starting material and an apparent preference for iridium to form dinuclear species. For example, $[Rh_2Cl_2(CO)_4]$ is an often used precursor for cluster synthesis, whereas, the iridium analogue is a highly insoluble polymeric material. Also, while $[Rh(H)(CO)(PPh_3)_3]$ upon pyrolysis forms $[Rh_3(\mu\text{-}PPh_2)_3(CO)_3(PPh_3)_2]$, $[Ir(H)(CO)(PPh_3)_3]$ yields $[Ir_2(\mu\text{-}PPh_2)_2(CO)_6]$.[144] In the search for starting materials to synthesize phosphido-bridged iridium clusters, $[Ir_2(COE)_2(Cl)_2]$ proved to be ideal.

The reaction of $[Ir_2(COE)_2(Cl)_2]$ with carbon monoxide

followed by reaction with diethylamine and PPh_2H affords $[Ir_3(\mu\text{-}PPh_2)_3(CO)_5]$. In solution this compound exists in equilibrium with the hexacarbonyl cluster, $[Ir_3(\mu\text{-}PPh_2)_3(CO)_6]$. Both complexes were only characterized by $^{31}P\{^1H\}$ NMR spectroscopy. These two clusters may be easily interconverted by either bubbling CO through the solution, or pumping on the mixture. The correctness of these assignments were subsequently proved upon the reaction with dppm and full characterization of the product. Addition of dppm to a solution of $[Ir_3(\mu\text{-}PPh_2)_3(CO)_5]$ proceeds with the substitution of two CO molecules to form $[Ir_3(\mu\text{-}PPh_2)_3(\mu\text{-}dppm)(CO)_3]$.

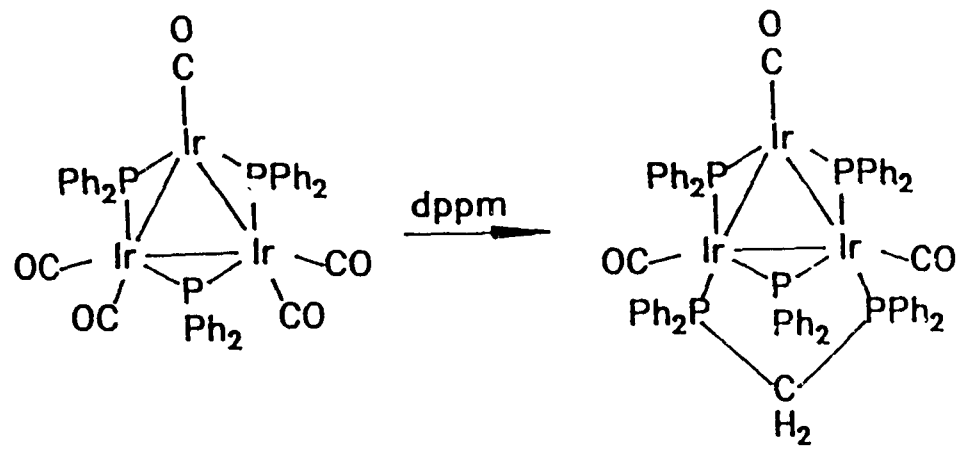

The $^{31}P\{^1H\}$ NMR spectrum of $[Ir_3(\mu\text{-}PPh_2)_3(\mu\text{-}dppm)(CO)_3]$ is shown in figure **5-3**. The peak at 100.7 ppm belongs to the two equivalent $\mu\text{-}PPh_2$ groups coupling to the unique phosphido bridge. The small coupling constant, 24 Hz, is

Figure 5-3

The $^{31}P\{^{1}H\}$ NMR Spectrum of
$[Ir_3(\mu\text{-}PPh_2)_3(\mu\text{-}dppm)(CO)_3]$

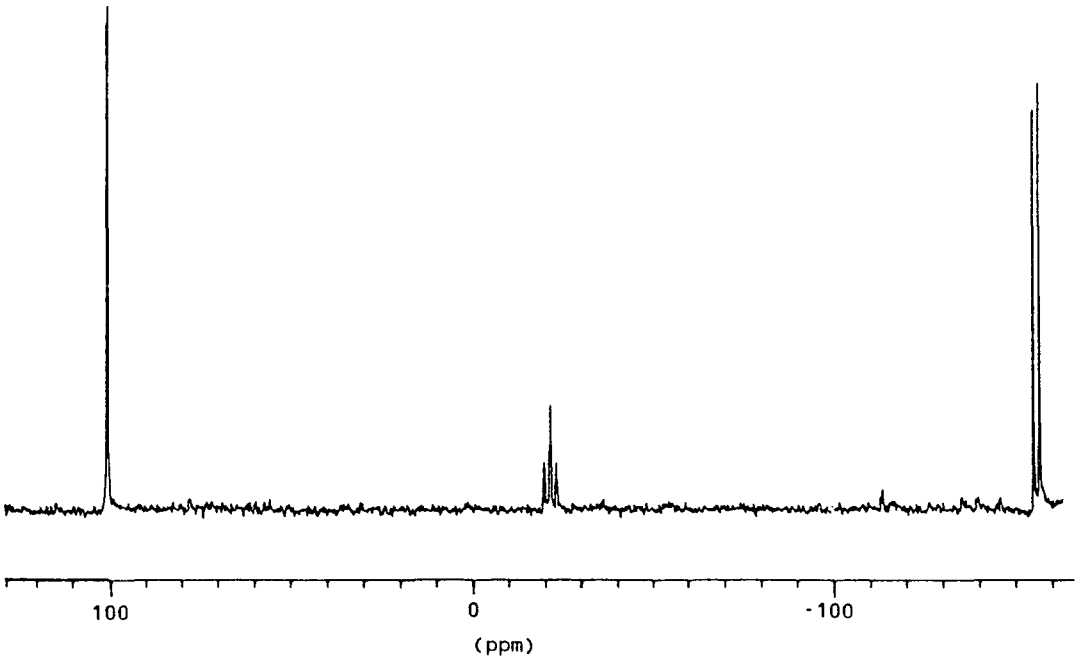

due to the cis arrangement of these groups to each other. The triplet of triplets at -21.7 ppm is due to the unique phosphido bridge. It is coupled to the other phosphido bridges and the dppm ligand trans to it. The coupling constants are 24 Hz and 169 Hz respectively. The other peak is the expected doublet (J= 169 Hz) at -155.9 ppm for the dppm ligand.

The crystal structure of $[Ir_3(\mu\text{-}PPh_2)_3(\mu\text{-}dppm)(CO)_3]$ was determined by Dr. Browning and is depicted in figure **5-4**. Tables **5-3** and **5-4** contain the relevant crystallographic parameters and a number of selected bond lengths and angles respectively. $[Ir_3(\mu\text{-}PPh_2)_3(\mu\text{-}dppm)(CO)_3]$ has nearly the same structure as its rhodium analogue. The metal-metal bond distances are, however, slightly longer. The dihedral angle between the tri-iridium plane and the plane formed by the unique phosphido bridge and the two equivalent iridiums is 103.4°. The dppm-Ir-Ir plane has a dihedral angle of 80.63° with the tri-iridium plane.

In chapter three, fragmentation of platinum clusters $[Pt_3(\mu\text{-}X)(\mu\text{-}PPh_2)_2(PPh_3)_3][BF_4]$ (X= H, Cl) with Bu^tNC were discussed. In contrast to that fragmentation reaction, the reaction between Bu^tNC and $[Ir_3(\mu\text{-}PPh_2)_3(CO)_5]$ proceeds with the addition of the two Bu^tNC molecules to the unsaturated

Figure 5-4

The Molecular Structure of
$[Ir_3(\mu\text{-}PPh_2)_3(\mu\text{-dppm})(CO)_3]$

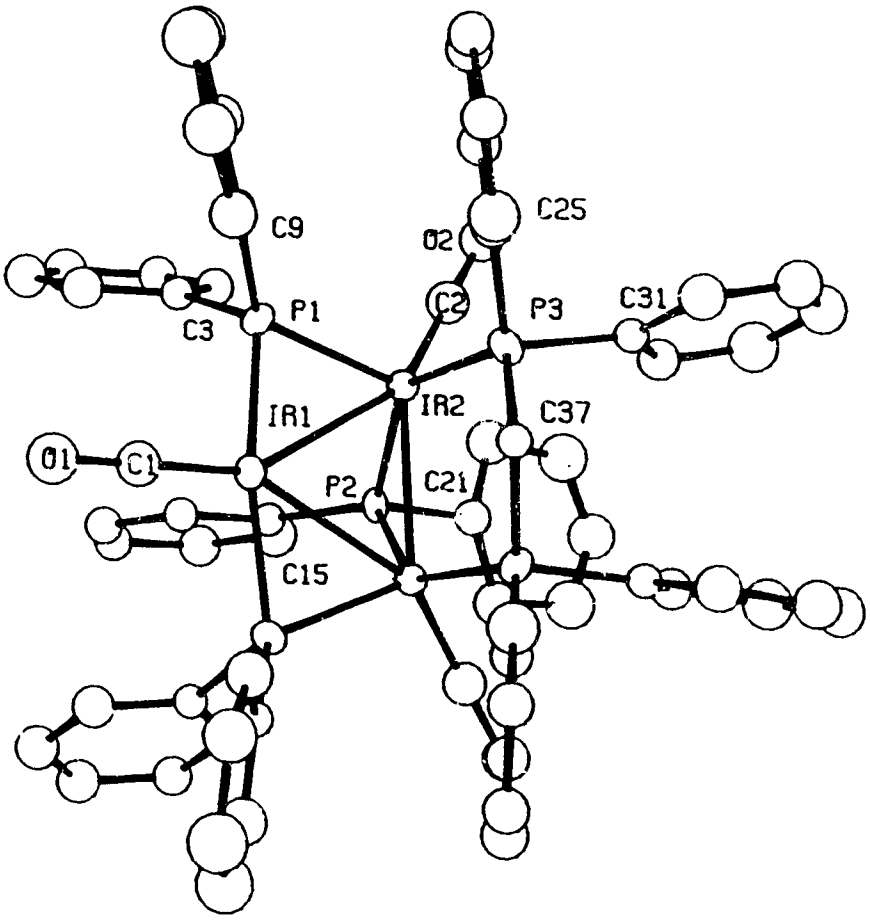

Table 5-3

Crystallographic Parameters for
$[Ir_3(\mu\text{-}PPh_2)_3(\mu\text{-dppm})(CO)_3]$

formula	$C_{64}H_{52}O_3P_5Ir_3$
fw	1601
space group	Pnma
a (Å)	23.963(5)
b (Å)	24.970(5)
c (Å)	11.080(2)
α (degrees)	90.00
β (degrees)	90.00
ϒ (degrees)	90.00
volume ($Å^3$)	6630
Z	4
calculated density (g/cm^3)	1.5926
μ (cm^{-1})	59.52
radiation (Å)	Mo 0.71069
temperature (K)	295
scan method	ω/2θ
total reflections collected	1929
parameters refined	113
R	0.0694
R_w	0.0646

Table 5-4

Selected Bond Lengths(Å) and Angles(°) for $[Ir_3(\mu\text{-}PPh_2)_3(\mu\text{-dppm})(CO)_3]$

Atoms	Distance
Ir(2)-Ir(1)	2.805(2)
Ir(2)-Ir(2')	2.743(3)
P(1)-Ir(1)	2.271(8)
C(1)-Ir(1)	1.75(6)
P(1)-Ir(2)	2.291(9)
P(2)-Ir(2)	2.30(1)
P(3)-Ir(2)	2.328(1)
C(2)-Ir(2)	1.75(1)
C(1)-O(1)	1.29(6)
C(2)-O(2)	1.25(3)

Atoms	Angle
Ir(2)-Ir(1)-Ir(2')	58.6(1)
Ir(1)-Ir(2)-Ir(2')	60.4(5)
Ir(1)-P(1)-Ir(2)	75.9(3)
C(1)-Ir(1)-Ir(2)	150.6(1)
P(1)-Ir(2)-Ir(1)	51.7(2)
P(1)-Ir(1)-Ir(2)	52.4(2)
C(1)-Ir(1)-P(1)	98.9(3)
C(2)-Ir(2)-P(1)	102.2(4)
C(2)-Ir(2)-P(2)	99.8(4)
C(2)-Ir(2)-P(3)	95.6(4)
P(2)-Ir(2)-P(3)	140.4(3)
P(2)-Ir(2)-Ir(1)	82.7(4)
P(3)-C(37)-P(3')	109(2)

(Estimated standard deviations are given in parentheses.)

iridium atom, accompanied by a lengthening of the Ir-Ir bond distances to yield $[Ir_3(\mu\text{-}PPh_2)_3(CO)_5(Bu^tNC)_2]$.

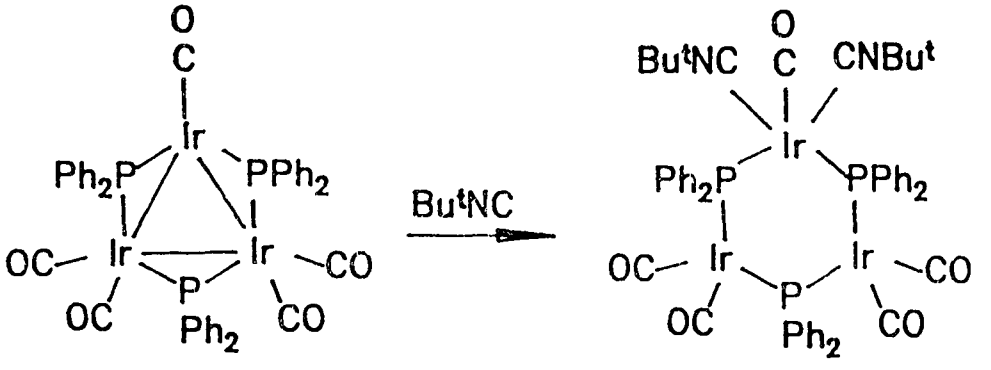

This addition is also accompanied by the rearrangement of the unique phosphido bridge into the plane of the three iridium atoms as determined by X-ray crystallographic structure determination (figure **5-5**). Relevant crystallographic parameters are listed in table **5-5**. Table **5-6** contains a list of selected bond lengths and angles. The Bu^tNC groups are trans to each other. A similar reaction was reported by Haines and coworkers where the addition of two moles of CO to $[Rh_3(\mu\text{-}PPh_2)_3(CO)_5]$ resulted in the symmetric expansion of the Rh_3P_3 ring with the accompanying rearrangement to a planar configuration.[145] This expansion with the concurrent elongation of the Rh-Rh bonds was

Figure 5-5

The Molecular Structure of
$[Ir_3(\mu\text{-}PPh_2)_3(CO)_5(Bu^tNC)_2]$

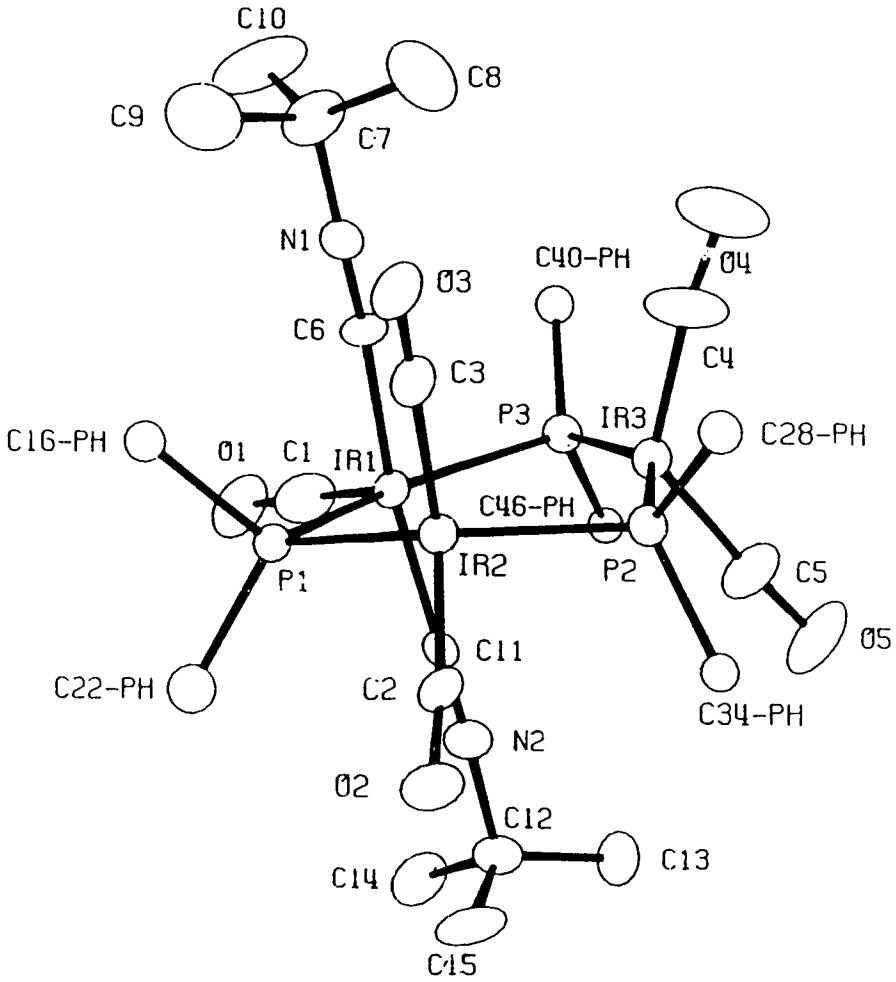

Table 5-5

Crystallographic Parameters for
$[Ir_3(\mu\text{-}PPh_2)_3(CO)_5(Bu^tNC)_2]$

formula	$C_{51}H_{48}N_2O_5P_3Ir_3$
fw	1439
space group	$P2_1/n$
a (Å)	23.015(4)
b (Å)	20.197(6)
c (Å)	11.849(5)
α (degrees)	90.0
β (degrees)	92.19(4)
ɣ (degrees)	90.0
volume ($Å^3$)	5504
Z	4
calculated density (g/cm^3)	1.736
μ (cm^{-1})	73.40
radiation (Å)	Mo 0.71069
temperature (K)	295
scan method	ω/2θ
total reflections collected	4570
parameters refined	397
R	0.0587
R_w	0.0563

Table 5-6

Selected Bond Lengths(Å) and Angles(°) for $[Ir_3(\mu\text{-}PPh_2)_3(CO)_5(Bu^tNC)_2]$

Atoms	Distance	Atoms	Distance
Ir(1)-Ir(2)	3.176(2)	P(2)-Ir(3)	2.332(7)
Ir(1)-Ir(3)	3.199(2)	P(2)-Ir(2)	2.321(7)
Ir(2)-Ir(3)	3.329(2)	C(1)-Ir(1)	1.80(4)
P(1)-Ir(1)	2.373(7)	C(3)-Ir(2)	1.86(4)
P(1)-Ir(2)	2.273(7)	C(2)-Ir(2)	1.77(3)
P(3)-Ir(1)	2.378(7)	C(4)-Ir(3)	1.87(4)
P(3)-Ir(3)	2.300(8)	C(5)-Ir(3)	1.93(4)
C(6)-Ir(1)	1.91(3)	C(1)-O(1)	1.16(5)
C(11)-Ir(1)	1.96(3)	C(2)-O(2)	1.23(4)
C(6)-N(1)	1.16(4)	C(3)-O(3)	1.18(4)
C(11)-N(2)	1.17(4)	C(4)-O(4)	1.16(5)
C(5)-O(5)	1.12(5)		

Atoms	Angle
Ir(3)-Ir(1)-Ir(2)	63.0(1)
Ir(3)-Ir(2)-Ir(1)	58.0(1)
Ir(2)-Ir(3)-Ir(1)	58.2(1)
Ir(1)-P(1)-Ir(2)	86.2(2)
Ir(1)-P(3)-Ir(3)	86.3(2)
Ir(2)-P(2)-Ir(3)	91.4(3)
C(6)-Ir(1)-C(11)	170(1)
C(3)-Ir(2)-C(2)	131(1)
C(14)-Ir(3)-C(5)	127(2)
C(1)-Ir(1)-P(1)	102(1)
C(1)-Ir(1)-P(3)	103(1)
P(1)-Ir(1)-C(6)	87(1)
P(1)-Ir(2)-C(3)	98.7(1)
P(2)-Ir(3)-P(3)	149.4(3)
C(11)-Ir(1)-P(1)	91.0(8)

(Estimated standard deviations are given in parentheses.)

attributed to the apparent population of a molecular orbital which is anti-bonding with respect to the rhodium atoms. The Ir-Ir bond distances in $[Ir_3(\mu\text{-}PPh_2)_3(CO)_5(Bu^tNC)_2]$ are 3.176Å, 3.199Å, and 3.329Å. Although these distances are longer than those expected for a single metal-metal bond; they are still shorter than those associated with a complete non-bonding metal-metal interaction. The two equivalent iridiums have two terminal carbonyl groups coordinated to them and have geometries intermediate between square planar and tetrahedral. The third iridium has two trans Bu^tNC groups and a carbonyl ligand attached to it and adopts a distorted trigonal bipyramidal geometry.

The $^{31}P\{^1H\}$ NMR spectrum of $[Ir_3(\mu\text{-}PPh_2)_3(CO)_5(Bu^tNC)_2]$ (figure **5-6**) consists of two sets of peaks. The triplet at -105 ppm belongs to the unique phosphido bridge, and the doublet at -140 ppm corresponds to the two equivalent phosphido bridges. The coupling constant between the phosphorus atoms is 150 Hz. This large phosphorus-phosphorus coupling is because the phosphido bridges are almost trans to each other. The high-field shift of the phosphido bridges is indicative of the almost non-bonding interaction of the iridium atoms. The IR spectrum of $[Ir_3(\mu\text{-}PPh_2)_3(CO)_5(Bu^tNC)_2]$ (figure **5-7**) also clearly indicates the presence of Bu^tNC (2178 and 2138 cm^{-1}) and CO

Figure 5-6

The $^{31}P\{^{1}H\}$ NMR Spectrum of $[Ir_3(\mu\text{-}PPh_2)_3(CO)_5(Bu^tNC)_2]$

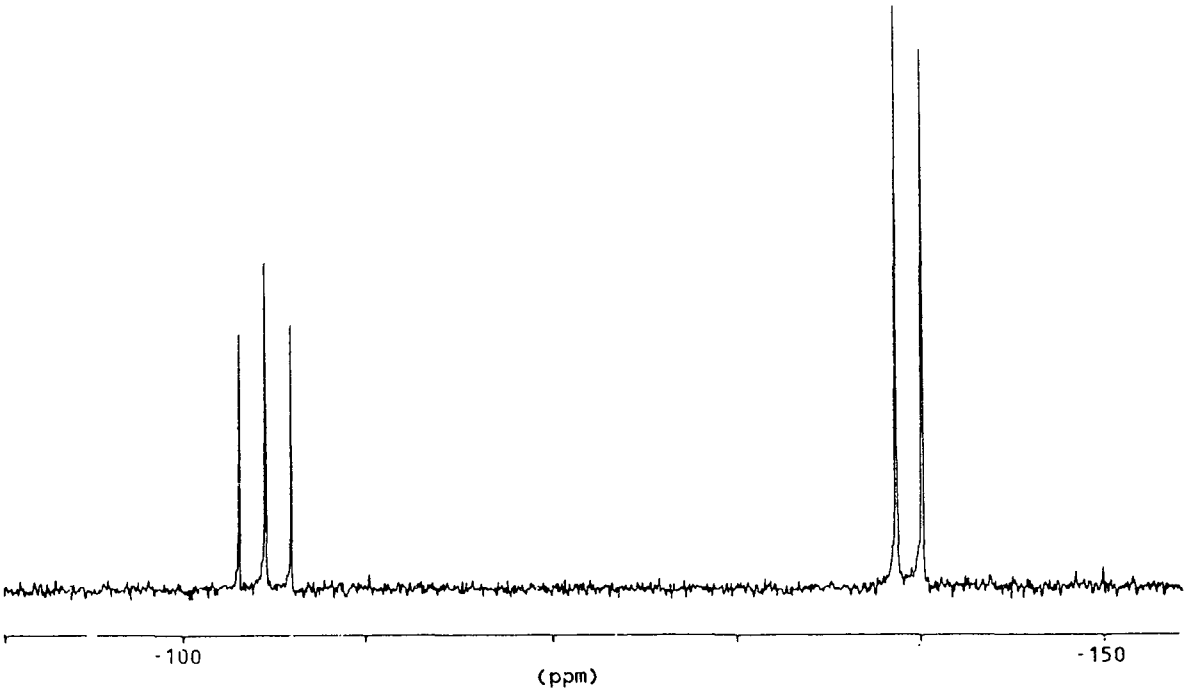

Figure 5-7

The IR Spectrum of
$[Ir_3(\mu\text{-}PPh_2)_3(CO)_5(Bu^tNC)_2]$

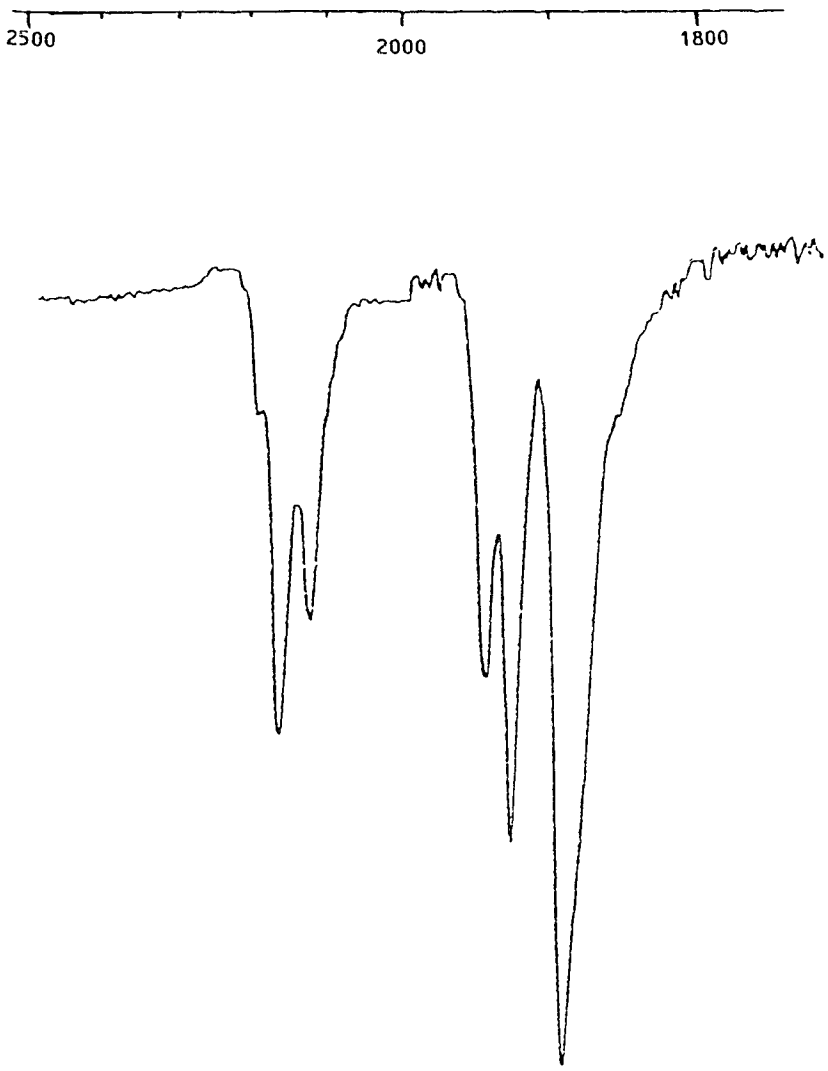

(1948, 1930, and 1892 cm^{-1}) ligands.

This area offers a great deal of potential for further study, both with respect to cluster fragmentation reactions, and reaction chemistry of strongly held adjacent metal centers.

CHAPTER SIX

GENERAL DISCUSSION

The last four chapters of this thesis dealt with the synthesis and reactivities of a number of phosphido-bridged transition-metal clusters. In accordance with the major focus of the project, each compound and all its spectroscopic and structural parameters were presented in order with some relevant discussion and examples of previously known analogues. This chapter summarizes some of the spectral and structural data and deals with some of the general points and trends.

A summary of the selected bond lengths and angles of the trinuclear clusters $[MM'_2(\mu\text{-}X)(\mu\text{-}PPh_2)(PPh_3)_3][BF_4]$ (M= Pd, Pt) may be found in tables **7-1** and **7-2**. Table **7-3** contains a number of selected $^{31}P\{^1H\}$ NMR parameters for these clusters and a few analogous complexes. Selected $^{31}P\{^1H\}$ NMR parameters for $[M_2(\mu\text{-}PPh_2)(\mu\text{-}R_2PCH_2PR_2)(PR'_3)_3]^+$ (M= Pd, Pt; R= Ph, Me; R'= Ph,Et) and similar compounds are summarized in table **7-4**.

$^{31}P\{^1H\}$ NMR Spectral Trends:

A number of points should be noted about the $^{31}P\{^1H\}$ NMR spectra of the palladium and platinum compounds described in this thesis. In $[M_3(\mu\text{-}X)(\mu\text{-}PPh_2)_2(PR_3)_3]^+$ (M= Pd, Pt) complexes, due to the relatively large coupling constant

Table 7-1

Selected Bond Lengths (Å) for
$[M_2M'(\mu\text{-}X)(\mu\text{-}PPh_2)_2(PR_{3,3}][BF_4]$

	I	II	III	IV	V	VI	VII
M(1)-M(2)	2.93(2)	2.933(2)	2.953(1)	2.886(1)	2.796(1)	2.914(1)	2.921(1)
M(1)-M(3)	2.93(2)	2.936(2)	2.977(1)	2.908(1)	2.795(1)	2.906(1)	2.916(1)
M(2)-M(3)	2.89(2)	2.906(2)	2.924(1)	2.878(2)	2.638(1)	2.849(1)	2.860(1)
P(1)-M(1)	2.31(2)	2.296(2)	2.293(3)	2.273(5)	2.299(3)	2.260(7)	2.258(5)
P(2)-M(2)	2.30(1)	2.296(6)	2.282(3)	2.287(5)	2.248(2)	2.243(7)	2.264(5)
P(3)-M(3)	2.29(1)	2.273(6)	2.273(3)	2.288(5)	2.241(4)	2.271(7)	2.264(6)
P(4)-M(1)	2.27(1)	2.274(6)	2.268(3)	2.274(5)	2.312(3)	2.266(6)	2.259(4)
P(4)-M(2)	2.22(2)	2.204(6)	2.237(3)	2.201(5)	2.220(3)	2.192(6)	2.186(5)
P(5)-M(1)	2.28(2)	2.282(6)	2.265(3)	2.260(5)	2.299(3)	2.279(6)	2.263(5)
P(5)-M(3)	2.23(2)	2.203(6)	2.231(3)	2.198(5)	2.212(2)	2.200(7)	2.186(5)
X-M(2)	2.41(1)	2.408(6)	2.355(1)	2.392(5)	---	2.420(7)	2.401(6)
X-M(3)	2.41(1)	2.394(6)	2.354(3)	2.389(5)	---	2.415(7)	2.406(6)
reference	36	36		36	51		

I $[Pd_3(\mu\text{-}Cl)(\mu\text{-}PPh_2)(PPh_3)_3][BF_4]$
II $[Pd_3(\mu\text{-}Cl)(\mu\text{-}PPh_2)_2(PEt_3)_3][BF_4]$
III $[Pd_3(\mu\text{-}SCH_2Ph)(\mu\text{-}PPh_2)_2(PEt_3)_3][BF_4]$
IV $[PtPd_2(\mu\text{-}Cl)(\mu\text{-}PPh_2)_2(PPh_3)_3][BF_4]$
V $[Pt_3(\mu\text{-}H)(\mu\text{-}PPh_2)_2(PPh_3)_3][BF_4]$
VI $[Pt_3(\mu\text{-}Cl)(\mu\text{-}PPh_2)_2(PPh_3)_3][BF_4]$
VII $[Pt_3(\mu\text{-}Cl)(\mu\text{-}PPh_2)_2(PEt_3)_3][BF_4]$

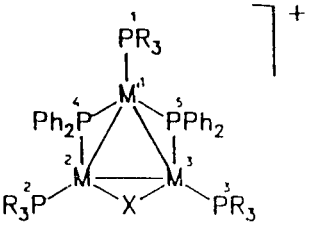

(Estimated standard deviations are given in parantheses)

Table 7-2

Selected Bond Angles (°) for $[M_2M'(\mu\text{-}X)(\mu\text{-}PPh_2)_2(PR_3)_3][BF_4]$

	I	II	III	IV	V	VI	VII
M(2)-M(1)-M(3)	59.1(8)	59.3(1)	59.1(1)	59.6(1)	56.3(1)	58.6(1)	58.7(1)
M(1)-M(2)-M(3)	60.3(4)	60.4(1)	60.9(1)	60.6(1)	61.8(1)	60.5(1)	60.6(1)
M(1)-M(3)-M(2)	60.5(5)	60.3(1)	60.0(1)	59.8(1)	61.9(1)	60.8(1)	60.7(1)
M(2)-X-M(3)	73.8(8)	74.5(2)	76.8(1)	74.0(1)	---	72.2(2)	73.0(2)
M(1)-P(4)-M(2)	81.7(6)	81.8(2)	81.9(1)	80.3(2)	76.2(1)	81.6(2)	82.2(2)
M(1)-P(5)-M(3)	81.1(6)	81.8(2)	82.9(1)	81.0(2)	76.6(1)	80.9(2)	81.9(2)
P(4)-M(1)-M(2)	48.3(2)	48.0(2)	48.6(1)	48.7(1)	50.4(1)	48.1(2)	47.8(1)
P(5)-M(1)-M(3)	48.7(3)	47.9(2)	48.1(1)	48.3(1)	50.3(1)	48.4(2)	47.9(1)
P(5)-M(3)-M(1)	50.2(9)	50.3(2)	49.0(1)	50.7(1)	53.1(1)	50.7(2)	50.2(1)
P(4)-M(2)-M(1)	50.0(7)	50.1(1)	59.5(1)	51.0(1)	53.4(1)	50.3(2)	50.1(1)
M(3)-M(2)-X	53.0(4)	52.5(1)	51.6(1)	52.9(1)	---	53.8(2)	53.6(1)
M(2)-M(3)-X	53.2(5)	53.0(1)	51.6(1)	53.0(1)	---	54.0(2)	53.4(1)
P(1)-M(1)-P(4)	102.9(4)	105.7(2)	104.1(1)	104.4(2)	104.6(1)	105.8(2)	104.7(2)
P(1)-M(1)-P(5)	100.7(4)	98.7(2)	100.7(1)	100.4(2)	101.0(1)	99.2(3)	101.4(2)
P(2)-M(2)-P(4)	101.8(8)	104.1(2)	102.9(1)	104.8(2)	108.1(1)	104.4(2)	102.3(2)
P(3)-M(3)-P(5)	103.0(9)	103.2(2)	101.3(1)	102.5(2)	105.9(1)	104.2(2)	102.6(2)
P(2)-M(2)-X	95.0(9)	93.8(2)	95.8(1)	91.3(2)	---	91.5(2)	93.7(2)
P(3)-M(3)-X	93.2(1)	93.3(2)	98.0(1)	94.8(2)	---	90.4(2)	93.3(2)
reference	36	36		36	51		

I $[Pd_3(\mu\text{-}Cl)(\mu\text{-}PPh_2)(PPh_3)_3][BF_4]$
II $[Pd_3(\mu\text{-}Cl)(\mu\text{-}PPh_2)_2(PEt_3)_3][BF_4]$
III $[Pd_3(\mu\text{-}SCH_2Ph)(\mu\text{-}PPh_2)_2(PEt_3)_3][BF_4]$
IV $[PtPd_2(\mu\text{-}Cl)(\mu\text{-}PPh_2)_2(PPh_3)_3][BF_4]$
V $[Pt_3(\mu\text{-}H)(\mu\text{-}PPh_2)_2(PPh_3)_3][BF_4]$
VI $[Pt_3(\mu\text{-}Cl)(\mu\text{-}PPh_2)_2(PPh_3)_3][BF_4]$
VII $[Pt_3(\mu\text{-}Cl)(\mu\text{-}PPh_2)_2(PEt_3)_3][BF_4]$

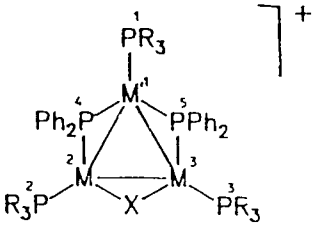

(Estimated standard deviations are given in parentheses)

Table 7-3

Selected $^{31}P\{^{1}H\}$ NMR Parameters for $[M'M_2(\mu\text{-}X)(\mu\text{-}Y)_2(PR_3)_3]^n$ Complexes

				$\delta_{4,5}$	J_{12}	J_{16}	J_{17}	J_{27}	J_{45}	J_{46}	J_{47}	ref.
				(ppm)				(Hz)				
$[M'M_2(\mu\text{-}X)(\mu\text{-}Y)_2(PR_3)_3]^n$												
M=M'=Pt												
X=H	Y=PPh_2	R=Ph	n=+1	85.8	86	3518	358	3940	260	1980	2500	
X=Cl	Y=PPh_2	R=Ph	n=+1	-13.2	75	4142	233	4406	243	2264	3523	
X=Cl	Y=PPh_2	R=Et	n=+1	-27.4	71	3763	253	3980	250	2309	3553	
X=Br	Y=PPh_2	R=Ph	n=+1	-1.9	76	4139	235	4279	244	2271	3474	
X=I	Y=PPh_2	R=Ph	n=+1	14.2	77	4156	233	4313	237	2301	3357	
X=S	Y=PPh_2	R=Ph	n=0	-47.8	83	3538	230	4784	177	2199	2637	
X=SH	Y=PPh_2	R=Ph	n=+1	-28.4	75	4366	215	4491	215	2255	2802	
X=SMe	Y=PPh_2	R=Ph	n=+1	-29.8	76	4332		4544	213	2284	2846	
X=Y=PPh_2		R=Ph	n=+1	-42.0	66	4597	166			2045		
X=Y=PPh_2		R=Et	n=+1	-56.9	64	2057	115			4177		
X=Cl	Y=SO_2	R=Ph	n=-1		62	4599	431	5469				48
X=Br	Y=SO_2	R=Ph	n=-1		62	4620	440	5482				48
X=Cl	Y=SO_2	R=Cy	n=-1		59	4341	352	4963				48
X=SO_2	Y=CO	R=Cy	n=-1		62	5134	449	4055				48
X=Y=CO		R=Cy	n=0		58	4412	430					158
X=Y=CO		R=Pr^i	n=0		56	4422	419					158
X=Y=CO		R=$PhBu^t_2$	n=0		48	4826	419					58
M=Pd,M'=Pt												
X=Cl	Y=PPh_2	R=Et	n=+1		83	4037	213			2621		36
M=Pd												
X=Cl	Y=PPh_2	R=Ph	n=+1	80.7	89							35
X=Cl	Y=PPh_2	R=Et	n=+1	63.8	93							35
X=S	Y=PPh_2	R=Ph	n=0	27.7	95							
X=S	Y=PPh_2	R=Et	n=0	0.3	103							
X=SH	Y=PPh_2	R=Ph	n=+1	66.1	85							
X=SMe	Y=PPh_2	R=Ph	n=+1	67.1	87							
X=SCH_2Ph	Y=PPh_2	R=Ph	n=+1	40.4	88							

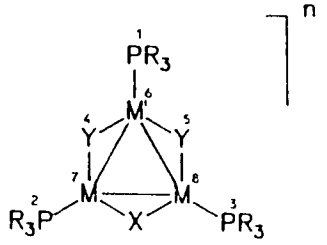

Table 7-4

Selected $^{31}P\{^{1}H\}$ NMR Parameters for $[M'M(\mu\text{-}X)(Y)(Z)(PR_3)_2]^{n+}$ Complexes

$[M'M(\mu\text{-}X)(Y)(Z)(PR_3)_2]^{n+}$				δ_1	J_{12}	J_{14}	J_{16}	J_{17}	J_{23}	J_{24}	J_{26}	J_{27}	J_{36}	J_{37}	J_{46}	J_{47}	ref.
				(ppm)	(Hz)												
M=M'=Pt																	
X=S	Y=Z=CO	$R=Bu^t_2Ph$	n=0						128		3169	107					58
$X=SO_2$	Y=Z=CO	$R=Bu^t_2Ph$	n=0						76		3957	318					58
X=SMe	Y=Z=CO	$R=Bu^t_2Ph$	n=1						110		3117	10					58
$X=SO_2$	$Y=Z=CNC_8H_9$	R=Cy	n=0						91								72
X=S	$Y=Z=CH_3NC$	R=Cy	n=0						178								59
X=S	$Y=PPh_3$, Z=CO	R=Ph	n=0						180	11							59
X=SMe	$Y=PPh_3$, Z=CO	R=Ph	n=1						164	13							59
$X=PPh_2$	$Y=PPh_3$, $Z=Bu^tNC$	R=Ph	n=1	26.6		250	2754	3101	162		3156	433	320	3024	3004		
$X=PPh_2$	Y,Z=dppm	R=Ph	n=1	53.9	11	251	2781	2781	149	6	3293	343	J_{27}	J_{26}	3065	53	
$X=PPh_2$	Y,Z=dppm	R=Et	n=1	50.6	9	252	2775	2775	134		3179	216	J_{27}	J_{26}	3072		
$X=PPh_2$	Y,Z=dmpm	R=Ph	n=1	42.4	4	253	2639	2639	155	7	3220	360	J_{27}	J_{26}	2853	57	
X=S	Y,Z=dppm	R=Ph	n=0						175	15	3191	231	J_{27}	J_{26}	3538	109	59
X=SMe	Y,Z=dppm	R=Ph	n=1						160	16	3040	175	J_{27}	J_{26}	3896	89	59
M=Pd,M'=Pt																	
$X=PPh_2$	Y,Z=dppm	R=Ph	n=1	78.3	6	227	3205										
M=M'=Pd																	
$X=PPh_2$	Y,Z=dppm	R=Ph	n=1	96.7	32	207			200								

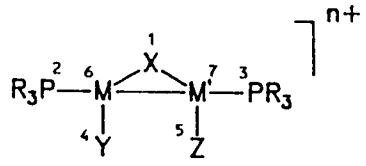

between the two phosphido bridges, the $^{31}P\{^{1}H\}$ NMR spectra become deceptively simple cases of a more complex spin system.[146] In the case of the Pd(I) and Pt(I) dimers, $[M_2(\mu\text{-}PPh_2)(\mu\text{-}dppm)(PR_3)_2]^+$ (M = Pd, Pt), the relatively large three bond coupling constant between the two terminal phosphines leads to the same effect. In both trinuclear and dinuclear compounds when the metal is palladium, these coupling constants cannot be determined directly from the spectrum. When the metal is platinum, then those coupling constants can be determined directly from the spectrum, as the presence of spin-active ^{195}Pt renders the two $\mu\text{-}PPh_2$ (in trinuclear complexes) and the two PR_3 (in dinuclear cases), different from each other making their coupling constant observable.

Simple first order approximation may also be used for the platinum sidebands in the $^{31}P\{^{1}H\}$ NMR spectra of all the trinuclear and dinuclear platinum complexes because of the relatively large size of the one bond platinum-phosphorus coupling constants (tables **7-3** and **7-4**). As is seen from the data in these tables the P-P and P-Pt coupling constants of the compounds reported in this thesis have similar magnitudes to those determined for related complexes.

The size of the three bond phosphorus-phosphorus coupling constant in the dimers depends on the spatial orientation of the terminal phosphines with respect to each other. The more linear or trans the geometry of the phosphines, the larger this coupling constant becomes. For example, in $[Pt_2(\mu\text{-}SO_2)(CNC_8H_6)_2(PCy_3)_2]$, the coupling constant between the two PCy_3 groups is 91 Hz,[147] while in $[Pt_2(\mu\text{-}PPh_2)(dmpm)(PPh_3)_2]^+$ the three bond P-P is 155 Hz (table **7-4**). This difference may be related to the crystal structures which show that in the first case the PCy_3 groups are bent towards the $\mu\text{-}SO_2$ by about 30°, whereas, in $[Pt_2(\mu\text{-}PPh_2)(dmpm)(PPh_3)_2]^+$ the PPh_3 groups are bent from the metal-metal axis by 20° only(table **3-5**).

There have been many attempts to relate $^{31}P\{^1H\}$ NMR parameters to structural parameters, but mostly they have been unsuccessful.[148] Two of the most successful correlations to date have been the relation of two bond phosphorus-phosphorus coupling constants, where the intervening atom is a metal, to stereochemistry; and the relation of $\mu\text{-}PPh_2$ chemical shifts to the extent of metal-metal interactions. Both of these are well documented in the review literature,[149-153] and are straightforward. Mutually trans phosphorus atoms have a large coupling constant whereas cis atoms have a small coupling constant;

and strong metal-metal interactions between two metals bridged by PPh_2 lead to downfield shifts of the μ-PPh_2 resonance. All the complexes synthesized and reported in this thesis follow both of these general trends.

The difference between two-bond trans P-P and cis P-P coupling constant can be clearly seen from the values compiled in table **7-4**. $[M_2(\mu\text{-}PPh_2)(R_2PCH_2PR_2)(PPh_3)_2]^+$(M= Pd, R= Ph; M= Pt, R= Me) complexes provide good examples. In both cases, X-ray diffraction has shown that the diphosphine ligand is almost trans to the μ-PPh_2 group and the terminal phosphines are cis to the μ-PPh_2. The coupling constants, 207 Hz and 253 Hz compared to 32 Hz and 4 Hz, reflect those geometries. Also in the rhodium and iridium clusters, $[M_3(\mu\text{-}PPh_2)_3(\mu\text{-dppm})(CO)_3]$, one of the μ-PPh_2 groups is trans to the μ-dppm and cis to the other two phosphido bridges. These orientations are clearly reflected in the coupling constants (151 Hz and 169 Hz for the trans, 26 Hz and 24 Hz for the cis).

The effect of the metal-metal distance on the μ-PPh_2 chemical shift can be most dramatically seen in the two compounds $[Pt_3(\mu\text{-}H)(\mu\text{-}PPh_2)_2(PPh_3)_3][BF_4]$ and $[Pt_3(\mu\text{-}Cl)(\mu\text{-}PPh_2)_2(PPh_3)_3][BF_4]$. In the μ-H cluster, the phosphido-bridged platinum-platinum bond lengths are 2.796Å and 2.795Å

(table 7-1) and the μ-PPh_2 chemical shift is +86 ppm (table 7-3). In the μ-Cl cluster, for reasons that were discussed in chapter two, the platinum-platinum bond lengths have increased to 2.921Å and 2.916Å, and the μ-PPh_2 shielding has increased to -13.2 ppm. An increase of about 0.1Å has led to a large upfield shift.

Because of the $1/\Delta E$ (ΔE = mean excitation energy) term in the paramagnetic contribution to shielding, large downfield shifts of μ-PPh_2 are proposed to be a result of a small gap between the highest occupied molecular orbital (HOMO) and the lowest unoccupied molecular orbital (LUMO).[153] This explanation seems to fit well with the observed μ-PPh_2 chemical shifts in $[Pt_3(\mu\text{-}X)(\mu\text{-}PPh_2)_2(PPh_3)_3]^+$ (X= H, Cl). As discussed in chapter two, molecular orbital calculations on model compounds have shown that for the triangular phosphido-bridged palladium and platinum clusters there are 22 low lying orbitals.[154] In the case of 42-electron clusters such as $[Pt_3(\mu\text{-}H)(\mu\text{-}PPh_2)_2(PPh_3)_3]^+$, the HOMO has its wavefunction mainly localized on the metals. The LUMO is a combination of μ-PR_2 p-orbitals and in-plane metal d-orbitals. This orbital places most of its electron density on the bridging μ-PPh_2, and is only slightly higher in energy than the HOMO. In the 42-electron cluster, $[Pt_3(\mu\text{-}H)(\mu\text{-}PPh_2)_2(PPh_3)_3]^+$, therefore, there is a small gap

between HOMO and LUMO, resulting in a large paramagnetic contribution to shielding which has a deshielding effect. Addition of two electrons, as in the 44 electron cluster $[Pt_3(\mu\text{-}Cl)(\mu\text{-}PPh_2)_2(PPh_3)][BF_4]$, leaves a large gap between filled and unfilled levels causing a decrease in the paramagnetic contribution to shielding.

A number of other examples in this thesis illustrate this trend. In $[Pd_2(\mu\text{-}PPh_2)(\mu\text{-}dppm)(PPh_3)_2][BF_4]$, the metal-metal distance is 2.715Å, and the $\mu\text{-}PPh_2$ chemical shift is 96.7 ppm. In $[Pd_2(\mu\text{-}PPh_2)(\mu\text{-}dppm)_2Cl_2][BF_4]$ where the metal-metal separation is 3.413Å, the $\mu\text{-}PPh_2$ chemical shift has shifted upfield to -67.6 ppm. The complexes $[M_3(\mu\text{-}PPh_2)_3(\mu\text{-}dppm)(CO)_3]$ (M= Rh, Ir), with metal-metal distances averaging 2.75Å (tables **5-2** and **5-4**), have $\mu\text{-}PPh_2$ shifts of 152.1 ppm and 100.7 ppm. In $[Ir_3(\mu\text{-}PPh_2)_3(CO)_5(Bu^tNC)_2]$, the addition of two molecules of Bu^tNC has caused the metal-metal bonds to increase to an average of 3.23Å, resulting in increased shielding of $\mu\text{-}PPh_2$ to -140.0 ppm.

The variation of $\mu\text{-}PPh_2$ chemical shifts with the change in the metal, the bridging unit X, and the terminal phosphines in $[M_3(\mu\text{-}X)(\mu\text{-}PPh_2)_2(PR_3)_3]^+$ (M= Pd, Pt) was discussed previously in chapter two. The same trends are observed for the dinuclear compounds, $[M_2(\mu\text{-}PPh_2)(\mu\text{-}dppm)(PR_3)_2]^+$ (M= Pd,

Pt). Replacement of palladium with platinum and substitution of the terminal triphenylphosphines and the dppm ligand with more basic groups, such as PEt_3 or dmpm causes an increase in the shielding of μ-PPh_2 (table **7-4**). Similar shifts have been observed in a number of related systems.[153] In $[M_3(\mu\text{-}H)_2(\mu\text{-}PPh_2)_2(CO)_8]$ (M= Fe, Ru, Os), for example, the μ-PPh_2 shielding increases when descending the triad,[155] and in $[Ru_3(\mu\text{-}PPh_2)_2(\mu^2\text{-}C{\equiv}CR)_3(Ph_2PC{\equiv}CR)(CO)_6]$ the μ-PPh_2 chemical shift moves to higher field as R is changed from Ph to Pr^i to Bu^t.[156] These trends could be in part due to the higher diamagnetic contribution to the shielding of the μ-PPh_2 phosphorus.

Several groups have also proposed correlations between one bond platinum-phosphorus coupling constants and platinum-phosphorus bond lengths.[157-158] This correlation can also be observed in the Pt-P couplings in $[Pt_3(\mu\text{-}X)(\mu\text{-}PPh_2)_2(PR_3)_3]^+$ (X= H, Cl; R= Ph, Et) compounds. As was discussed in chapter two, there is an asymmetry in the Pt-P (μ-PPh_2) bond lengths due to the different trans influences of the other bridging ligands (table **7-1**). In $[Pt_3(\mu\text{-}Cl)(\mu\text{-}PPh_2)_2(PPh_3)_3][BF_4]$, for example, the length of the phosphorus-platinum bond trans to the μ-Cl is 2.192Å and the Pt-P coupling constant is 3523 Hz, and the Pt-P bond length trans to the other μ-PPh_2 is 2.266Å with a platinum-

phosphorus coupling constant of 2264 Hz. A change in the bond length of 0.074Å has caused a decrease of 1259 Hz in the coupling constant. This trend is also observed with the terminal phosphines. For example the platinum-phosphorus (unique terminal phosphine) bond length in $[Pt_3(\mu\text{-}Cl)(\mu\text{-}PPh_2)_2(PPh_3)_3][BF_4]$ is 2.260Å, which is shorter than the Pt-P bond length in $[Pt_3(\mu\text{-}H)(\mu\text{-}PPh_2)_2(PPh_3)_3]^+$ (2.299Å). The Pt-P coupling constants (4142 Hz compared to 3518 Hz)(table **7-3**) reflect this difference in bond lengths . Present theory suggests that the decrease in this one-bond platinum-phosphorus coupling constant is the result of the removal of metal s-electron density by the stronger trans influencing ligand, which leads to a decrease in the Fermi contact contribution to the coupling constant.

The correlation of $\mu\text{-}PPh_2$ phosphorus to metal bond lengths with platinum-phosphorus coupling constants may be used to assign coupling constants in cases where there is ambiguity. For example, in $[Pt_2(\mu\text{-}PPh_2)(PPh_3)_3(Bu^tNC)]^+$ the Pt-P bond trans to the PPh_3 group is 2.270Å compared to 2.217Å for the M-P bond trans to the Bu^tNC group (table **3-7**). Thus the larger Pt-P coupling constant (3101 Hz) is assigned to that interaction (the other coupling constant is 2754 Hz).

Structural Trends

Three general points should be noted regarding the structure and bonding in the complexes reported in this thesis. First, the eighteen electron and sixteen electron rules for transition metal complexes apply in all cases, and consequently all the metal-metal bonds may be considered as two-electron/two-center bonds. Second, the structures may be viewed in terms of different sized metal fragments sharing common bridging groups. Finally, for the trinuclear clusters, the skeletal electron pair[159-160] approach (discussed in chapter two) may be used to explain their structures.

All the triangular platinum and palladium clusters reported in the literature to date, including $[M_3(\mu\text{-}X)(\mu\text{-}PPh_2)_2(PPh_3)_3]^+$ (M= Pd, Pt) complexes, with a few exceptions,[161] have similar structures which are based on a triangular arrangement of metal atoms with three bridging ligands and each metal atom bearing one terminal ligand . The metal-metal distances range from 2.60Å to 2.95Å, and there is little deviation from planarity. These structures may be considered as being composed of three distorted T-shaped ML_3 fragments sharing common bridging groups.[161] Palladium and platinum ML_3 fragments can each contribute two atomic

orbitals and two electrons to cluster bonding, making in total six orbitals and six electrons available for metal-metal bonding.[160] X-ray crystallographic data supports this view of the structures. In $[M_3(\mu\text{-}X)(PPh_2)_2(PPh_3)_3][BF_4]$ (M= Pd, Pt), for example, the phosphido bridge-metal-phosphido bridge bond angles average 146° and the X-M-P(μ-PPh_2) angles average 163°, while the terminal phosphine-metal-phosphido bridge bond angles average 103° and X-M-P(PR_3) angles average 94° (tables **7-1** and **7-2**). These angles are compared to 180° and 90° angles of an idealized T-shaped fragment. In terms of the skeletal electron pair theory all of these trinuclear clusters are electron precise which means that the total number of electrons available for cluster bonding equals the total number of atomic orbitals available. A triangular arrangement of metal atoms, therefore, requires six electrons and six atomic orbitals.[160]

The structure of the dimers $[M_2(\mu\text{-}PPh_2)(\mu\text{-}R_2PCH_2PR_2)(PPh_3)_2]^+$ (M= Pd, Pt) may also be viewed in terms of two distorted T-shaped ML_3 fragments bonded together. The bond angles for these complexes support this formulation. For example, in $[M_2(\mu\text{-}PPh_2)(\mu\text{-}R_2PCH_2PR_2)(PPh_3)_2]^+$ (M=Pd, Pt) and $[M_2(\mu\text{-}PPh_2)(PPh_3)_3(Bu^tNC]^+$ compounds, the phosphido bridge-metal- diphosphine angles are an average of 148°, and the phosphido bridge-metal-terminal phosphine angles are 109°

(tables 3-3, 3-5, and 3-7). Similar models have been proposed for other Pd(I) and Pt(I) dimers and have been used in molecular orbital calculations.[162]

For the 46 electron compounds $[M_3(\mu\text{-}PPh_2)_3(CO)_5]$ (M= Rh, Ir), skeletal electron pair theory predicts an electron count of 48. By this standard, these complexes are electron deficient and should react with electron donor molecules. The ease by which they react with additional molecules of CO or Bu^tNC provides evidence of this deficiency. $[M_3(\mu\text{-}PPh_2)_3(\mu\text{-dppm})(CO)_3]$ (M= Rh, Ir) may be viewed as one ML_3 and two ML_4 fragments sharing bridging units. A rhodium(I) or iridium(I) ML_3 fragment contributes two orbitals and two electrons, and each ML_4 fragment contibutes two orbitals and two electrons to cluster bonding.

$[Ir_3(\mu\text{-}PPh_2)_3(CO)_5(Bu^tNC)_2]$ is a 50 electron cluster, and approximately follows the prediction made by the skeletal electron pair theory that the addition of extra electrons to the stable electron count will lead to cleavage of metal-metal bonds. This complex may be considered as two ML_4 fragments and one ML_5 fragment sharing bridges. The ML_5 fragment does not contribute any orbitals or electrons to cluster bonding. Structural data for $[Ir_3(\mu\text{-}PPh_2)_3(CO)_5(Bu^tNC)_2]$ shows that the iridium-iridium bond

lengths have increased to essentially non-bonding distances (table **5-6**).

The complexes reported here also provide good examples of the flexibility of the μ-PPh_2 group to accommodate a variety of M-M distances and M-P-M angles. The M-M distances and M-P-M angles range from 2.688Å and 73.1° (in $[Pd_2(\mu\text{-}PPh_2)(\mu\text{-}Pr^i_2PCH_2PPh_2)(PPh_3)_2]^+$) (table **3-3**) to 3.373Å and 91.4° (in $[Ir_3(\mu\text{-}PPh_2)_3(CO)_5(Bu^tNC)_2]$) (table **5-6**).

As the examples in this chapter illustrate, the spectroscopic and structural parameters of the trinuclear and dinuclear compounds reported in this thesis provide important new examples of several known trends in cluster chemistry. In particular, the availability of detailed $^{31}P\{^1H\}$ NMR studies offers new understanding of the structural and bonding trends and moves us closer to a comprehensive understanding of these molecules.

CHAPTER SEVEN

EXPERIMENTAL

Unless otherwise stated, all of the syntheses described in this thesis were carried out under an atmosphere of dry nitrogen gas using standard Schlenck tube techniques at ambient temperatures (but the products are generally stable in air). The solvents were dried with suitable reagents and redistilled prior to their use:

1) Dichloromethane from phosphorus pentoxide

2) Tetrahydrofuran, diethyl ether, benzene, toluene and hexane from potassium/benzophenone

3) acetone, ethanol, and methanol from anhydrous sodium carbonate.

Infrared spectra were recorded on either a Perkin-Elmer 283 or a Perkin-Elmer 1320 spectrophotometer calibrated against the 1601 cm^{-1} absorption of polystyrene film. Solid examples were examined either as potassium bromide discs or Nujol mulls.

$^{31}P\{^{1}H\}$, $^{195}Pt\{^{1}H\}$ NMR spectra were recorded on a Brüker WM250 FT-spectrometer operating at 101.3, and 53.5 MHz respectively. Protons were decoupled by broad-band irradiation at appropriate frequencies. Chemical shifts are reported in parts per million with respect to external $P(OMe)_3$ for ^{31}P. The $^{195}Pt\{^{1}H\}$ chemical shifts are reported as absolute frequency values (≡ MHz) with reference to

$Si(CH_3)_4$ at exactly 100 MHz. Coupling constants are in Hertz (Hz). Positive chemical shift values are deshielded relative to references. Second order $^{31}P\{^1H\}$ NMR spectra were analyzed by computer simulation using VEAITR and NMRPLOT programs.[163-164] Elemental microanalyses were performed by Canadian Microanalytical Service Ltd., New Westminster, British Columbia. The crystal structures were solved by Dr. J. Browning using either an Enraf-Nonius CAD4 or a Picker 4-circle diffractometer. Both instruments use Mo K_α radiation.

Most of the commonly used reagents and $RhCl_3.3H_2O$ were purchased from Aldrich Chemicals Ltd. $PdCl_2$, $PtCl_2$ and K_2PtCl_4 were obtained from Johnson-Mathey Ltd. Strem Chemicals Ltd. was the source of Pr^i_2PCl, Bu^tNC. All reagents were used as supplied.

$[Pd_3(\mu\text{-}Cl)(\mu\text{-}PPh_2)_2(PR_3)_3][BF_4]$, $[Pd_3(\mu\text{-}PPh_2)_3(PR_3)_3][BF_4]$ (R= Et, Ph), $[PtPd_2(\mu\text{-}PPh_2)_2(PPh_3)_3][BF_4$,[165] $[Pt_3(\mu\text{-}H)(\mu\text{-}PPh_2)_2(PPh_3]_3[BF_4]$,[166] $[Rh_3(\mu\text{-}PPh_2)_3(CO)_3(PPh_3)_2]$,[167] $[Ir_2(COE)_2Cl_2]$,[168] $Pr^i_2PCH_2PPh_2$ [169] were prepared as described before.

$[Pd_3(\mu\text{-}S)(\mu\text{-}PPh_2)_2(PR_3)_3]$ (R= Ph,Et):

These complexes were prepared in a similar manner. e.g. $[Pd_3(\mu\text{-}S)(\mu\text{-}PPh_2)_2(PPh_3)_3]$:
Excess $Na_2S.9H_2O$ (0.216 g, 0.900 mmol) in water (1 mL) was added to a stirred solution of $[Pd_3Cl(PPh_2)_2(PPh_3)_3][BF_4]$ (0.150 g, 0.094 mmol) in methanol (10 mL). The solution turned dark red immediately. After being stirred for 1 h, the solvent was removed <u>in vacuo</u> leaving a dark red powder which was extracted with THF (15 mL). The extract was filtered through celite and the solvent removed <u>in vacuo</u> to give $[Pd_3S(PPh_2)_2(PPh_3)_3]$ (0.120 g, 0.080 mmol) as a dark red powder. Yield: 85% (based on the conversion of $[Pd_3Cl(PPh_2)_2(PPh_3)_3][BF_4]$).
A satisfactory elemental analysis of this compound was not obtained.

$^{31}P\{^1H\}$ NMR:[170] δ_1 -124.4, $\delta_{2,3}$ -110.7, $\delta_{4,5}$ 27.7; J_{12} 95. solvent: $CDCl_3$.

$[Pd_3(\mu\text{-}S)(\mu\text{-}PPh_2)_2(PEt_3)_3]$: Yield: 65% (based on the conversion of $[Pd_3Cl(PPh_2)_2(PPh_3)_3][BF_4]$).
<u>Anal.</u> calc'd for $C_{42}H_{65}P_5SPd_3$: C 46.9, H 6.09; <u>Found:</u> C 48.2, H 6.18).

$^{31}P\{^1H\}$ NMR:[170] δ_1 -140.4, $\delta_{2,3}$ -122.7, $\delta_{4,5}$ 8.1; J_{12} 103. Solvent: $CDCl_3$.

$[Pd_3(\mu\text{-}SH)(\mu\text{-}PPh_2)_2(PPh_3)_3][BF_4]$:

Excess $HBF_4.Et_2O$ (0.112 g, 0.690 mmol) was added to a stirred solution of $[Pd_3S(PPh_2)_2(PPh_3)_3]$ (0.070 g, 0.046 mmol) in THF (5 mL). There was no noticeable change in the initial red color of the solution. After stirring, for 10 minutes, the solvent was removed in vacuo and the excess $HBF_4.Et_2O$ was removed by successive washings with ether (3x10 mL). The remaining dark red powder was recrystallized from THF/hexane at 24°C to yield $[Pd_3SH(PPh_2)_2(PPh_3)_3][BF_4]$ as dark red crystals (0.050 g, 0.034 mmol). Yield: 75% (based on the conversion of $[Pd_3S(PPh_2)_2(PPh_3)_3]$).
A satisfactory elemental analysis of this compound was not obtained.

$^{31}P\{^1H\}$ NMR:[170] δ_1 -126.5, $\delta_{2,3}$ -120.1, $\delta_{4,5}$ 66.1; J_{12} 85. Solvent: THF.

$[Pd_3(\mu\text{-}SMe)(\mu\text{-}PPh_2)_2(PPh_3)_3][BF_4]$:

Excess $(CH_3)_3OBF_4$ (0.013 g, 0.087 mmol) was added to a stirred solution of $[Pd_3S(PPh_2)_2(PPh_3)_3]$ (0.080 g, 0.054 mmol) in THF (5 mL). Over a period of 15 minutes the color of the solution changed from red to dark orange. After 1.5 h of stirring, the solvent was removed in vacuo to obtain an orange powder. The orange powder was recrystallized from CH_2Cl_2/hexane at 24°C to afford $[Pd_3SMe(PPh_2)_2(PPh_3)_3][BF_4]$

as orange crystals (0.052 g, 0.032 mmol). Yield: 60% (based on the conversion of $[Pd_3S(PPh_2)_2(PPh_3)_3]$).

Anal. Calc'd for $C_{81}H_{70}BCl_2F_4P_5Pd_3S$: C 57.0, H 4.13; Found: C 57.7, H 4.19.

$^{31}P\{^1H\}$ NMR:[170] δ_1 -125.7, $\delta_{2,3}$ -119.2, $\delta_{4,5}$ 57.1; J_{12} 87. Solvent: $CDCl_3$.

$[Pd_3(\mu\text{-}SCH_2Ph)(\mu\text{-}PPh_2)_2(PEt_3)_3][BF_4]$:

Excess $PhCH_2Br$ (0.719 g, 4.203 mmol) was added to a stirred solution of $[Pd_3S(PPh_2)_2(PEt_3)_3]$ (0.100 g, 0.093 mmol) in THF (7 mL). The color changed from dark red to orange red instantly. After stirring for 20 minutes, the solvent was removed in vacuo. The oily residue obtained was washed with ether (3x 15 mL) to remove excess $PhCH_2Br$. The red powder obtained was dissolved in ethanol and excess $NaBF_4$ (0.100 g, 0.911 mmol) was then added. After one hour of stirring, the solvent was removed in vacuo and the remaining solid was extracted with CH_2Cl_2 (5mL). The extract was filtered through celite and then layered with hexane and stored at 24°C. $[Pd_3SCH_2Ph(PPh_2)_2(PEt_3)_3][BF_4]$ was obtained as dark red crystals (0.020 g, 0.015 mmol). Yield 30% (based on the conversion of $[Pd_3S(PPh_2)_2(PEt_3)_3]$).

Anal. Calc'd for $C_{49}H_{72}BF_4P_5Pd_3S$: C 46.9, H 5.79; Found: C 46.8, H 5.76.

$^{31}P\{^{1}H\}$ NMR:[170] δ_1 -139.2, $\delta_{2,3}$ -128.2, $\delta_{4,5}$ 40.4; J_{12} 88. Solvent: $CDCl_3$.

$[Pd_3(\mu\text{-}Se)(\mu\text{-}PPh_2)_2(PEt_3)_3][BF_4]$:

Excess Na_2Se (0.100 g, 0.800 mmol) was added to a stirred solution of $[Pd_3Cl(PPh_2)_2(PEt_3)_3][BF_4]$ (0.100 g, 0.085 mmol) in THF (5 mL). After 1 h of stirring, the solvent was removed in vacuo leaving a dark red powder which was extracted with THF (20 mL). The extract was filtered and the solvent removed in vacuo to give $[Pd_3Se(PPh_2)_2(PEt_3)_3]$ (0.070 g, 0.062 mmol) as a dark red powder. Yield: 73% (based on the conversion of $Pd_3Cl(PPh_2)_2(PEt_3)_3][BF_4]$. Anal. Calc'd. for $C_{42}H_{65}P_5Pd_3Se$: C 44.9, H 5.83; Found: C 42.6, H 4.83.

$^{31}P\{^{1}H\}$ NMR:[170] δ_1 -137.3, $\delta_{2,3}$ -123.6, $\delta_{4,5}$ 2.2; J_{12} 105, J_{14} 11. Solvent: THF.

$[Pt_3(\mu\text{-}Cl)(\mu\text{-}PPh_2)_2(PPh_3)_3][BF_4]$:

HCl gas was bubbled through a solution of $[Pt_3H(PPh_2)_2(PPh_3)_3]_2[C_2O_4]$ (0.300 g, 0.084 mmol) in ethanol (10 mL) for 20 seconds. The solution changed color from dark orange to light yellow. Excess $NaBF_4$ (0.100 g, 0.910 mmol) in water (0.5 mL) was then added to the stirred

solution. After 10 minutes of stirring, the solvent was removed in vacuo and the remaining light yellow powder was extracted with THF (10 mL). The extract was filtered and the solvent was removed in vacuo. The orangish yellow powder detained was recrystallized from CH_2Cl_2/hexane at 24°C to yield $[Pt_3Cl(PPh_2)_2(PPh_3)_3[BF_4]$ as orangish yellow crystals (0.270 g, 0.145 mmol). Yield: 86% (based on the conversion of $[Pt_3H(PPh_2)_2(PPh_3)_3]_2[C_2O_4]$).

Anal. Calc'd. for $C_{78}H_{65}BClF_4Pt_3$: C 50.2, H 3.51; Found: C 49.8, H 3.50.

$^{31}P\{^1H\}$ NMR:[171] δ_1 -137.9, $\delta_{2,3}$ -124.6, $\delta_{4,5}$ -13.1; J_{12} 76, J_{16} 4143, J_{17} 233, J_{27} 4406, J_{45} 243, J_{46} 2264, J_{47} 3523, J_{48} 95. Solvent: $CDCl_3$.

$^{195}Pt\{^1H\}$ NMR: δ_6 21.368749 MHz; δ_7 21.382223; J_{67} 651. Solvent: CH_2Cl_2.

$[Pt_3(\mu\text{-}Cl)(\mu\text{-}PPh_2)_2(PEt_3)_3][BF_4]$:

PEt_3 (0.020 g, 0.169 mmol) was added to a stirred solution of $[Pt_3Cl(PPh_2)_2(PPh_3)_3][BF_4]$ (0.100 g, 0.054 mmol) in CH_2Cl_2 (5 mL). There was a slight change in the initial yellow color of the solution to light orange. After stirring for 0.5 hour, the solvent was removed in vacuo and the remaining yellow powder was washed with ether (3x10

mL) to remove produced PPh_3. The yellow powder was then recrystallized from CH_2Cl_2/hexane at 24°C to afford $[Pt_3Cl(PPh_2)_2(PEt_3)_3][BF_4]$ (0.020 g, 0.014 mmol) as yellow crystals. Yield: 26% (based on the conversion of $[Pt_3Cl(PPh_2)_2((PPh_3)_3][BF_4]$).

Anal. Calc'd. for $C_{42}H_{65}BClF_4P_5Pt_3$: C 35.2, H 4.57; Found: C 35.8, H 4.53.

$^{31}P\{^1H\}$ NMR:[171] δ_1 -143.3, $\delta_{2,3}$ -125.1, $\delta_{4,5}$ -27.4; J_{12} 70.7, J_{16} 3764, J_{17} 253, J_{27} 3980, J_{45} 250, J_{46} 2309, J_{47} 3553, J_{48} 104. Solvent: $CDCl_3$.

$[Pt_3(\mu\text{-}Br)(\mu\text{-}PPh_2)_2(PPh_3)_3][Br]$:

Excess KBr (0.100 g, 0.840 mmol) in water (1 mL) was added to a stirred solution of $[Pt_3Cl(PPh_2)_2(PPh_3)_3][BF_4]$ (0.100 g, 0.054 mmol) in methanol (10 mL). After 10 minutes of stirring, the solvent was removed in vacuo and the remaining light yellow powder was extracted with CH_2Cl_2 (10 mL). The extract was filtered and the solvent was removed in vacuo. Recrystallization of the residue from CH_2Cl_2/hexane at 24°C afforded orange crystals of $[Pt_3Br(PPh_2)_2(PPh_3)_3][Br]$ (0.070 g, 0.035 mmol). Yield= 65% (based on the conversion of $[Pt_3Cl(PPh_2)_2(PPh_3)_3][BF_4]$).

Anal. Calc'd. for $C_{79}H_{67}Br_2Cl_2P_5Pt_3$: C 47.6, H 3.39; Found: C 47.9, H 3.37.

$^{31}P\{^{1}H\}$ NMR:[171] δ_1 -136.5, $\delta_{2,3}$ -123.6, $\delta_{4,5}$ -2.0; J_{12} 76.0, J_{16} 4139, J_{17} 235, J_{27} 4279, J_{45} 244, J_{46} 2271, J_{47} 3474, J_{48} 98. Solvent: CH_2Cl_2.

$[Pt_3(\mu\text{-}I)(\mu\text{-}PPh_2)_2(PPh_3)_3][I]$:

This complex can be prepared by two methods:

1) Excess KI (0.100 g, 0.602 mmol) in water (1 mL) was added to a stirred solution of $[Pt_3Cl(PPh_2)_2(PPh_3)_3][BF_4]$ (0.200 g, 0.107 mmol) in ethanol (15 mL). The solution turned dark red immediately. After 0.5 hour of stirring, the solvent was removed <u>in vacuo</u> and the remaining dark red powder was extracted with CH_2Cl_2 (25 mL). The extract was filtered through celite and the solvent was removed <u>in vacuo</u> to obtain a dark red powder. Recrystallization from CH_2Cl_2/hexane gave dark red crystals of $[Pt_3I(PPh_2)_2(PPh_3)_3][I]$ (0.175 g, 0.088 mmol). Yield: 82% (based on the conversion of $[Pt_3Cl(PPh_2)_2(PPh_3)_3][BF_4]$). <u>Anal.</u> Calc'd. for $C_{78}H_{65}I_2P_5Pt_3$: C 46.9, H 3.25; <u>Found:</u> C 46.9, H 3.28.

$^{31}P\{^{1}H\}$ NMR:[171] δ_1 -134.7, $\delta_{2,3}$ -120.4, $\delta_{4,5}$ 14.1; J_{12} 76.9, J_{16} 4157, J_{17} 233, J_{27} 4313, J_{45} 237, J_{46} 2301, J_{47} 3357, J_{48} 86. Solvent: CH_2Cl_2.

2) Excess CH_3I (0.570 g, 4.015 mmol) was added to a

stirred solution of $[Pt_3H(PPh_2)_2(PPh_3)_3]_2[C_2O_4]$ (0.040 g, 0.011 mmol) in THF (5 mL). Solution turned dark red almost immediately. After 0.5 hour of stirring, the solvent was removed <u>in vacuo</u> to obtain a dark red powder. The $^{31}P\{^1H\}$ spectrum of the red powder matched that of $[Pt_3I(PPh_2)_2(PPh_3)_3][I]$ exactly.

$[Pt_3(\mu\text{-}S)(\mu\text{-}PPh_2)_2(PPh_3)_3]$:

Excess $Na_2S.9H_2O$ (0.200 g, 0.833 mmol) in water (0.5 mL) was added to a stirred yellow suspension of $[Pt_3Cl(PPh_2)_2(PPh_3)_3][BF_4]$ (0.300 g, 0.161 mmol) in methanol (20 mL). The suspension became orange instantly. After 15 minutes of stirring, the solvent was removed <u>in vacuo</u>. The resulting orange powder was extracted with THF (35 mL). The extract was filtered and the solvent removed <u>in vacuo</u> to give $[Pt_3S(PPh_2)_2(PPh_3)_3]$ (0.270 g, 0.130 mmol) as an orange powder. Yield: 81% (based on the conversion of $[Pt_3Cl(PPh_2)_2(PPh_3)_3]$).

<u>Anal.</u> Calc'd. for $C_{78}H_{65}P_5SPt_3$: C 52.8, H 3.69; <u>Found:</u> C 49.5, H 3.63.

$^{31}P\{^1H\}$ NMR:[171] δ_1 -134.7, $\delta_{2,3}$ -123.7, $\delta_{4,5}$ -47.8; J_{12} 82.7, J_{16} 3538, J_{17} 230, J_{27} 4784, J_{45} 177.2, J_{46} 2199, J_{47} 2637, J_{48} 74.5. Solvent: THF.

$[Pt_3(\mu\text{-}SCH_2Ph)(\mu\text{-}PPh_2)_2(PPh_3)_3][BF_4]$:

Excess $PhCH_2Br$ (0.288 g, 1.681 mmol) was added to a stirred orange solution of $[Pt_3S(PPh_2)_2(PPh_3)_3]$ (0.050 g, 0.028 mmol) in THF (5 mL). The color of the solution turned lighter from red to orange. After 15 minutes of stirring, the solvent was removed in vacuo. The residue was washed with hexane (4x15 mL) and ether (3x15 mL) to remove excess $PhCH_2Br$. The orange powder obtained was dissolved in ethanol (5 ml) and excess $NaBF_4$ (0.100 g, 0.911 mmol) in water (0.5 mL) was then added. After 5 minutes of stirring, the solvent was removed in vacuo and the remaining orange powder extracted with CH_2Cl_2 (5 mL). The extract was filtered and the solvent was removed in vacuo. Recrystallization from THF/hexane at 24°C yielded $[Pt_3SCH_2Ph(PPh_2)_2(PPh_3)_3][BF_4]$ (0.025 g, 0.013 mmol) as orange crystals. Yield: 46% (based on the conversion of $[Pt_3S(PPh_2)_2(PPh_3)_3]$).

Anal. Calc'd. for $C_{85}H_{72}BF_4P_5SPt_3$: C 52.3, H 3.72; Found: C 52.1, H 3.89.

$^{31}P\{^1H\}$ NMR:[171] δ_1 -139.4, $\delta_{2,3}$ -131.1, $\delta_{4,5}$ -29.8; J_{12} 76, J_{16} 4332, J_{27} 4544, J_{45} 213, J_{46} 2284, J_{47} 2846, J_{48} 101. Solvent: CH_2Cl_2.

$[Pt_3(\mu\text{-}SH)(\mu\text{-}PPh_2)_2(PPh_3)_3][BF_4]$:

Excess $HBF_4.Et_2O$ (0.100 g, 0.618 mmol) was added to a stirred solution of $[Pt_3S(PPh_2)_2(PPh_3)_3]$ (0.050 g, 0.028 mmol) in benzene (10 mL). Immediately the solution changed from red to light yellow. After 1 hour of stirring, the solvent was removed in vacuo. the remaining bright yellow powder was washed with ether (3x10 mL). Recrystallization from CH_2Cl_2/hexane at 24°C afforded $[Pt_3SH(PPh_2)_2(PPh_3)_3][BF_4]$ (0.030 g, 0.016 mmol) as yellow crystals. Yield= 58% (based on the conversion of $[Pt_3S(PPh_2)_2(PPh_3)_3]$).

Anal. Calc'd for $C_{79}H_{68}BCl_2F_4P_5Pt_3S$: C 48.7, H 3.52; Found: C 48.4, H 3.52.

$^{31}P\{^1H\}$ NMR:[171] δ_1 -137.6, $\delta_{2,3}$ -130.0, $\delta_{4,5}$ -21.9; J_{12} 73, J_{16} 4355, J_{17} 207, J_{27} 4423, J_{45} 214, J_{46} 2243, J_{47} 2980, J_{48} 96. Solvent: THF

$[Pt_3(\mu\text{-}SMe)(\mu\text{-}PPh_2)(PPh_3)_3][I]$:

Excess CH_3I (0.228 g, 1.606 mmol) was added to a stirred solution of $[Pt_3S(PPh_2)_2(PPh_3)_3]$ (0.230 g, 0.130 mmol) in THF (5 mL). The color of the solution changed from red to orange almost immediately. After 15 minutes of stirring, the solvent was removed in vacuo. The orange powder was washed with hexane (3x10 mL) and recrystallized from

THF/hexane at 24°C to give $[Pt_3SMe(PPh_2)_2(PPh_3)][I]$ (0.220 g, 0.115 mmol) as orange crystals. Yield: 88% (based on the conversion of $[Pt_3S(PPh_2)_2(PPh_3)_3]$).

Anal. Calc'd. for $C_{79}H_{68}IP_5SPt_3$: C 49.5, H 3.58; Found: C 49.6, H 3.73.

$^{31}P\{^1H\}$ NMR:[171] δ_1 -137.4, $\delta_{2,3}$ -129.2, $\delta_{4,5}$ -28.6; J_{12} 75, J_{16} 4366, J_{17} 215, J_{27} 4491, J_{45} 215, J_{46} 2255, J_{47} 2802, J_{48} 98. Solvent: $CDCl_3$.

$[Pt_3(\mu\text{-}SMe)(\mu\text{-}PPh_2)_2(PR_3)_3][I]$ (R= Et, Bu^n):

These complexes were prepared in a similar manner. e.g. $[Pt_3(\mu\text{-}SMe)(\mu\text{-}PPh_2)_2(PEt_3)_3][I]$:

PEt_3 (0.040 g, 0.064 mmol) was added to a stirred solution of $[Pt_3SMe(PPh_2)_2(PPh_3)_3][BF_4]$ (0.040 g, 0.021 mmol) in CH_2Cl_2 (5 mL). The solution changed color from bright orange to a lighter orange. After 15 minutes of stirring, the solvent was removed in vacuo and the remaining light orange powder was washed with ether (3x10 mL) to remove liberated PPh_3. Recrystallization from CH_2Cl_2/hexane yielded $[Pt_3SMe(PPh_2)_2(PEt_3)_3][BF_4]$ (0.026 g, 0.018 mmol) as light orange crystals. Yield: 86% (based on the conversion of $[Pt_3SMe(PPh_2)_2(PPh_3)_3]$).

Anal. Calc'd. for $C_{43}H_{68}BF_4P_5SPt_3$: C 35.8, H 4.75; Found:

C 36.8, H 4.82.

$^{31}P\{^{1}H\}$ NMR:[171] δ_1 -145.0, $\delta_{2,3}$ -136.8, $\delta_{4,5}$ -46.0; J_{12} 63, J_{16} 4046, J_{27} 4125, J_{46} 2366. Solvent: THF.

$[Pt_3(\mu\text{-}SMe)(\mu\text{-}PPh_2)_2(PBu^n{}_3)_3][I]$: Yield: 53%. Isolated as a light orange oil.

$^{31}P\{^{1}H\}$ NMR:[171] δ_1 -154.0, $\delta_{2,3}$ -145.1, $\delta_{4,5}$ -46.5; J_{12} 70, J_{16} 4036, J_{27} 4095, J_{45} 213, J_{46} 2344, J_{47} 2805, J_{48} 104. Solvent: $CDCl_3$.

$[Pt_3(\mu\text{-}PPh_2)_3(PPh_3)_3][Cl]$:

PPh_2H (0.015 g, 0.083 mmol) was added to a stirred solution of $[Pt_3Cl(PPh_2)_2(PPh_3)_3][Cl]$ (0.0150 g, 0.083 mmol) and p-toluidine (0.008 g, 0.075 mmol) in THF (5 mL). The solution changed from yellow to deep red almost instantly. After 1 hour of stirring, the solvent was removed <u>in vacuo</u> and the product was washed with ether (3x15 mL). Recrystallization from CH_2Cl_2/hexane at 24°C afforded $[Pt_3(PPh_2)_3(PPh_3)_3][Cl]$ (0.130 g, 0.066 mmol) as red crystals. Yield: 80% (based on the conversion of $[Pt_3Cl(PPh_2)_2(PPh_3)_3][Cl]$).

A satisfactory elemental analysis of this compound was not obtained.

$^{31}P\{^{1}H\}$ NMR:[172] $\delta_{1,2,3}$ -129.3, $\delta_{4,5,6}$ -42.0; J_{12} 66, J_{17} 4597, J_{27} 166, J_{47} 2045. Solvent: THF.

$[Pt_3(\mu\text{-}PPh_2)_3(PEt_3)_3][BF_4]$:

PEt_3 (0.017 g, 0.147 mmol) was added to a stirred red solution of $[Pt_3(PPh_2)_3(PPh_3)_3][BF_4]$ (0.090 g, 0.045 mmol) in CH_2Cl_2 (5 mL). The solution turned slightly darker in color. After 0.5 hour of stirring, the solvent was removed in vacuo and the resulting red powder was washed with ether (3x10 mL). Recrystallization from CH_2Cl_2/hexane at 24°C gave $[Pt_3(PPh_2)_3(PEt_3)_3][BF_4]$ (0.053 g, 0.038 mmol) as red crystals. Yield: 74% (based on the conversion of $[Pt_3(PPh_2)_3(PPh_3)_3][BF_4]$).

Anal. Calc'd for $C_{54}H_{75}BF_4P_6Pt_3$: C 41.0, H 4.78; Found: C 40.3, H 4.83.

$^{31}P\{^1H\}$ NMR: ^{172} $\delta_{1,2,3}$ -141.1, $\delta_{4,5,6}$ -56.9; J_{12} 64, J_{17} 2057, J_{27} 115, J_{47} 4178. Solvent: CH_2Cl_2.

$^{195}Pt\{^1H\}$ NMR: δ_{Pt} 21.364350 MHz. Solvent: CH_2Cl_2.

Reaction of $[Pt_3(\mu\text{-}H)(\mu\text{-}PPh_2)_2(PPh_3)_3]_2[C_2O_4]$ with $PhCH_2Br$ and CH_2I_2:

These reactions were carried out in a similar manner:

e.g. Excess $PhCH_2Br$ (0.075 g, 0.438 mmol) was added to a stirred solution of $[Pt_3(H)(PPh_2)_2(PPh_3)_3]_2[C_2O_4]$ (0.050 g, 0.014 mmol) in CH_2Cl_2 (2 mL). After 1 hour of stirring, the

$^{31}P\{^{1}H\}$ NMR spectrum of the solution was recorded which indicated only the presence of the starting cluster.

Reaction of $[M_3(\mu\text{-}Cl)(\mu\text{-}PPh_2)(PR_3)_3][BF_4]$ (M= Pd, R= Et; M= Pt, R= Ph) with Zn/AcOH/CH_3OH:

These reactions were carried out in a similar manner: e.g. Reaction of $[Pt_3(\mu\text{-}Cl)(\mu\text{-}PPh_2)_2(PPh_3)_3][BF_4]$ with Zn/AcOH/MeOH:

Zn dust (0.050 g, 0.765 mmol) and glacial acetic acid (1 mL) were added to a stirred $[Pt_3(Cl)(PPh_2)_2(PPh_3)_3][BF_4]$ (0.100 g, 0.054 mmol) in CH_3OH (20 mL). There was no noticeable change in the color of the solution. After 4 days of stirring, excess K_2CO_3 (0.300 g, 2.171 mmol) was added to neutralize the solution. The solvent was removed in vacuo leaving an orange-yellow powder which was extracted in CH_2Cl_2 (20 mL) to obtain a yellow solution. The solvent was then removed in vacuo to obtain a yellow powder which was identified as $[Pt_3(\mu\text{-}H)(\mu\text{-}PPh_2)_2(PPh_3)_3][BF_4]$ by $^{31}P\{^{1}H\}$ NMR spectroscopy.

In the case of $[Pd_3(\mu\text{-}Cl)(\mu\text{-}PPh_2)_2(PR_3)_3][BF_4]$ (R= Ph,Et) there was a color change from light red to dark red upon the addition of reagents. The only products identified in these cases were $[Pd_3(\mu\text{-}PPh_2)_3(PR_3)_3][BF_4]$ (R= Ph, Et), through their identical $^{31}P\{^{1}H\}$ NMR spectrum with authentic

samples.

$[Pd_2(\mu\text{-}PPh_2)(\mu\text{-}Ph_2PCH_2PPh_2)(PPh_3)_2][BF_4]$ and $[Pd_2(\mu\text{-}PPh_2)(\mu\text{-}Ph_2PCH_2PPh_2)_2Cl_2][BF_4]$:

Dppm (0.049 g, 0.130 mmol) was added to a stirred solution of $[Pd_3Cl(PPh_2)_2(PPh_3)_3][BF_4]$ (0.200 g, 0.125 mmol) in CH_2Cl_2 (15 mL). The solution changed color from light red to dark red immediately. After 24 hours of stirring, during which the solution changed color back to light red the volume of the solvent was reduced to 4 mL. The solution was layered with hexane (5 mL) and stored at 0°C. After 24 hours, the yellow crystals of $[Pd_2(PPh_2)(dppm)_2Cl_2][BF_4]$ (0.018 g, 0.014 mmol) that had formed were separated from the red supernatant. The red supernatant was dried <u>in vacuo</u> to yield an orange powder. Recrystallization from CH_2Cl_2/hexane at 24°C afforded $[Pd_2)(PPh_2(dppm)(PPh_3(_2][BF_4]$ (0.080 g, 0.057 mmol) as orange crystals.
$[Pd_2(PPh_2)(dppm)_2Cl_2][BF_4]$: Yield: 7% (based on the conversion of $[Pd_3Cl(PPh_2)_2(PPh_3)_3][BF_4]$).
<u>Anal.</u> Calc'd. for $C_{62}H_{54}BF_4P_5Pd_2$: C 56.2, H 4.11; <u>Found:</u> C 56.3, H 4.84.

$^{31}P\{^1H\}$ NMR:[173] δ_1 -66.7, δ_2 -129.3; J_{12} 11.5. Solvent: $CDCl_3$.

$[Pd_2(PPh_2)(dppm)(PPh_3)_2][BF_4]]$: Yield: 30% (based on the conversion of $(Pd_3(Cl(PPh_2)_2(PPh_3)_3][BF_4])$.

Anal. Calc'd. for $C_{73}H_{62}BF_4P_5Pd_2$: C 62.9, H 4.48; Found: C 62.0, H 4.72.

$^{31}P\{^1H\}$ NMR:[174] δ_1 96.7, $\delta_{2,3}$ -125.4, $\delta_{4,5}$ -135.0; J_{12} 32, J_{14} 207, J_{23} 200, J_{24} -31.8, J_{25} 7.4, J_{45} 60. Solvent: $CDCl_3$.

$[Pd_2(\mu\text{-}PPh_2)(\mu\text{-}Ph_2PCH_2PPh_2)(PR_3)_2][BF_4]$ (R= Et, Bu^n):

Similar methods were used to synthesize the above compounds: e.g. $[Pd_2(\mu\text{-}PPh_2)(\mu\text{-}dppm)(PEt_3)_2][BF_4]$:

PEt_3 (0.015 g, 0.125 mmol) was added to a stirred solution of $[Pd_2(PPh_2)(dppm)(PPh_3)_2][BF_4]$ (0.050 g, 0.036 mmol) in CH_2Cl_2 (10 mL). The orange solution turned slightly darker. After 1 h of stirring, the solvent was reduced in volume (5 mL) and was layered with hexane. After 24 h at 24°C light orange crystals of $[Pd_2(PPh_2)(dppm)(PEt_3)_2][BF_4]$ (0.035 g, 0.032 mmol) had formed and were separated. Yield: 88% (based on the conversion of $[Pd_2(PPh_2)(dppm)(PPh_3)_2][BF_4]$).

Anal. Calc'd for $C_{50}H_{64}BCl_2F_4P_5Pd_2$: C 50.9, H 5.37; Found: C 51.8, 55.

$^{31}P\{^1H\}$ NMR:[174] δ_1 82.5, $\delta_{2,3}$ -132.9, $\delta_{4,5}$ -135.4; J_{12} 30, J_{14} 210. Solvent: $CDCl_3$.

$[Pd_2(\mu\text{-}PPh_2)(\mu\text{-}dppm)(PBu^n{}_3)_2][BF_4]$: Isolated as light orange crystals. Yield: 70% (based on the conversion of $[Pd_2(PPh_2)(dppm)(PPh_3)_2][BF_4]$).

Anal. Calc'd for $C_{61}H_{86}BF_4P_5Pd_2$: C 57.5, H 6.81; Found: C 58.1, H 6.69.

$^{31}P\{^1H\}$ NMR:[174] δ_1 81.9, $\delta_{2,3}$ -144.3, $\delta_{4,5}$ -134.3; J_{12} 28, J_{14} 210. Solvent: CH_2Cl_2.

$[Pd_2(\mu\text{-}PPh_2)(\mu\text{-}dppm)(PEt_3)_2][BF_4]$ was also prepared by the following method:

Dppm (0.022 g, 0.057 mmol) was added to a stirred solution of $[Pd_3Cl(PPh_2)_2(PEt_3)_3][BF_4]$ (0.066 g, 0.056 mmol) in CH_2Cl_2 (5 mL). The solution became slightly darker. After 1 hour of stirring, the solvent was removed in vacuo. Crystallization from CH_2Cl_2/hexane at 24°C yielded orange crystals of $[Pd_2(PPh_2)(dppm)(PEt_3)_2]_2[C_2O_4]$ (0.030 g, 0.030 mmol).

$[Pd_2(\mu\text{-}PPh_2)(\mu\text{-}Pr^i{}_2PCH_2PPh_2)(PPh_3)_2][BF_4]$:

$Pr^i{}_2PCH_2PPh_2$ (0.052 g, 0.163 mmol) was added to a stirred solution of $[Pd_3Cl(PPh_2)_2(PPh_3)_3][BF_4]$ (0.237 g, 0.149 mmol) in CH_2Cl_2 (15 mL). The solution changed color to dark red instantly. After 24 hours of stirring, the volume

of the solvent was reduced to 3 mL and hexane (5 mL) was layered on top. After 24 hours at 0°C the orange supernatant was separated from the yellow precipitate that had formed. The solvent was then removed <u>in vacuo</u> to obtain an orange powder. Successive crystallizations from CH_2Cl_2/hexane at 24°C afforded $[Pd_2(PPh_2)(Pr^i{}_2PCH_2PPh_2)(PPh_3)_2][BF_4]$ (0.015 g, 0.011 mmol) as orange crystals. Yield: 5% (based on the conversion of $[Pd_3Cl(PPh_2)_2(PPh_3)_3][BF_4]$).

<u>Anal.</u> Calc'd. for $C_{68}H_{68}BCl_2F_4P_5Pd_2$: C 58.3, H 4.82; <u>Found:</u> C 58.3, H 4.83.

$^{31}P\{^1H\}$ NMR:[175] δ_1 95.8, $\delta_{2,3}$ -124.4, δ_4 -121.5, δ_5 -138.2; J_{12} 30, J_{13} 40, J_{14} 205, J_{15} 195, J_{23} 160, J_{24} -20, J_{25} 9, J_{34} 6, J_{35} -17, J_{45} 55. Solvent: $CDCl_3$.

$[Pd_2(\mu\text{-}PPh_2)(\mu\text{-}(EtO)_2(POP(OEt)_2)(PPh_3)_2][BF_4]$:

$(EtO)_2POP(OEt)_2$ (0.050 g, 0.194 mmol) was added to a stirred solution of $[Pd_3Cl(PPh_2)_2(PPh_3)_3][BF_4]$ (0.100 g, 0.063 mmol) in CH_2Cl_2 (5 mL). The solution changed color from red to dark red and after 30 seconds returned to red again. After 16 hour of stirring, the solvent was removed <u>in vacuo</u>. The orange residue was washed with hexane (3x15 mL). Recrystallization from CH_2Cl_2/hexane 24°C gave $[Pd_2(PPh_2)(POP)(PPh_3)_2][BF_4]$ (0.077 g, 0.061 mmol) as orange

crystals. Yield: 65% (based on the conversion of $[Pd_3Cl(PPh_2)_2(PPh_3)_3][BF_4]$.

Anal. Calc'd. for $C_{56}H_{60}BF_4O_5P_5Pd_2$: C 53.1, H 4.77; Found: C 52.2, H 4.89.

$^{31}P\{^1H\}$ NMR:[174] δ_1 85.2, $\delta_{2,3}$ -123.3, $\delta_{4,5}$ -15.2; J_{12} 25, J_{14} 330, J_{23} 70, J_{24} 10, J_{45} 30. Solvent: $CDCl_3$.

$[PtPd(\mu\text{-}PPh_2)(\mu\text{-}Ph_2PCH_2PPh_2)(PPh_3)_2][BF_4]$ and $[Pt_2(\mu\text{-}PPh_2)(\mu\text{-}Ph_2PCH_2PPh_2)_2Cl_2][BF_4]$:

Dppm (0.060 g, 0.156 mmol) was added to a stirred solution of $[PtPd_2Cl(PPh_2)_2(PPh_3)_3][BF_4]$ and $[Pd_3Cl(PPh_2)_2(PPh_3)_3][BF_4]$ (0.200 g) in CH_2Cl_2 (15 mL). Immediately the color changes from light red to dark red and after 30 minutes to light red again. After stirring for 24 hours, the solution was concentrated to 5 mL and layered with hexane (5 mL). After 24 h at 0°C the yellow crystals formed were collected and by $^{31}P\{^1H\}$ and $^{195}Pt\{^1H\}$ NMR spectroscopy were shown to contain $[Pt_2(PPh_2)(dppm)_2Cl_2][BF_4]$. The solvent of the orange supernatant was removed in vacuo and the $^{31}P\{^1H\}$ and $^{195}Pt\{^1H\}$ of the orange powder isolated showed the presence of $[PtPd(PPh_2)(dppm)(PPh_3)_2][BF_4]$.

There is always some $[Pd_3Cl(PPh_2)(PPh_3)_3][BF_4]$ present in the preparation of $[PtPd_2Cl(PPh_2)_2(PPh_3)_3][BF_4]$, therefore,

the reaction with dppm also yields $[Pd_2(PPh_2)(dppm)(PPh_3)_2]^+$ and $[Pd_2(PPh_2)(dppm)_2(Cl)_2]^+$ as described earlier.

$[Pt_2(PPh_2)(dppm)_2Cl_2][BF_4]$: $^{31}P\{^1H\}$ NMR:[176] δ_1 -94.3, δ_2 -134.1; J_{12} 10, J_{13} 2552, J_{23} 2715. Solvent: $CDCl_3$.

$^{195}Pt\{^1H\}$ NMR: δ_{Pt} 21.401337 MHz. Solvent: $CDCl_3$.

$[PtPd(PPh_2)(dppm)(PPh_3)_2][BF_4]$: $^{31}P\{^1H\}$ NMR:[177] δ_1 78.3, δ_2 -130.3, δ_3 -132.6, δ_4 -137.8, δ_5 -140.0; J_{12} 6, J_{13} 52, J_{14} 227, J_{15} 238, J_{16} 3205. Solvent: $CDCl_3$.

$^{195}Pt\{^1H\}$ NMR: δ_{Pt} 21.406287 MHz. Solvent: $CDCl_3$.

$[Pt_2(\mu\text{-}PPh_2)(\mu\text{-}R_2PCH_2PR_2)(PPh_3)_2][Y]$ (R= Ph, Me):

These complexes were prepared by similar methods: e.g. $[Pt_2(\mu\text{-}PPh_2)(\mu\text{-}Ph_2PCH_2PPh_3)_2]_2[BF_4]$:

Dppm (0.049 g, 0.127 mmol) was added to a stirred solution of $[Pt_3H(PPh_2)_2(PPh_3)_3][BF_4]$ (0.200 g, 0.109 mmol) in CH_2Cl_2 (20 mL). There was no noticeable change in the color of the solution. After 1 hour of stirring, the solvent was removed <u>in vacuo</u>. The remaining light orange powder was washed with hexane (2x10 mL). Recrystallization from CH_2Cl_2/hexane at 24°C afforded $[Pt_2(PPh_2)(dppm)(PPh_3)_2][BF_4]$ (0.210 g, 0.134 mmol) as orange crystals. Yield: 82% (based on the conversion of $[Pt_3H(PPh_2)_2(PPh_3)_3][BF_4]$).

Anal. Calc'd for $C_{73}H_{62}BF_4P_5Pt_2$: C 55.8, H 3.98; Found: C 56.3, H 3.99.

$^{31}P\{^1H\}$ NMR:[178] δ_1 53.9, $\delta_{2,3}$ -120.3, $\delta_{4,5}$ -134.7; J_{12} 11, J_{14} 251.4, J_{16} 2781, J_{23} 149, J_{24} 5.8, J_{25} 0, J_{26} 3293, J_{36} 343, J_{45} 54.6, J_{46} 3065, J_{56} 53.4. Solvent: $CDCl_3$.

$^{195}Pt\{^1H\}$ NMR: δ_{Pt} 21.387240 MHz. Solvent: $CDCl_3$.

$[Pt_2(\mu\text{-}PPh_2)(\mu\text{-}Me_2PCH_2PMe_2)(PPh_3)_2]_2[C_2O_4]$: Yield: 52%. Isolated as orange crystals.

Anal. Calc'd for $C_{108}H_{108}O_4P_{10}Pt_4$: C 50.8, H 4.25; Found: C 49.8, H 4.26.

$^{31}P\{^1H\}$ NMR:[178] δ_1 42.4, $\delta_{2,3}$ -119.7, $\delta_{4,5}$ -160.7; J_{12} 3.7, J_{14} 253, J_{16} 2639, J_{23} 155, J_{24} 7, J_{26} 3220, J_{36} 360, J_{45} 45, J_{46} 2853, J_{56} 57.8. Solvent: $CDCl_3$.

$^{195}Pt\{^1H\}$ NMR: δ_{Pt} 21.387682 MHz. Solvent: $CDCl_3$.

$[Pt_2(\mu\text{-}PPh_2)(\mu\text{-}Ph_2PCH_2PPh_2)(PR_3)_2][C_2O_4]$ (R= Et, Bu^n):

These complexes were prepared in a similar manner: e.g. $[Pt_2(\mu\text{-}PPh_2)(\mu\text{-}Ph_2PCH_2PPh_2)(PEt_3)_2]_2[C_2O_4]$:
PEt_3 (0.014 g, 0.121 mmol) was added to a stirred solution of $[Pt_2(PPh_2)(dppm)(PPh_3)_2]_2[C_2O_4]$ (0.060 g, 0.019 mmol) in CH_2Cl_2 (5 mL). After 3 hours of stirring, the solvent was removed in vacuo and the remaining orange powder was washed

with hexane (3x10 mL). Recrystallization from CH_2Cl_2/hexane at 24°C yielded $[Pt_2(PPh_2)(dppm)(PEt_3)_2][C_2O_4]$ (0.050 g, 0.016 mmol) as orange crystals. Yield: 84% (based on the conversion of $[Pt_2(PPh_2)(dppm)(PPh_3)_2]_2[C_2O_4]$).
Anal. Calc'd for $C_{100}H_{124}O_4P_{10}Pt_4$: C 48.4, H 5.04; Found: C 47.8, H 5.18.

$^{31}P\{^1H\}$ NMR:[178] δ_1 50.6, $\delta_{2,3}$ -127.9, $\delta_{4,5}$ -136.2; J_{12} 9.4, J_{14} 252, J_{16} 2775, J_{23} 134, J_{26} 3179, J_{36} 216, J_{45} 56, J_{46} 3072. Solvent: $CDCl_3$.

$^{195}Pt\{^1H\}$ NMR: δ_{Pt} 21.387236 MHz. Solvent: $CDCl_3$.

$[Pt_2(\mu\text{-}PPh_2)(\mu\text{-}Ph_2PCH_2PPh_2(PBu^n_3)_2]_2[C_2O_4]$: Yield: 44% Isolated as orange crystals.
Anal. Calc'd. for $C_{63}H_{88}Cl_2O_2P_5Pt_2$: C 51.9, H 6.02; Found: C 51.5, H 6.10.

$^{31}P\{^1H\}$ NMR:[178] δ_1 49.4, $\delta_{2,3}$ -136.5, $\delta_{4,5}$ -136.2; J_{14} 255, J_{16} 1645, J_{26} 3036, J_{45} 52, J_{46} 3034. Solvent: $CDCl_3$.

$[Pt_2(\mu\text{-}PPh_2)(\mu\text{-}Bu^t_2PCH_2PPh_2)(Bu^tNC)_2]_2[C_2O_4]$:

$Bu^t_2PCH_2PPh_2$ (0.033 g, 0.096 mmol) was added to a stirred solution of $[Pt_3H(PPh_2)_2(PPh_3)_3]_2[C_2O_4]$ (0.150 g, 0.042 mmol). After 3 hours of stirring, excess Bu^tNC (0.079 g, 0.950 mmol) was added to the solution. There was no

noticeable change in the color of the solution. After 1 hour of stirring, the volume of the solvent was reduced to 2 mL. The $^{31}P\{^{1}H\}$ NMR spectrum of the solution at this stage indicated the presence of $[Pt_2(\mu\text{-}PPh_2)(\mu\text{-}Bu^t{}_2PCH_2PPh_2)(Bu^tNC)_2]_2[C_2O_4]$. However, after recrystallization for 48 hours at 24°C, all the product had converted to $[Pt_2(\mu\text{-}PPh_2)(PPh_3)_3(Bu^tNC)]^+$ as evident by $^{31}P\{^{1}H\}$ NMR spectroscopy.

$[Pt_2(\mu\text{-}PPh_2)(\mu\text{-}Bu^t{}_2PCH_2PPh_2)(Bu^tNC)_2]_2[C_2O_4]$: $^{31}P\{^{1}H\}$ NMR:[179] δ_1 53.5, δ_2 -95.7, δ_3 -138.7; J_{12} 233, J_{13} 254, J_{14} 3011, J_{15} 2546, J_{23} 55, J_{24} 2924, J_{35} 3149. Solvent: CH_2Cl_2.

$[Pt_2(\mu\text{-}PPh_2)(PPh_3)_3(Bu^tNC)]_2[C_2O_4]$:

Bu^tNC (0.008 g, 0.092 mmol) was added to a stirred solution of $[Pt_3H(PPh_2)_2(PPh_3)_3]_2[C_2O_4]$ (0.300 g, 0.084 mmol) in CH_2Cl_2 (3 mL). The color of the solution changed from orange to light yellow. After 0.5 hour of stirring, the solvent was removed <u>in vacuo</u>. Recrystallization from THF/hexane at 24°C afforded $[Pt_2(PPh_2)(PPh_3)_3(Bu^tNC)]_2[C_2O_4]$ (0.270 g, 0.088 mmol) as yellow crystals. Yield: 70% (based on the conversion of $[Pt_3H(PPh_2)_2(PPh_3)_3]_2[C_2O_4]$).
<u>Anal.</u> Calc'd. for $C_{145}H_{130}Cl_2N_2O_4P_8Pt_4$: C 56.9, H 4.28; <u>Found:</u> C 56.6, H 4.48.

$^{31}P\{^{1}H\}$ NMR:[180] δ_1 26.6, δ_2 128.3, δ_3 122.0, δ_4 110.0; J_{14}

250, J_{15} 3101, J_{16} 2754, J_{23} 162, J_{25} 3156, J_{26} 433, J_{35} 320, J_{45} 3004. Solvent: $CDCl_3$.
IR: 2160.

Reaction of $[Pd_2(\mu\text{-}PPh_2)(\mu\text{-}(EtO)_2POP(OEt)_2(PPh_3)_2][BF_4]$ with $Ph_2PCH_2PPh_2$:

Dppm (0.007 g, 0.018 mmol) was added to a stirred solution of $[Pd_2(PPh_2)(POP)(PPh_3)_2][BF_4]$ (0.022 g, 0.018 mmol) in CH_2Cl_2 (5 mL). The solution immediately changed color from yellow to orange. After 24 hours of stirring, the solvent was removed in vacuo. The $^{31}P\{^1H\}$ NMR spectrum of the isolated orange powder showed that POP was completely replaced by dppm to afford $[Pd_2(\mu\text{-}PPh_2)(\mu\text{-}dppm)(PPh_3)_2][BF_4]$.

Reactions of $[M_3(M\text{-}X)(\mu\text{-}PPh_2)_2(PR_3)_3][Y]$ (M= Pd, X= SH, R= Ph; M= Pd, X= SCH_2Ph, R= Et; M= Pd, X= S, R= Ph; M= Pd, X= S, R= Et; M= Pd, X= PPh_2, R= Et; M= Pt, X= SMe, R= Ph; M= Pt, X= SCH_2Ph, R= Ph; M= Pt, X= S, R= Et; M= Pt, X= PPh_2, R= Ph; M= Pt, X= PPh_2, R= Et) with Dppm:

These reactions were carried out in a similar way and their results are summarized in chapter three. Two examples are:

Reaction of $[Pd_3(\mu\text{-}SH)(\mu\text{-}PPh_2)_2(PPh_3)_3][BF_4]$ with Dppm:

Dppm (0.020 g, 0.052 mmol) was added to a stirred solution of $[Pd_3(\mu\text{-}SH)(\mu\text{-}PPh_2)_2(PPh_3)_3][BF_4]$ (0.055 g, 0.034 mmol) in THF (2 mL) in a 10 mm NMR tube. After 1 hour of stirring, the $^{31}P\{^1H\}$ of the solution was taken which showed the complete conversion of the starting material to $[Pd_2(\mu\text{-}PPh_2)(\mu\text{-}dppm)(PPh_3)_2][BF_4]$ (0.055 g, 0.039 mmol).

Reaction of $[Pd_3(\mu\text{-}SCH_2Ph)(\mu\text{-}PPh_2)_2(PEt_3)_3][BF_4]$ with Dppm:

Dppm (0.012 g, 0.032 mmol) was added to a solution of $[Pd_3(\mu\text{-}SCH_2Ph)(\mu\text{-}PPh_2)_2(PEt_3)_3][BF_4]$ (0.040 g, 0.032 mmol) in THF (3 mL). There was no noticeable change in the color of the solution. After stirring the solution for 3 days, the $^{31}P\{^1H\}$ NMR spectrum of the solution was recorded which indicated the presence of unreacted starting cluster and dppm.

Reaction of $[Pt_2(\mu\text{-}PPh_2)(\mu\text{-}dppm)(PPh_3)_2][BF_4]$ with CH_3I:

Excess CH_3I (1.368 g, 9.635 mmol) was added to a stirred solution of $[Pt_2(PPh_2)(dppm)(PPh_3)_2][C_2O_4]$ (0.090 g, 0.029 mmol) in THF (2 mL). Almost immediately the color of the solution turned from dark orange to dark green. After stirring for 6 hours, the $^{31}P\{^1H\}$ NMR spectrum of the solution indicated the presence of $[Pt_2(PPh_2)(dppm)(PPh_3)(I)]$ and $[Ph_3PCH_3I]^+$. The product

could not be isolated because in solution it decomposes to yield $[Ph_3PCH_3I]^+$ and $[Pt(dppm)I_2]$ as monitored by $^{31}P\{^1H\}$ NMR spectroscopy.

$[Pt_2(PPh_2)(dppm)(PPh_3)(I)]$: $^{31}P\{^1H\}$ NMR:[181] δ_1 16.2, δ_2 -131.5, δ_3 -134.5, δ_4 -153.1; J_{12} 0, J_{13} 376, J_{14} 270, J_{15} 2036, J_{16} 2863, J_{23} 0, J_{24} 8, J_{25} 614, J_{26} 3688, J_{34} 59, J_{35} 2527, J_{36} 49, J_{45} 59, J_{46} 3020. Solvent: $CDCl_3$.

Reaction of $[Pt_2(\mu\text{-}PPh_2)(\mu\text{-}dmpm)(PPh_3)_2]_2[C_2O_4]$ with H_2:

This reaction was carried out under different conditions:

(a) H_2 was bubbled through a solution of $[Pt_2(\mu\text{-}PPh_2)(\mu\text{-}dmpm)(PPh_3)_2]_2[C_2O_4]$ (0.050 g, 0.020 mmol) in CH_2Cl_2 (10 mL) for 24 hours. There was no noticeable change in the color of the solution. The $^{31}P\{^1H\}$ NMR spectrum of the solution indicated that no reaction had taken place.

(b) $[Pt_2(\mu\text{-}PPh_2)(\mu\text{-}dmpm)(PPh_3)_2]_2[C_2O_4]$ (0.050 g, 0.020 mmol) dissolved in CH_2Cl_2 (2 mL) in a small Erlenmeyer flask was placed in a Parr high pressure reactor. After 24 hours at 800 psi H_2 pressure and 80°C temperature, the flask was removed from the reactor. There was no change in the color of the solution which contained some black precipitate. The $^{31}P\{^1H\}$ NMR spectrum of the solution showed only the presence of the starting dimer.

Reaction of $[M_2(\mu\text{-}PPh_2)(\mu\text{-}dppm)(PPh_3)_2][Y]$ with Different Oxidative Addition Reagents (M= Pt, Reagent= CH_3CH_2I, CH_2I_2, $PhCH_2Br$, Bu^tOOH; M= Pd, Reagent= CH_2I_2, CH_3I, CH_2N_2):

All of these reactions were carried out in a similar manner with similar results: e.g. Reaction of $[Pt_2(PPh_2)(dmpm)(PPh_3)_2]_2[C_2O_4]$ with CH_2I_2:

Excess CH_2I_2 (0.665 g, 2.483 mmol) was added to a stirred solution of $[Pt_2(PPh_2)(dmpm)(PPh_3)_2]_2[C_2O_4]$ (0.050 g, 0.020 mmol) in THF (2 mL). After 8.5 hours of stirring, the $^{31}P\{^1H\}$ NMR spectrum of the solution was recorded which indicated that no reaction has taken place. Additional stirring for 24 hours did not lead to any further reaction as was shown by $^{31}P\{^1H\}$ NMR spectroscopy.

Reaction of $[M_2(\mu\text{-}PPh_2)(\mu\text{-}dppm)(PPh_3)_2][Y]$ (M= Pt, Pd) with $LiBEt_3H$:

These reactions were carried out in a similar manner with similar results, for example:

$LiBEt_3H$ (0.004 g, 0.040 mmol) was added to a stirred solution of $[Pd_2(PPh_2)(dppm)(PPh_3)_2][BF_4]$ (0.050 g, 0.036 mmol) in THF (10 mL). After stirring for 24 hours the $^{31}P\{^1H\}$ NMR spectrum of the solution was recorded which showed that no reaction had occurred.

Reaction of $[Pd_2(\mu\text{-}PPh_2)(\mu\text{-}dppm)(PPh_3)_2][BF_4]$ with C_4F_6:

Excess C_4F_6 was condensed into a vessel containing a solution of $[Pd_2(PPh_2)(dppm)(PPh_3)_2][BF_4]$ (0.100 g, 0.072 mmol) in THF (15 mL) at -196°C. The vessel was slowly warmed up to 24°C and stirred for 24 hours. The $^{31}P\{^1H\}$ NMR spectrum of the solution indicated that no reaction had occurred.

Reaction of $[Pd_2(\mu\text{-}PPh_2)(\mu\text{-}dppm)(PPh_3)_2][BF_4]$ with CO:

CO was bubbled through a solution of $[Pd_2(PPh_2)(dppm)(PPh_3)_2][BF_4]$ (0.050 g, 0.036 mmol) in THF (15 mL). After 24 hours of bubbling the $^{31}P\{^1H\}$ NMR spectrum of the solution was recorded which indicated that no reaction had taken place.

Reaction of $[Pd_2(\mu\text{-}PPh_2)(\mu\text{-}dppm)(PPh_3)_2][BF_4]$ with $HBF_4.Et_2O$:

$HBF_4.Et_2O$ (0.030 g, 0.072 mmol) was added to a stirred solution of $[Pd_2(PPh_2)(dppm)(PPh_3)_2][BF_4]$ (0.050 g, 0.036 mmol) in CH_2Cl_2 (3 mL). There was no noticeable change in the color of the solution. After stirring for 24 hours, the $^{31}P\{^1H\}$ NMR spectrum of the solution was recorded which showed that no reaction had taken place.

Reaction of $[Pt_2(\mu\text{-}PPh_2)(\mu\text{-}dppm)(PPh_3)_2]_2[C_2O_4]$ with HCl:

HCl was bubbled through a solution of $[Pt_2(PPh_2)(dppm)(PPh_3)_2]_2[C_2O_4]$ (0.030 g, 0.010 mmol) in CH_2Cl_2 (5 mL) for a period of 5 minutes. The color of the solution turned from orange to light yellow almost immediately. The $^{31}P\{^1H\}$ NMR spectrum of the solution was recorded and indicated only the presence of the starting dimer.

Reaction of $[Pt_2(\mu\text{-}PPh_2)(\mu\text{-}dppm)(PPh_3)_2]_2[C_2O_4]$ with I_2:

I_2 (0.011 g, 0.043 mmol) was added to a stirred solution of $[Pt_2(PPh_2)(dppm)(PPh_3)_2]_2[C_2O_4]$ (0.050 g, 0.016 mmol) in THF (5 mL). The color of the solution turned dark red immediately. After 24 hours of stirring, the color of the solution changed to light orange. The solvent was removed in vacuo and the light yellow powder isolated was identified as $[PtI_2(dppm)]$ by comparing its $^{31}P\{^1H\}$ NMR parameters with published values.

Reaction of $[Pd_2(\mu\text{-}PPh_2)(\mu\text{-}dppm)(PPh_3)_2][BF_4]$ with H_2:

This reaction was carried out under different conditions:

a) H_2 was bubbled through a solution of $[Pd_2(PPh_2)(dppm)(PPh_3)_2][BF_4]$ (0.050 g, 0.036 mmol) in

CH_2Cl_2 (10 mL) for four days. After that time, the $^{31}P\{^1H\}$ NMR spectrum of the solution indicated that no reaction had taken place. The starting compound was recovered in over 90% yield.

b) A solution of $[Pd_2(PPh_2)(dppm)(PPh_3)_2][BF_4]$ (0.050 g, 0.036 mmol) in CH_2Cl_2 (5 mL) was placed in a Parr bench-top high pressure reactor and pressurized to 1200 psi with H_2. After 18 hours at 75°C, the solution was removed. The $^{31}P\{^1H\}$ NMR spectrum of the solution only showed the presence of the starting material.

Reaction of $[Pt_2(\mu\text{-}PPh_2)(\mu\text{-}dmpm)(PPh_3)_2]_2[C_2O_4]$ with CO:

This reaction was carried out under different conditions:

(a) CO was bubbled through a solution of $[Pt_2(PPh_2)(dmpm)(PPh_3)_2]_2[C_2O_4]$ (0.050 g, 0.020 mmol) in CH_2Cl_2 (4 mL) for 0.5 hour. There was no change in the color of the solution. The $^{31}P\{^1H\}$ NMR spectrum of the solution showed that no reaction had taken place.

(b) $[Pt_2(PPh_2)(dmpm)(PPh_3)_2]_2[C_2O_4]$ (0.050 g, 0.020 mmol) was dissolved in THF (2 mL) in a small erlenmeyer flask which was then placed in a Parr bench-top high pressure reactor. After 45 minutes at 540 psi CO pressure and 25°C temperature, the solution which had turned lighter in color

was removed and its $^{31}P\{^{1}H\}$ NMR spectrum recorded. The $^{31}P\{^{1}H\}$ NMR spectrum showed only the presence of the starting material. The reaction was repeated at a higher CO pressure (800 psi) and temperature (80°C) for a longer period (24 hours) but no reaction took place.

Reaction of $[Pd_2(\mu\text{-}PPh_2)(\mu\text{-}dppm)(PPh_3)_2][BF_4]$ with Cl_2:

Cl_2 was bubbled through a solution of $[Pd_2(\mu\text{-}PPh_2)(\mu\text{-}dppm)(PPh_3)_2][BF_4]$ (0.050 g, 0.036 mmol) in CH_2Cl_2 (10 mL) for 2 minutes. During this time the solution changed color from dark orange to light yellow to colorless and then immediately back to red with some white precipitate. The $^{31}P\{^{1}H\}$ NMR spectrum of the red solution indicated complete decomposition of the starting material.

Reaction of $[Pd_2(\mu\text{-}PPh_2)(\mu\text{-}dppm)(PPh_3)_2][BF_4]$ with $HCCCO_2Me$:

Excess $HCCCO_2Me$ (0.095 g, 1.124 mmol) was added to a stirred solution of $[Pd_2(PPh_2)(dppm)(PPh_3)_2][BF_4]$ (0.050 g, 0.036 mmol) in THF (15 mL). After 24 hours of stirring, the color of the solution had changed from orange red to dark red. The $^{31}P\{^{1}H\}$ NMR spectrum of the solution showed that no reaction had occurred.

Reaction of $[Pt_2(\mu\text{-}PPh_2)(\mu\text{-}dppm)(PPh_3)_2]_2[C_2O_4]$ with $NOBF_4$:

$NOBF_4$ (0.050 g, 0.214 mmol) was added to a stirred solution of $[Pt_2(PPh_2)(dppm)(PPh_3)_2]_2[C_2O_4]$ (0.050 g, 0.016 mmol) in CH_2Cl_2 (2 mL). The color of the solution turned darker orange. After stirring for 24 hours, the $^{31}P\{^1H\}$ NMR spectrum of the solution was recorded which showed that no reaction had occurred.

Reaction of $[Pt_2(\mu\text{-}PPh_2)(\mu\text{-}dppm)(PPh_3)_2]_2[C_2O_4]$ with KCN:

KCN (0.005 g, 0.075 mmol) was added to a stirred solution of $[Pt_2(PPh_2)(dppm)(PPh_3)_2]_2[C_2O_4]$ (0.050 g, 0.016 mmol) in THF (5 mL). After refluxing the solution at 65°C for 30 hours, the $^{31}P\{^1H\}$ NMR spectrum of the solution was recorded which indicated that no reaction had occurred.

Reaction of $[Pd_2(\mu\text{-}PPh_2)(\mu\text{-}Ph_2PCH_2PPh_2)(PPh_3)_2][BF_4]$ with KCN:

KCN (0.005 g, 0.075 mmol) was added to a stirred solution of $[Pd_2(PPh_2)(dppm)(PPh_3)_2][BF_4]$ (0.050 g, 0.036 mmol) in THF (8 mL). After refluxing the solution at 65°C for 18 hours the solvent was removed <u>in vacuo</u>. The $^{31}P\{^1H\}$ NMR spectrum of the orange powder isolated showed the presence of $[Pd_2(\mu\text{-}PPh_2)(\mu\text{-}dppm)(PPh_3)(CN)]$ along with some starting material. Further refluxing did not improve the ratio.

$[Pd_2(PPh_2)(dppm)(PPh_3)(CN)]$: $^{31}P\{^1H\}$ NMR:[182] δ_1 82.9; J_{12} 15, J_{13} 204, J_{14} 255. Solvent: $CDCl_3$.

Reaction of $[M_2(\mu\text{-}PPh_2)(\mu\text{-}Ph_2PCH_2PPh_2)(Bu^tNC)_2][BF_4]$ (M= Pd, Pt) with Bu^tNC:

These reactions were carried out in a similar manner: e.g. the reaction of $[Pt_2(\mu\text{-}PPh_2)(\mu\text{-}dppm)(PPh_3)_2]_2[C_2O_4]$ with Bu^tNC:

Bu^tNC (0.011 g, 0.032 mmol) was added to a stirred solution of $[Pt_2(PPh_2)(dppm)(PPh_3)_2]_2[C_2O_4]$ (0.050 g, 0.016 mmol) in CH_2Cl_2 (5 mL). There was no noticeable change in the dark orange color of the solution. After stirring the solution for 1 hour, the $^{31}P\{^1H\}$ NMR spectrum of the solution was recorded which indicated that the terminal triphenylphosphines had been replaced by Bu^tNC. This compound was not isolated because during recrystallization from CH_2Cl_2/hexane at 24°C the substituted product reverts back to the starting dimer $[Pt_2(PPh_2)(dppm)(PPh_3)_2]_2[C_2O_4]$.

$[Pt_2(PPh_2)(dppm)(Bu^tNC)_2]_2[C_2O_4]$: $^{31}P\{^1H\}$ NMR:[183] δ_1 53.1, $\delta_{2,3}$ -135.2; J_{12} 251, J_{14} 2781, J_{24} 3065. Solvent: CH_2Cl_2.

$[Pd_2(PPh_2)(dppm)(Bu^tNC)_2][BF_4]$: $^{31}P\{^1H\}$ NMR:[183] δ_1 97.3, $\delta_{2,3}$ -136.2; J_{12} 208. Solvent: CH_2Cl_2.

$[Rh_3(\mu\text{-}PPh_2)_3(\mu\text{-}dppm)(CO)_3]$:

Dppm (0.026 g, 0.068 mmol) was added to a stirred sclution of $[Rh_3(PPh_2)_3(PPh_3)_2(CO)_3]$ (0.100 g, 0.068 mmol) in CH_2Cl_2 (15 mL). The color changed rapidly from a dark green to a bright emerald green. After 15 minutes of stirring, the solvent was removed <u>in vacuo</u> and the residue was recrystallized from CH_2Cl_2/hexane at 24°C to yield $[Rh_3(PPh_2)_3(dppm)(CO)_3]$ as dark green crystals (0.070 g, 0.052 mmol). Yield: 76% (based on the conversion of $[Rh_3(PPh_2)_3(PPh_3)_2(CO)_3]$).

<u>Anal.</u> Calc'd for $C_{64}H_{51}O_3P_5Rh_3$: C 57.7, H 3.86; <u>Found:</u> C 57.3, H 3.84.

$^{31}P\{^1H\}$ NMR:[184] $\delta_{1,2}$ 152.1, δ_3 74.0, $\delta_{4,5}$ -127.1; J_{12} 202, J_{13} 26, J_{14} 0, J_{16} 128, J_{17} 104, J_{18} 0, J_{34} 151, J_{37} 128, J_{47} 132, J_{45} 54. Solvent: CH_2Cl_2.

IR: 1932, 1925.

$[Ir_3(\mu\text{-}PPh_2)_3(\mu\text{-}dppm)(CO)_3]$:

CO was bubbled vigorously through a solution of $[Ir_2(COE)_4Cl_2]$ (0.300 g, 0.324 mmol) in benzene (20 mL) resulting in the rapid precipitation of a dark green solid. Diethylamine (0.047 g, 0.648 mmol) was added dropwise to this stirred mixture. After stirring for 10 minutes, a pale

yellow solution had formed. Addition of PPh_2H (0.120 g, 0.648 mmol) caused an immediate change to a reddish brown solution containing a mixture of $[Ir_3(PPh_2)_3(CO)_5]$ and $[Ir_3(PPh_2)_3(CO)_6]$. After stirring for a further 30 minutes, the solution was filtered and the solvent was removed <u>in vacuo</u> to obtain an oily red residue. The red residue was dissolved in CH_2Cl_2 (15 mL) and dppm (0.085 g, 0.221 mmol) was added. After stirring for 2 hours, the volume of the solvent was reduced <u>in vacuo</u> to 5 mL, and then transferred to an alumina column. A light red band was eluted from the column with benzene (10 mL). Removal of the solvent <u>in vacuo</u>, followed by recrystallization from CH_2Cl_2/hexane at 24°C afforded $[Ir_3(PPh_2)_3(dppm)(CO)_3]$ as dark red crystals (0.070 g, 0.044 mmol). Yield: 20% (based on the conversion of $[Ir_2(COE)_4Cl_2]$).

<u>Anal.</u> Calc'd for $C_{64}H_{51}O_3P_5Ir_3$: C 48.1, H 3.21; <u>Found:</u> C 47.1; H 3.38.

$^{31}P\{^1H\}$ NMR:[185] $\delta_{1,2}$ 100.7, δ_3 -21.7, $\delta_{4,5}$ -155.9; J_{12} 202, J_{13} 24, J_{14} 0, J_{34} 169, J_{45} 54. Solvent: CH_2Cl_2.

$[Ir_3(PPh_2)_3(CO)_5]$: $^{31}P\{^1H\}$ NMR:[185] $\delta_{1,2}$ 99.5, δ_3 -41.0; J_{12} 16.

$[Ir_3(PPh_2)_3(CO)_6]$: $^{31}P\{^1H\}$ NMR:[185] $\delta_{1,2,3}$ 39.0.

$[Ir_3(\mu\text{-}PPh_2)_3(CO)_5(Bu^tNC)_2]$:

Bu^tNC (0.033 g, 0.399 mmol) was added to a stirred solution of $[Ir_3(\mu\text{-}PPh_2)_3(CO)_5]$ (0.230 g, 0.132 mmol) in CH_2Cl_2 (15 mL). The color of the solution changed from red to yellow-orange almost immediately. After 1 hour of stirring, the volume of the solvent was reduced and the solution passed through alumina and the solvent removed in vacuo to obtain powder. Recrystallization from CH_2Cl_2/hexane at 24°C yielded $[Ir_3(PPh_2)_3(CO)_5(Bu^tNC)_2]$ as bright yellow crystals (0.030 g, 0.021 mmol). Yield: 16% (based on the conversion of $[Ir_3(PPh_2)_3(CO)_5]$).
Anal. Calc'd for $C_{52}H_{50}Cl_2N_2O_5P_3Ir_3$: C 41.0, H 3.31 ; Found: C 40.6, H 2.93.

$^{31}P\{^1H\}$ NMR:[185] $\delta_{1,2}$ -103.1, δ_3 -148.8; J_{13} 150.
IR: 2178, 2138, 1948, 1930, 1892.

SUGGESTIONS FOR FURTHER WORK

During the course of this project a large area was covered and explored. The reaction chemistry of $[M_3(\mu\text{-}X)(\mu\text{-}PPh_2)_2(PPh_3)_3]^+$ (M= Pd, X= Cl; M= Pt, X= H) clusters both with respect to substitution and fragmentation reactions was described (figure **8-1**). It was shown that these clusters react with diphosphine ligands to afford unique M(I) dimers, $[M_2(\mu\text{-}PPh_2)(\mu\text{-}R_2PCH_2PR_2)(PPh_3)_2]^+$ (M= Pt, Pd), which were unreactive towards a number of different reagents. Finally, analogous phosphido-bridged iridium and rhodium trinuclear clusters were synthesized and their reactions with dppm and Bu^tNC ligands were discussed. Some areas that could be further pursued in the future to obtain promising results are:

1. Further Reactions of Palladium and Platinum Trinuclear Clusters:

(a) Reactions of CO and small organic molecules such as C_2H_4 with transition metal clusters are of interest due to their relevance to many homogeneous and heterogeneous catalytic systems.[186-187] Preliminary studies have shown that bubbling CO through a solution of $[Pt_3(\mu\text{-}Cl)(\mu\text{-}PPh_2)_3(PPh_3)_3]^+$ for more than one minute and up to 24 hours leads to the reversible addition of one equivalent of CO to produce what appears to be $[Pt_3(\mu\text{-}PPh_2)_2(Cl)(CO)(PPh_3)_3]^+$.

Figure 8-1

Summary of the Reactions of
$[M_3(\mu\text{-}X)(\mu\text{-}PPh_2)_2(PPh_3)_3][BF_4]$

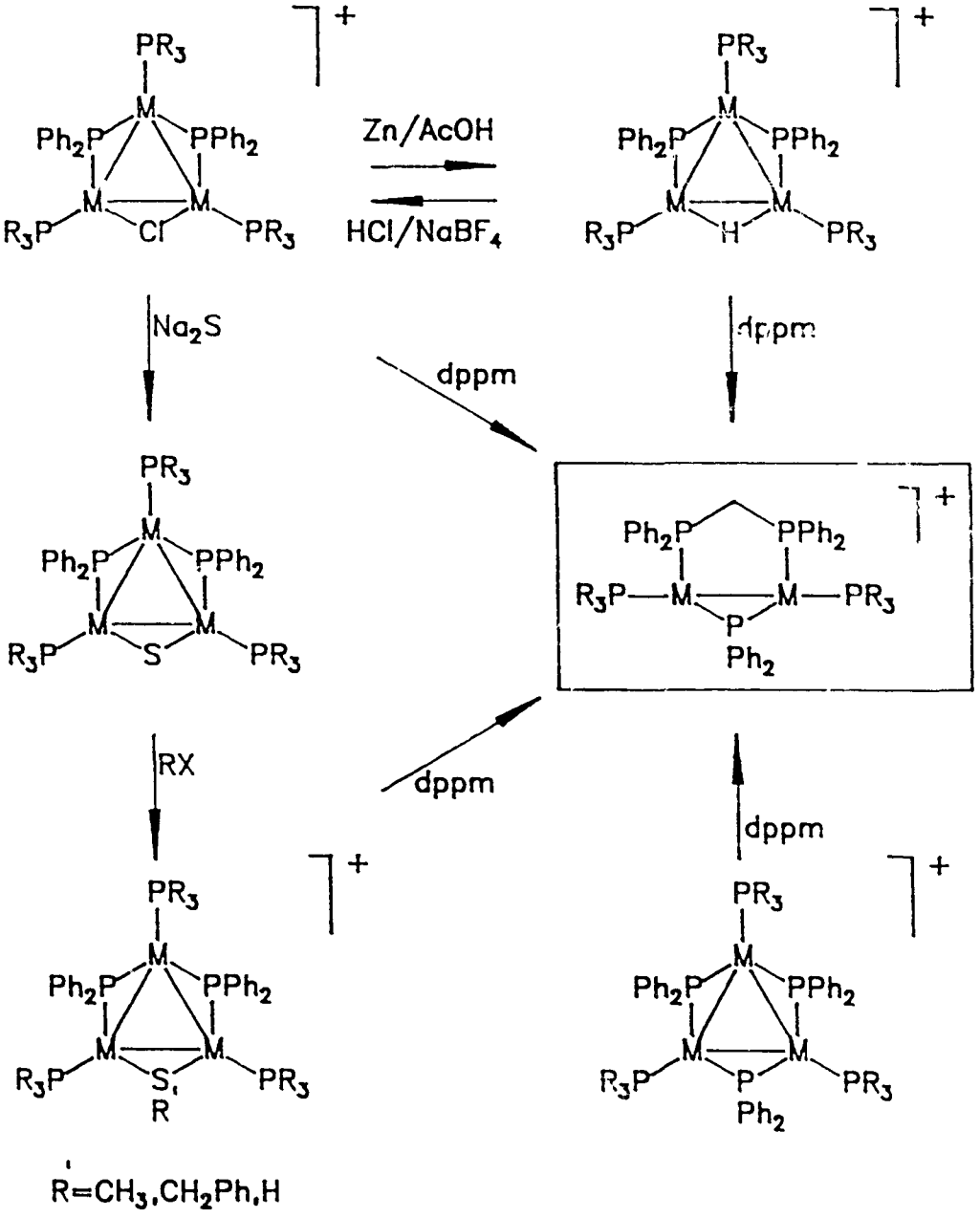

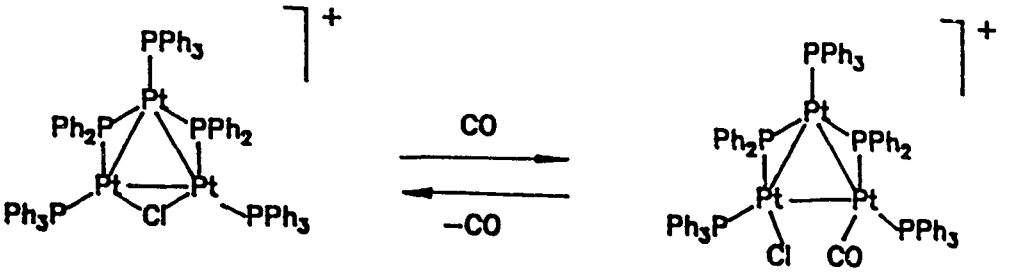

This compound which was formulated as $[Pt_3(\mu\text{-}PPh_2)_2(Cl)(CO)(PPh_3)_3]^+$ readily loses CO upon pumping or over a period of a few hours in solution. This reaction is not unique, and there are other examples of reversible additions of CO to clusters in the literature.[189-190] Preliminary investigation has also shown that the reaction of the μ-Cl platinum cluster with CH_2=CHMgBr leads to the formation of a μ-CH=CH_2 cluster similar to compounds reported by several groups.[191-193]

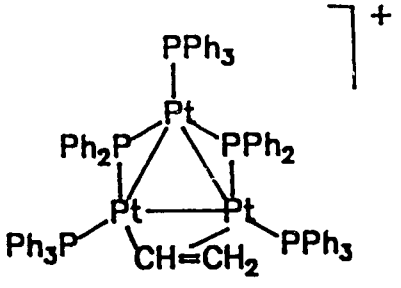

The reactions of this compound with other molecules such as CO, alkenes and alkynes should, in principle, lead to a number of products where new C-C bonds have formed.

b) Reaction of the trinuclear palladium platinum clusters with $R'_2P\text{-}RN\text{-}PR'_2$,[194] $Ph_2PCH_2PPh_2CH_2PPh_2$,[195] and $Ph_2PCH_2CH_2PPh_2$ ligands could lead to novel complexes. $Ph_2PCH_2PPh_2CH_2PPh_2$ has recently been used extensively to stabilize two and three adjacent metal centers.[196-197] In the case of $Ph_2PCH_2CH_2PPh_2$ ligand, preliminary investigation indicates that it reacts with $[Pt_3(\mu\text{-}Cl)(\mu\text{-}PPh_2)_2(PPh_3)_3][BF_4]$ to yield the substitution product, $[Pt_3(\mu\text{-}Cl)(\mu\text{-}PPh_2)_2(PPh_3)_2(Ph_2PCH_2CH_2PPh_2)][BF_4]$.

c) As was mentioned before successful separation of $[PtPd_2(\mu\text{-}Cl)(\mu\text{-}PPh_2)_2(PPh_3)_3][BF_4]$ and $[Pd_3(\mu\text{-}Cl)(\mu\text{-}PPh_2)_2(PPh_3)_3][BF_4]$ has not been possible yet. Once that has been achieved, the study of the reactivity of the mixed platinum/palladium compounds would be of interest with respect to preferential reactivity of the different metal centers.

d) Alternative methods of synthesizing these trinuclear clusters would be of interest. UV irradiation has been underutilized in this respect. Preliminary investigation has shown that UV irradiation of $[PdCl(PPh_3)_3][BF_4]$ in ethanol leads to the formation of a number of multimetallic compounds including the trinuclear cluster $[Pd_3Cl(\mu\text{-}PPh_2)_2(PPh_3)_3][BF_4]$. The UV irradiation of $[Pt(PPh_3)_4]$ was also discovered to yield a number of multimetallic species.

2. Mechanistic Studies:

The mechanism of the fragmentation reactions reported are not at all clear. A detailed mechanistic study would afford a better understanding of the processes involved.

3. Electrochemical Studies:

In spite of the great interest in clusters and in Pd(I) and Pt(I) dimers there is little known about their electrochemical behavior. The only example of such study showed that Pd(I) and Pt(I) dimers, $[M_2(\mu\text{-dppm})_2X_2]$ (M= Pd, Pt; X= Cl, Br, I), undergo either an irreversible two-electron reduction to yield $[Pd(dppm)_2]$ among other products; or an irreversible one-electron oxidation to yield $[PdCl_2(dppm)]$.[198] In both cases all the fragments formed were not identified. The triangular clusters and dimers reported in this thesis make ideal candidates for a comprehensive electrochemical study.

4. Further Reaction Chemistry of Pd(I) and Pt(I) Dimers:

(a) Preliminary Studies have shown that the terminal triphenylphosphines in $[M_2(\mu\text{-}PPh_2)(\mu\text{-dppm})(PPh_3)_2]^+$ (M= Pd, Pt) may be replaced by two moles of dppm to afford $[M_2(\mu\text{-}PPh_2)(\mu\text{-dppm})(dppm)_2]^+$.

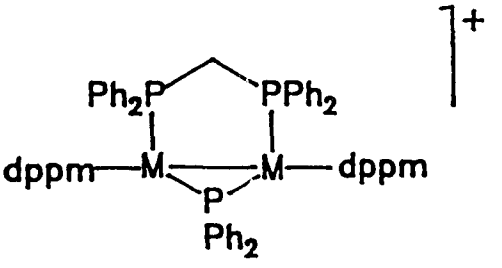

This compound might be used as a bidentate (the two dangling dppm phosphorus atoms) ligand for square planar metal atoms to synthesize homonuclear and heteronuclear clusters $[M'M_2(\mu\text{-}PPh_2)(\mu\text{-}dppm)_3(X)_2]^+$ (M'= Pd, Pt, Rh, Ir; M= Pd, Pt; X= Cl, CO, R).

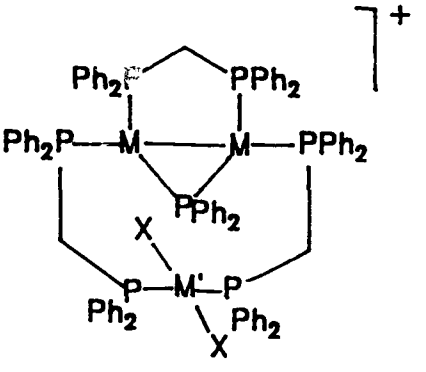

Similar reactions were reported by Puddephatt and co-workers where $[Pt_2(\mu\text{-}S)(\mu\text{-}dppm)(dppm)_2]$ was reacted with a number of square planar complexes such as $[PdCl_2(PhCN)_2]$ and $[Pt(X)Cl(SMe_2)_2]$ to yield trinuclear clusters.[199]

c) The Pd(I) and Pt(I) dimers might show enhanced or different reactivity under ultraviolet conditions.

d) The lability of the terminal iodide in [$Pt_2(\mu\text{-}PPh_2)(\mu\text{-}dppm)(PPh_3)(I)$] might be used to synthesize other dimers where the iodide is replaced by other ligands such as CO, H, and C_2H_4.

5. Reaction chemistry of [$M_3(\mu\text{-}PPh_2)_3(\mu\text{-}dppm)(CO)_3$] (M= Rh, Ir):

[$M_3(\mu\text{-}PPh_2)_3(\mu\text{-}dppm(CO)_3$] (M= Rh, Ir) clusters contain unsaturated sites, therefore, in principle they should react with donor molecules. Reactions with alkenes and alkynes would be of particular interest. Reaction of these clusters with oxidative addition reagents such as HCl, I_2, CH_3I, H_2O would also be interesting and should yield valuable data.

6. NMR Studies:

The compounds reported in this thesis have interesting and sometimes complicated NMR spectra. 2-D NMR techniques can be used to solve some of these problems and to add to the knowledge of signs and magnitudes of coupling constants. These in turn will add to the understanding of bonding and stability in those complexes.

REFERENCES

1. King, R.B. **Prog. Inorg. Chem.** (1972), 15, 287.

2. Johnson, B.F.G. Ed. **"Transition Metal Clusters"**; John Wiley and Sons, New York, (1980).

3. Moskovits, M., (Ed.) **"Metal Clusters"**; John Wiley and Sons, New York, (1986).

4. Mutterties, E.L.; Rhodin, T.N.; Band, E.; Brucker, C.F.; Pretzer, N.R. **Chem. Rev.** (1979), 79, 91.

5. Mutterties, E.L.; Krause, M.J. **Angew. Chem. Int. Ed. Engl.** (1983), 22, 135.

6. Huttner, G.; Knol, K. **Angew. Chem. Int. Ed. Engl.** (1987), 26, 743.

7. Puddephatt, R.J. **Canadian Chemical News**, March 1986.

8. Atwood, J. D. **Coord. Chem. Rev.** (1988), 83, 93.

9. Martinez, J.M.; Adams, H.; Bailey, N.A.; Maitlis, P.M. **J. Chem. Soc. Chem. Commun.** (1989), 286.

10. Hermann, W. A. **Angew. Chem. Int. Ed. Engl.** (1982), 21, 117.

11. Holt, E.M.; Whitmire, K.H.; Shriver, D.H. **J. Organometal. Chem.** (1981), 213, 125.

12. Beaman, L.R.; Rahman, Z.A.; Keister, J.B. **Organometallics** (1983), 2, 1062.

13. Zilter, J.W.; Bower, D.K.; Dalton, D.M.; Keister, J.B.; Churchill, M.R. **Organometallics** (1989), 8, 492.

14. Geoffrey, G.L.; Rosenberg, S.; Shulman, P.M.; Wittle, R.R. **J. Amer. Chem. Soc.** (1984), 106, 1519.

15. Davies, S.J.; Howard, J.A.K.; Pilotti, M.V.; Stone, F.G.A. **J. Chem. Soc. Chem. Comm.** (1989), 19[illegible].

16. Sappa, E.; Tiripicchio, A.; Braunstein, P. **Coord. Chem. Rev.** (1985), 65, 219.

17. Jones, R.A.; Wright, T.C.; Atwood, J.L.; Hunter, W.E. **Organometallics** (1983), 3, 114.

18. Brandon, J.B.; Dixon, K.R. **Can. J. Chem.** (1981), 59, 1188.

19. Huttner, G.; Born, J.; Zsolnai, L. **J. Organomet. Chem.** (1984), 263, C33.

20. Carty, A.J.; Maclaughlin, S.A.; Nucciarone, D. **Phosphorus 31 NMR Spectroscopy in Stereochemical Analysis**, VCH Publishers, Inc. (1987).

21. Roberts, D.A.; Geoffrey, G.L. in **Comprehensive Organometallic Chemistry**; Wilkinson, G.; Stone, F.G.A.; Abel, E.W., Eds. Pergamon Press, Oxford (1982), Chapter 40.

22. Colbran, S.B.; Lahoz, F.J.; Raithby, P.R.; Lewis, J.; Johnson, B.F.G.; Cardin, C.J. **J. Chem. Soc. Dalton Trans.** (1988), 173.

23. Adams, R.D.; Horváth, I.T.; Wang, S. **Inorg. Chem.** (1986), 25, 1617.

24. Van Gastel, F.; Taylor, N.J.; Carty, A.J. **Inorg. Chem.** (1989),28, 384.

25. Braunstein, P.; de Meric de Bellefon, C.; Reis, M. **J. Organometal. Chem.**,(1984), 262, C14.

26. Bermúdez, M.D.; Brown, F.P.E.; Stone, F.G.A. **J. Chem. Soc. Dalton Trans.** (1988), 1139.

27. Chihara, T.; Komoto, R.; Kobayashi, K.; Yamazaki, H.; Matsuua, Y. **Inorg. Chem.** (1989), 28, 964.

28. Douglas, G.; Manojlovic-Muir, L.; Muir, K.W.; Jennings, M.C.; Lloyd, B.R.; Rashidi, M.; Puddephatt, R.J. **J. Chem. Soc. Chem. Comm.** (1988), 149.

29. Hidai, M.; Kokura, M.; Uchida, Y. **J. Organomet. Chem.** (1973), 52, 431.

30. Yoshida, T.; Otsuka, S. **J. Amer. Chem. Soc.** (1977), 99, 2134.

31. Otsuka, S.; Tatsuno, Y.; Miki, M.; Aoki, T.; Matsumoto, M.; Yoshioka, H.; Nakatsu, K. **J. Chem. Soc. Chem. Commun.** (1973), 445.

32. Manojlovic-Muir, L.; Muir, K.W.; Lloyd, B.R.; Puddephatt, R.J. **J. Chem. Soc. Chem. Comm.** (1983), 83, 1336.

33. Arif, A.M.; Heaton, D.E.; Jones, R.A.; Nunn, C.M. **Inorg. Chem.** (1987), 26, 4228.

34. Boag, N.M.; Boucher, D.; Davies, J.A.; Miller, R.W.; Pinkerton, A.A.; Syed, R. **Organometallics** (1988), 7, 791.

35. Dixon, K.R.; Rattray, A.D. **Inorg. Chem.** (1978), 17, 1099.

36. Berry, D.E.; Bushnell, G.W.; Dixon, K.R.; Moroney, P.M.; Wan, C. **Inorg. Chem.** (1985), 24, 2625.

37. Cartwright, S.J.; Dixon, K.R.; Rattray, A.D.; **Inorg.Chem.** (1980), 19, 1120.

38. Albinati, A.**Inorg. Chim. Acta.** (1977), 22, L31.

39. Browning, C.S.; Farrar, D.H.; Gukathasan, R.R.; Morris, S.A.**Organometallics** (1985), 4, 1750.

40. Evans, D.G.; Hallam, M.F.; Mingos, D.M.P.; Wardle, R.W.M.**J. Chem. Soc. Dalton Trans.** (1987), 1889.

41. Albinati, A.; Canturan, G.; Musco, A. **Inorg. Chim. Acta.** (1976), 16, L3.

42. Moody, D.C.; Ryan, R.R. **Inorg. Chem.** (1977), 16, 1052.

43. Briant, C.E.; Gilmour, D.I.; Mingos, D.M.P. **J. Chem. Soc. Dalton Trans.** (1986) 1535.

44. Green, M.; Howard, J.A.K.; Murray, M.; Spencer, J.L.; Stone, F.G.A. **J. Chem. Soc. Dalton Trans.** (1977), 1509.

45. Yamamoto, Y.; Takahashi, K.; Yamazaki, H. **Chem Lett.** (1985), 201.

46. Ferguson, G.; Lloyd, B.R.; Puddephatt, R.J. **Organomettalics** (1986), 5, 344.

47. Ling, S.S.M.; Hadj-Bagheri, N.; Manojlovic-Muir, L.; Muir, K.W.; Puddephatt, R.J. **Inorg. Chem.** (1987), 26, 231.

48. Bott, S.G.; Hallarn, M.F.; Ezomo, O.J.; Mingos, D.M.P.; Williams, I.D. **J. Chem. Soc. Dalton Trans.** (1988), 1461.

49. Taylor, N.J.; Chieh, P.C.; Carty, A.J. **J. Chem. Soc. Chem. Comm.** (1975), 448.

50. Evans, D.G.; Hughes, G.R.; Mingos, D.M.P.; Bassett, J.M.; Welch, A.J. **J. Chem. Soc. Chem. Comm.** (1980), 1255.

51. Bellon, D.E.; Ceriotti, A.; Demartin, F.; Langoni, G.; Heaton, B.T. **J. Chem. Soc. Dalton Trans.** (1982), 1671.

52. See reference 36.

53. Rakowski DuBois, M. **Chem. Rev.** (1989), 89, 1.

54. Li, P.; Curtis, M.D. **Inorg. Chem.** (1990), 29, 1242.

55. Hogarth, G.; Taylor, N.J.; Carty, A.J.; Meyer, A. **J. Chem. Soc. Chem. Comm.** (1988), 834.

56. Adams, R.D.; Babin, J.E.; Wang, J.-G.; Wu, W. **Inorg. Chem.** (1989), 28, 703.

57. Gukathasan, R.R.; Morris, R.H.; Walker, A. **Can. J. Chem.** (1983), 61, 2490.

58. Browning, C.S.; Farrar, D.H. **Organometallics** (1989), 8, 813.

59. Hunt, C.T.; Matson, G.B.; Balch, A.L. **Inorg. Chem.** (1981), 20, 2270.

60. Evans, D.G. **J. Organomet. Chem.** (1988), 352, 397.

61. Mingos, D.M.P.; Evans, D.G. **J. Organomet. Chem.** (1983), 251, C13.

62. Mingos, D.M.P. **Acc. Chem. Res.** (1984), 17, 311.

63. Evans, D.G.; Mingos, D.M.P. **J. Organomet. Chem.** (1982), 240, 321.

64. Hoffman, R. **Angew. Chem. Int. Ed. Engl.** (1982), 21, 711.

65. Underwood, D.J.; Hoffmann, R.; Tatsumi, K.; Nakamura, A.; Yamamoto, Y. **J. Amer. Chem. Soc.** (1985), 107, 5968.

66. Gilmour, D.I.; Mingos, D.M.P. **J. Organometal. Chem.** (1986), 302, 127.

67. See reference 48.

68. See reference 39 and 58.

69. Hallam, M.F.; Mingos, D.M.P. **J. Organomet. Chem.** (1986), 315, C35.

70. Yamamoto, Y. **Coord. Chem. Rev.** (1980), 32, 193.

71. Yamamoto, Y.; Yamazaki, H. **J. Chem. Soc. Dalton Trans.** (1986)

72. Mingos, D.M.P.; Williams, I.D.; Watson, M.J. **J. Chem. Soc. Dalton Trans.** (1988) 1509.

73. See reference 33.

74. Puddephatt, R.J. **Chem. Soc. Rev.** (1983), 12, 99.

75. Blagg, A.; Shaw, B.L. **J. Chem. Soc. Dalton Trans.** (1987), 221.

76. Fanwick, P.E.; Root, D.R.; Watton, R.A. **Inorg. Chem.** (1989), 28, 397.

77. Obendorf, D.; Probst, M.; Peringer, P.; Falk, H.; Müller, N. **J. Chem. Soc. Dalton Trans.** (1988), 1709.

78. Hämmerle, B.; MÜller, E.P.; Wilkinson, D.L.; MÜller, G.; Peringer, P. **J. Chem. Soc. Chem. Comm.** (1989), 1527.

79. Neher, A.; Lorenz, I-P. **Angew. Chem. Int. Ed. Eng.** (1989), 10, 28.

80. Hogarth, G.; Knox, S.A.R.; Lloyd, B.R.; MacPherson, K.A.; Morton, D.A.V.; Orpen, A.G. **J. Chem. Soc. Chem. Comm.** (1988), 360.

81. Grist, N.J.; Hogarth, G.; Knox, S.A.R.; Lloyd, B.R.; Morton, D.A.V.; Orpen, A.G. **J. Chem. Soc. Chem. Comm.** (1988), 673.

82. Puddephatt, R.J.; Thompson, M.A.; Manojlovic-Muir, L.; Muir, K.W.; Frew, A.A.; Brown, M.P. **J. Chem. Soc. Chem. Comm.**, (1981), 805.

83. Hadj-Bagheri, N." **Masters Thesis**", University of Victoria, 1985.

84. Hansen, B.E.; Fanwick, P.E.; Mancini, J.S. **Inorg. Chem.** (1982), 21, 3811.

85. Karsh, H.H.; Milewski-Mahrla, B. **Angew. Chem. Int. Ed. Eng.** (1981), 20, 814.

86. Calcas, J.A.; Harding, M.M.; Nichols, B.S.; Smith, A.K. **J. Chem. Soc. Dalton Trans.** (1985), 1835.

87. Hoffmann, D.M.; Hoffmann, R. **Inorg. Chem.** (1981), 20, 3543.

88. Puddephatt, R.J.; Azam, K.A.; Hill, R.H.; Brown, M.P.; Nelson, C.D.; Moulding, R.P., Seddon, K.R.; Grossel, M.C. **J. Amer. Chem Soc.** (1983), 105, 5642.

89. See reference 83.

90. Maitlis, P.M.; Espinet, P.; Russell, M.J.H. In **"Comprehensive Organometallic Chemistry"** Wilkinson, G.; Stone, F.G.A.; Abel, E.W.; Eds.; Pergamon Press: Oxford, (1982).

91. See reference 72.

92. Skapski, A.C.; Troughton, P.G.H. **J. Chem. Soc. A.** (1969), 2772.

93. See reference 71.

94. See reference 59.

95. Collman, J.P.; Hegedus, L.S. **"Principles and Applications of Organotransition Metal Chemistry"** University Science Books, Mill Valley, CA., (1980).

96. Cotton, F.A.; Wilkinson, G. **"Advanced Inorganic Chemistry"** 6th Edition, John Wiley and Sons, New York, (1988).

97. Harrison, D.H. **" Ph.D. Dissertation"**, University of Victoria, 1987.

98. Chisholm, M.H.; Kirkpatric, C.C.; Huffman, J.C. **Inorg. Chem.** (1981),20, 871.

99. Fanke, R.; Schmidbauer, H. **Inorg. Chim. Acta.** (1976), 13, 85.

100. Jalenik, P.d.; Schubert, U.; Schmidbauer, H. **Agnew. Chem. Int. Ed. Engl.** (1982), 21, 73.

101. Fackler, J.P.; Murray, H.H.; Trzcinska.Bancroft, B. **Organometallics** (1985), 4, 1633.

102. Murray, H.H; Fackler, J.P.; Porter, L.C.; Briggs, D.A.; Guerra, M.A.; Lagow, R.J. **Inorg. Chem.** (1987), 26, 357.

103. Harrison, D.G.; Stobart, S.R. **J. Chem. Soc. Chem. Comm.** (1986), 285.

104. Brost, R.D.; Fjeldsted, D.O.K.; Stobart, S.R. **J. Chem. Soc. Chem. Comm.** (1989), 488.

105. Atwood, J.L.; Beveridge, K.A.; Bushnell, G.W.; Dixon, K.R.; Eadie, D.T.; Stobart, S.R.; Zaworotko, M.J. **Inorg. Chem.** (1984), 23, 4050.

106. Bonnet, J.-J.; Galy, J.; Klack, P.; Mayanza, A.; Poilblanc, R. **J. Chem. Res. (s)** (1980), 146.

107. Jobe, I.R.; Ling, S.S.M.; Manojlovic-Muir, L.; Muir, K.W.; Puddephatt, R.J. **Organometallics** (1985), 4, 773.

108. See reference 95.

109. Langrick, C.R.; Pringle, P.G.; Shaw, B.L. **J. Chem. Soc. Dalton Trans.** (1985), 1015.

110. Davies, J.A.; Pinkerton, A.A.; Syed, R.; Vilmer, M. **J. Chem. Soc. Chem. Comm.** (1988), 47.

111. Kullberg, M.L.; Kubiak, C.P. **Inorg. Chem.** (1986), 25, 2119.

112. Balch, A.L.; Benner, L.S.; Olmstead, M.M. **Inorg. Chem.** (1979), 18, 2996.

113. Chung-Li, L.; Hunt, C.T.; Balch, A.L. **Organometallics** (1982), 1, 824.

114. Besenyei, G.; Chung-Li, L.; Gulinski, J.; Rettig,

S.J.; James, B.R.; Nelson, D.A.; Lilga, M.A. **Inorg. Chem.** (1987), 26, 3622.

115. Benner, L.S.; Balch, A.L. **J. Amer. Chem. Soc.** (1978), 100, 6099.

116. Frew, A.A.; Hill, R.H,; Manojlovic-Muir, L.; Muir, K.W.; Puddephatt, R.J. **J. Chem. Soc. Chem. Comm.** (1982), 198.

117. See reference 14.

118. Shyu, S.; Wojcicki, A. **Organometallics** (1984), 3, 809.

119. Chau, C.-N.; Yu, Y.-F; Wojcicki, A.; Calligaris, M.; Giorgio, N.; Balducci, G. **Organometallics** (1987), 6, 308.

120. Regragui, R.; Dixneuf, P.H.; Taylor, N.J.; Carty, A.J. **Organometallics** (1984), 3, 816.

121. See reference 59.

122. Browntree, G.S.; Carty, P.; Cash, D.N.; Walker, A. **Inorg. Chem.** (1975), 14, 323.

123. Cheng, P.T.; Nyburg, S.C. **Inorg. Chem.** (1975), 14, 327.

124. Arif, A.M.; Heaton, D.E.; Jones, R.A.; Kidd, K.B.; Wright, T.C.; Whittlesey, B.R.; Atwood, J.L.; Hunter, W.E.; Zhang, H. **Inorg. Chem.** (1987), 26, 4065.

125. See reference 118.

126. Grossel, M.C.; Batson, J.R.; Moulding, R.P.; Seddon, K.R. **J. Organometal. Chem.** (1986), 304, 391.

127. See reference 59.

128. Galli, D.; Garlaschelli, L.; Ciani, G.; Fumagalli, A.; Martinengo, S.; Sironi, A. **J. Chem. Soc. Dalton Trans.** (1984), 55.

129. Pergola, R.D.; Garlaschelli, L.; Martinengo, S.; Demartin, F.; Manassero, M.; Sansoni, M. **J. Chem. Soc. Dalton Trans.** (1986), 2463.

130. Lawson, R.J.; Shapley, J.R. **J. Amer. Chem. Soc.** (1976), 98, 7433.

131. Shapley, J.R.; Adair, P.C.; Lawson, R.J.; Pierpont, C.G. **Inorg. Chem.** (1982), 21, 1701.

132. Vazquez de Miguel, A.; Isobe, K.; Bailey, P.M.; Meanwell, N.J.; Maitliss, P.M. **Organometallics** (1982), 1, 1605.

133. Isobe, K.; Vazquez de Miguel, A.; Nutton, A.; Maitlis, P.M. **J. Chem. Soc. Dalton Trans.** (1984), 929.

134. Herrmann, W.A.; Plank, J.; Reidel, D.; Zeigler, M.L.; Weidenhammer, K.; Guggloz, E.; Balbach, B. **J. Amer. Chem. Soc.** (1981), 103, 63.

135. Harding, M.M.; Nicholls, B.S.; Smith, A.K. **J. Chem. Soc. Dalton Trans.** (1983), 1479.

136. Wang, H-H.; Casalnuovo, B.J., Johnson, B.J.; Mueting, A.M.; Pignolet, L.H. **Inorg. Chem.** (1988), 27, 325.

137. Billig, E.; Jamerson, J.D.; Pruett, R.L. **J. Organomet. Chem.** (1980), 192, C49.

138. Haines, R.J.; Steen, N.D.C.T.; English, R.B. **J. Organomet. Chem.** (1981), 209, C34.

139. Haines, R.J.; Steen, N.D.C.T.; English, R.B. **J. Chem. Soc. Chem. Comm.** (1981), 407.

140. Haines, R.J.; Steen, N.D.C.T.; English, R.B. **J. Chem. Soc. Dalton Trans.** (1984), 515.

141. Atwood, J.L.; Hunter, W.E.; Jones, R.A.; Wright, T.C. **Inorg. Chem.** (1983), 22, 993.

142. Jones, R.A.; Wright, T.C. **Inorg. Chem.** (1986), 25, 4058.

143. See reference 124.

144. Mason, R.; Sotofte, I.; Robinson, S.D.; Uttley, M.F. **J.Organometal. Chem.** (1972), 46, C61.

145. See Reference 140.

146. See Reference 35.

147. See Reference 72.

148. Dixon, K.R. In **Multinuclear NMR** Mason, J.M.; Ed., Plenum Press, NewYork, (1987).

149. Appelton, T.G.; Clark, H.C.; Mazner, L.E. **Coord. Chem. Rev.** (1973), 10, 378.

150. Meek, D.W.; Maznec, T.J. **Acc. Chem. Res.** (1981), 14, 266.

151. Pregosin, P.S.; Kunz, R.W. **^{31}P and ^{13}C NMR of Transition Metal Phosphorus Complexes**, No. 16 in series NMR Basic Principles and Progress, Diehl, P.; Fluck, E.; Kosfeld, R., Eds.; Springer-Verlog, NewYork,(1979).

152. Pidcock, A. In **Catalytic Aspects of Metal Phosphine Complexes**, No. 169 in series Advances in Chemistry, Alyea, E.C.; Meak, D.W., Eds. American Chemical Society, Washington,(1982).

153. See Reference 20.

154. See Reference 65.

155. Patel, V.; Cherkos, A.; Nucciarone, D.; Taylor, N.J.; Carty, A.J. **Organometallics** (1985), 4, 1795.

156. Smith, W.F.; Carty, A.J.; Taylor, N.J. **J. Chem. Soc. Chem. Comm.** (1979), 750.

157. Mather, G.G.; Pidcock, A.; Rapsey, G.N. **J. Chem. Soc. Dalton Trans.** (1973), 2095.

158. Moor, A.; Pregosin, P.S.; Venanzi, L.M. **Inorg. Chim. Acta.** (1982), 61, 135.

159. See Reference 60-64.

160. Johnson, B.F.G.; Benfield, R.E. in **Top. Stereo. Chem.** (1981), 12, 253.

161. Hallam, M.F.; Howells, N.D.; Mingos, D.M.P.; Wardle, R.W.M. **J. Chem. Soc. Dalton Trans.** (1985), 845.

162. See Reference 87.

163. Fenetti, J.A.; Harris, R.K., Johannsen, R.B. **J. Mag. Res.** (1970), 3, 84.

164. Swalen, J.D. **"Computer Programmes for Chemistry, Vol. 1"** Edited by D.F. Detar, W.A. Benjamin Inc., New York (1968).

165. See Reference 36.

166. See Reference 51.

167. See reference 137.

168. van der Ent, A.; Onderdelinden, A.L. **Inorg. Synth.** (1973), 14, 94.

169. Peterson, D.J. **J. Organomet. Chem.** (1967), 8, 199.

170. The following numbering scheme is used for the $^{31}P\{^{1}H\}$ NMR data of the trinuclear palladium complexes: unique terminal phosphine (1); other terminal phosphines (2,3); phosphido bridges (4,5).

171. The following numbering scheme is used for the $^{31}P\{^{1}H\}$ NMR data of these trinuclear platinum complexes: unique terminal phosphine (1); other terminal phosphines (2,3); phosphido bridges (4,5); unique platinum (6); other platinum (7,8).

172. The following numbering scheme is used for the $^{31}P\{^{1}H\}$ NMR data of this complex: terminal phosphines (1,2,3); phosphido bridges (4,5,6); platinum (7).

173. The following numbering scheme is used for the $^{31}P\{^{1}H\}$ NMR data of this complex: phosphido bridge (1); dppm (2).

174. The following numbering scheme is used for the $^{31}P\{^{1}H\}$ NMR data of the Pd(I) dimeric complexes: phosphido bridge (1); terminal phosphines (2,3); diphosphine ligand (4,5).

175. The following numbering scheme is used for the $^{31}P\{^{1}H\}$ NMR data of this complex: phosphido bridge (1); terminal phosphines (2,3); $Pr^{i}_{2}P$-end of diphosphine (4); $Ph_{2}P$-end of diphosphine (5).

176. The following numbering scheme is used for the $^{31}P\{^{1}H\}$ NMR data of this complex: phosphido bridge (1); dppm (2); platinum (3).

177. The following numbering scheme is used for the $^{31}P\{^{1}H\}$ NMR data of the Pt(I)/Pd(I) dimeric complexe: phosphido bridge (1); terminal phosphines (2,3); diphosphine ligand (4,5); platinum (6). 2 and 4 are attached to 6.

178. The following numbering scheme is used for the $^{31}P\{^{1}H\}$ NMR data of the Pt(I) dimeric complexes: phosphido bridge (1); terminal phosphines (2,3); diphosphine ligand (4,5); platinum (6).

179. The following numbering scheme is used for the $^{31}P\{^{1}H\}$ NMR data of this Pt(I) dimeric complex: phosphido bridge (1); $Bu^{t}_{2}P$- end of diphsphine (2); $Ph_{2}P$-end of diphosphine (3); platinum (4,5). 4 is attached directly to 2, and 5 to 3.

180. The following numbering scheme is used for the $^{31}P\{^{1}H\}$ NMR data of this Pt(I) dimeric complex: phosphido bridge (1); terminal triphenylphosphines (2,3,4); platinum (5,6). 4 is trans to 1, 2 and 3 are cis to 1.

181. The following numbering scheme is used for the $^{31}P\{^{1}H\}$ NMR data of these dimeric complexes: phosphido bridge (1); terminal phosphine (2); diphosphine ligand (3,4); platinum (5). 2 and 4 are cis to each other.

182. The following numbering scheme is used for the $^{31}P\{^{1}H\}$ NMR data of this complex: phosphido bridge (1); terminal phosphines (2); diphosphine ligand (3,4).

183. The following numbering scheme is used for the $^{31}P\{^{1}H\}$ NMR data of this complex: phosphido bridge (1); diphosphine ligand (2,3), platinum (4).

184. The following numbering scheme is used for the $^{31}P\{^{1}H\}$ NMR data of the rhodium cluster complex: equivalent phosphido bridges (1,2); unique phosphido bridge (3); dppm (4,5); unique rhodium (6); other rhodium (7,8).

185. The following numbering scheme is used for the $^{31}P\{^{1}H\}$ NMR data of the iridium cluster complexes: equivalent phosphido bridges (1,2); unique phosphido bridge (3); dppm (4,5).

186. See reference 96.

187. Schneider, J.; Minelli, M.; Huttner, G. **J. Organomet. Chem.** (1985), 294, 75.

188. Lloyd, B.; Bradford, A.; Puddephatt, R.J. **Organometallics** (1987), 6, 424.

189. See reference 142.

190. Adams, R.D.; Wang, S. **Organometallics** (1986), 5, 1272.

191. Colborn, R.E.; Dyke, A.F.; Gracey, B.P.; Knox, S.A.R.; MacPherson, K.A.; Mead, K.A.; Orpen, A.G. **J. Chem. Soc. Dalton Trans.** (1990), 761.

192. Fontaine, X.L.R.; Jacobson, G.B.; Shaw, B.L.; Thornton-Pett, M. **J. Chem. Soc. Dalton Trans.** (1988), 741.

193. Boyer, E.; Deeming, A.J.; Felix, M.S.B.; Kalin, S.F.; Adatia, T.; Bhusater, R.; Mcpartlin, M.; Powell, R. **J. Chem. Soc. Dalton Trans.** (1989), 5.

194. Colquhoun, I.J.; McFarlane, W. **J. Chem. Soc. Dalton Trans.** (1977), 1674.

195. Appel, R.; Geisler, K.; Scholer, H.F. **Chem. Ber.** (1979), 112, 648.

196. Balch, A.L.; Fossett, L.A.; Linehan, J.; Olmstead, M.M. **Organometallics** (1986), 5, 691.

197. Balch, A.L.; Fossett, L.A.; Guimerans, R.R.; Olmstead, M.M.; Reedy, P.E.; Wood, F.E. **Inorg. Chem.** (1986), 25, 1248.

198. Nemra, R.; Lemoine, P.; Braunstein, P.; de Meric de Bellefon, C.; Reis, M. **J. Organometal. Chem.** (1986), 304, 245.

199. Hadj-Bagheri, N.; Puddephatt, R.J. **J. Chem. Soc. Chem. Comm.** (1987), 1269.